

# Power production from radioactively contaminated biomass and forest litter in Belarus - Phase 1b

**Roed, Jørn; Andersson, Kasper Grann; Fogh, C.L.; Olsen, S.K.; Prip, H.; Junker, H.; Kirkegaard, N.; Jensen, J.-M.; Grebenkov, A.J.; Solovjev, V.N.**

*Total number of authors:*
16

*Publication date:*
2000

*Document Version*
Publisher's PDF, also known as Version of record

**Risø-R-1146(EN)**

# Power Production from Radioactively Contaminated Biomass and Forest Litter in Belarus - Phase 1b

**Jørn Roed, Kasper G. Andersson, Christian L. Fogh, Svend K. Olsen and Henrik Prip**
Risø National Laboratory, Denmark

**Helle Junker, Niels Kirkegaard and Jens-Martin Jensen**
ELSAMPROJEKT, Denmark

**Alexandre J. Grebenkov, Vitalij N. Solovjev, Gregory G. Kolchanov, Leonid A. Bida, Peter M. Klepatzky, Igor G. Pleshchenkov, Arnold A. Gvozdev**
IPEP, Belarus

**Larry Baxter**
Sandia National Laboratories, USA

**Risø National Laboratory, Roskilde**
**March 2000**

**Abstract** The Chernobyl accident has led to radioactive contamination of vast Belarussian forest areas. A total scheme for remediation of contaminated forest areas and utilisation of the removed biomass in safe energy production is being investigated in a Belarussian-American-Danish collaborative project. Here the total radiological impact of the scheme is considered. This means that not only the dose reductive effect of the forest decontamination is taken into account, but also the possible adverse health effects in connection with the much needed bio-energy production. This report presents the results of an in-country, commercial-scale investigation of the effect of a baghouse filter in retaining contaminants so that they are not released to the atmosphere in the biomass energy production process. Approximately 99.5% of the activity of a commercially representative, dust-laden boiler flue gas was removed from the stream by using a combination of a cyclone and a baghouse filter.

ISBN 87-550-2619-2
ISBN 87-550-2620-6 (Internet)
ISSN 0106-2840

Information Service Department, Risø, 2000

# Summary

The Chernobyl Bio-energy Project focuses on remediation of the forest areas contaminated by the 1986 Chernobyl power plant disaster. The combustion of biomass in an electric-power-producing boiler plays a central role in this strategy. A primary concern in connection with this combustion is the fate of the radionuclides. Experiments under carefully controlled laboratory conditions and under larger-scale commercial conditions typical of western technology were conducted earlier in separate programs. However, boiler design and operation differ significantly between the West and the Former Soviet Union. This report documents results obtained from commercially operating facilities of a design and operating style typical of the region of Belarus considered in this project.

The facility selected is a boiler at a sawmill that uses mildly contaminated wood as a feedstock. A slipstream from the flue gas of one boiler from this stream was redirected to a baghouse equipped with filters manufactured in the Former Soviet Union (but of western specification and design). The baghouse design and construction were completed under the direction of the Institute of Power Engineering Problems with funding and technical collaboration by Sandia National Laboratories. This document reports on the results of tests conducted at this facility that were supervised by Risø National Laboratory and in which all of the principal institutions played a role.

In comparison with western systems, boilers in the Former Soviet Union lack sophisticated control or particle cleanup systems. The selected boiler is typical in both regards. The boiler is hand fed and has a stationary grate. These features lead to large fluctuations in combustion conditions, particle loading, etc. It was anticipated that such fluctuations would compromise the quality of the data obtained from this investigation, and this anticipation proved well founded. High quality equipment and a careful experimental plan were both deployed during this investigation. In most cases, the features of the equipment and technique were compromised by boiler operation. However, the system was operated as carefully as possible and the results obtained are probably as high of quality as can be expected from such equipment.

Analyses of the samples have shown that sufficient information was obtained to characterise the filter performance. The filter efficiency was found to be around 99.5 % for $^{137}$Cs. This means that about 0.5 % of the caesium that is entrained in the flue gas prior to the filter passed through the filter and would be emitted from the stack. This is a significantly higher fraction of the material than would be released in similar western boilers with baghouse filters, but it is also significantly below the level that would pose a significant risk to surrounding individuals.

Calculations show that under the conditions given in the final report on Phase 1a of the project, the number of expected fatal cancers due to stack releases would be reduced from less than 2 per decade to less than one per century if furnaces were equipped with this type of particle collection system.

As the mentioned calculation was done considering highly contaminated wood fuel, the conclusion can be made that by applying a filter system and maintaining it, the radiation risk from the exhaust from the chimney is so low that it does not constitute a problem.

In addition to this, previous studies within the project have shown that:

1. The radiological risk to personnel operating the suggested type of biomass-fired power plant must be considered very low and below the recommended limit.
2. Harvesting and transporting processes in connection with fuel and ash handling can be planned in a way that would keep the doses below the limits.
3. The radioactive waste deposited in the recommended type of repositories will constitute a negligible risk to the population.

The goal of the project has been achieved, despite the problems with the stability. The results obtained were in agreement with the results expected, namely that it was possible to greatly reduce the exhaust of radiocaesium from the stack by applying a filter system based on baghouse technology.

The results of the whole project showed that it is possible to environmentally safely use forestry waste, forest litter and unclaimed biomass from radioactively contaminated forest for producing heat / power. This will enable a new production of significantly less contaminated wood at the harvested field.

Harvesting the contaminated forest and deep ploughing will reduce the dose to the population living in or near contaminated forest areas in two ways: external dose (from direct radiation) and internal dose (from intake of radioactive substances). Another environmental benefit in this context is that restricted forest areas can again be taken into use.

In Belarus, as much as 623 wood-fired boilers are currently operated in contaminated regions. These boilers utilise the woody waste from a number of local sawmills and have the total capacity of 25 MW. None of these are equipped with flue gas filtration systems, and consequently, their operation result in an annual release of about 1.5 thousand tonnes of airborne dust with an average activity of 30,000 Bq/kg. The project has shown that if these existing boilers were mounted with a filter of the tested type, the emission to the atmosphere of radioactive dust would be greatly reduced.

The project is linked to several projects previously accomplished under the auspices of programs of both the European Commission and the USA Department of Energy. A new TACIS program on addressing the clean-up and secondary medical effects of the Chernobyl disaster will disseminate the results of our project through a pilot information project in the CIS countries, which all have contaminated forests.

# Contents

# Preface

This report presents the results of a field test hosted at the Rechitza Drew Joint-Stock Sawmill in Rechitza, Belarus. This test is one of a series of experiments designed to determine the potential release of caesium from combustors designed as part of an environmental restoration project for forests contaminated by fallout from the Chernobyl accident. Previously, pilot-scale tests with fuels from Belarus were conducted under highly controlled laboratory conditions. Commercial-scale field tests with surrogate fuels were conducted in an operating boiler in the US, and models of combustion processes were completed. This field test was the first to include commercial-scale operation with contaminated fuels within Belarus.

The choice of a capture system type and its design is one of the most important tasks for future construction and operation of an industrial scale boiler that would safely utilise contaminated woody waste. Therefore, as a part of the pilot plant being built at IPEP to investigate all tasks related to combustion of radioactively contaminated wood fuel, the installation that includes a cyclone and a baghouse was constructed and then tested at the site of an existing boiler routinely fired with contaminated biomass. This boiler is at the site of the Rechitza Drew Joint Stock Sawmill. The management of the sawmill co-operated in providing access to the boiler and its operational parameters to allow this project to be completed. The boiler was inspected by members of the investigating team prior to the test. However, the boiler was shutdown for the weekend during the inspection.

The report serves as the final report from the project partners to the Danish Energy Agency of the Phase 1b in the Chernobyl Bio-energy project. RISØ carried out this phase in close collaboration with Institute of Power Engineering Problems, Sandia National Laboratories, and ELSAMPROJEKT. The Danish Energy Agency, the US Department of Energy (DOE), Wheelabrator Environmental System, Inc. (USA), and Belarus National Academy of Sciences, supported the work reported in this report.

# 1 Introduction

Vast areas of forestland in Belarus were severely contaminated by the Chernobyl accident. Many settlements, villages and towns are surrounded by the contaminated forests, which will often have a significant bearing on the external doses received by people living here. Further, it is generally popular, also for city people, to spend time in the forests, for instance for holidays, walks or collecting forest fruit (mushrooms and berries). Particularly the mushrooms accumulate relatively high levels of contaminants and the consumption of these is currently responsible for about one-fourth of the total radiation dose in the severely contaminated areas.

By removal of the contamination (i.e. vegetation and organic top soil) from the forest significant external and consumption doses can be averted. At the same time, the removed biomass may be applied to redress the Belarussian energy resource problem. By far, most of the energy consumed in Belarus is currently imported, and the option of applying biomass, which the country is very rich on, in energy production, is therefore highly attractive.

Firing with contaminated biomass removed in decontamination operations, however, demands careful analyses ensuring its radiological safety. In Phase 1a of the current project a number of studies were made of the general feasibility of the biomass power production scheme, focusing on factors such as radiological consequences, power plant design, biomass harvesting technologies and safe treatment and storage of the generated ash. These factors were addressed in a general sense on the basis of available data, and it was stressed that many influencing factors should be examined carefully in connection with analyses to evaluate the feasibility of the scheme in relation to specific sites and conditions.

Analyses of the radiological safety of the power plant are highly sensitive to the magnitude of contaminant stack releases. It was therefore deemed necessary to set up a series of tests to improve the estimate of the fraction of the contaminants in the biomass fuel that would be retained through the introduction of a baghouse filter. It was decided to carry out this test in Belarus, using contaminated biomass from the Belarussian forests, so as to make the test conditions as realistic as possible. The purpose of the test was not only to examine the filter efficiency, but also to measure the amount of radiocaesium per unit of mass in the slag and fly-ash relative to that in the fuel. Although the latter figures would be highly sensitive towards the actual firing conditions, the test would improve the understanding of the waste problem as well as the calculations of worker doses at the power plant. It is this test, which constitutes Phase 1b of the Chernobyl Bio-energy Project that is described in this report.

The main objective of the test was to investigate the capture and operational efficiency of the designed baghouse filter system under realistic operational conditions of an industrial boiler, the wood fuel of which being contaminated with $^{137}Cs$ and $^{90}Sr$ due to the Chernobyl Accident.

Further, the test is to be focused on full characterisation of wood fuel as well as boiler parameters, ashes, and flue gas before and after the filter system during the regular operation of the boiler. These data will help to quantify the extent of release of radioactive materials from the facility, and thus, to evaluate the actual radiological doses from an industrial boiler to its personnel and to the general public.

## 1.1 Description of the Rechitza Test Facility

The boiler selected for the tests is located at Rechitza Drew Sawmill, Rechitza City, ca. 260 km Southeast of Minsk and ca. 100 km North of Chernobyl. The boiler house was not equipped with any flue gas treatment system. It was therefore possible to introduce baghouse filter technology, as recommended for the actual energy generating power plant. Although the sawmill lies in a zone with a relatively low contamination level (40-200 kBq $m^{-2}$), the wood that is treated here comes from a large area, which includes much more severely contaminated spots. Within the closest 50 km there are areas with a contamination level of several MBq $m^{-2}$. For comparison the limit for relocation of people has been set at 1.5 MBq $m^{-2}$. According to the radiological survey carried out by the BelLesBumProm Concern each year, raw wood materials supplied to the Mill on average have a specific activity

of 120 Bq $kg^{-1}$. In 1998, additional measurements were carried out by IPEP. The maximum content of $^{137}Cs$ detected in wood chips and bottom slag was 162.8 Bq $kg^{-1}$ and 4703 Bq $kg^{-1}$, respectively.

**Description of the Boiler and its Operation**

The boiler was built more than 50 years ago by TAMPELLA in Finland. The boiler is a 9 tonnes $hr^{-1}$ steam boiler, producing steam at 230 °C and 10 bar. The combustion chamber is brick-built (i.e. non-cooled), and the wood is fired on a fixed grate. The boiler is intermittently fired with wood-residues from the sawmill. The combustion on the grate is seen on Figures 1.1 and 1.2 in situations when fuel has just been added and when all the fuel is burning, respectively. As can be seen on the photos the two combustion conditions are very different. Some key data is given in Table 1.1 below.

In modern boilers the combustion chamber is usually built using membrane wall construction. Such construction is essentially non-existent in Belarus but it provides for more compact and generally cooler combustors.

The specific objectives of the boiler investigation include:

- Characterise transient combustion conditions. Combustion conditions strongly impact data interpretation.
- Determine the potential impact of combustion conditions on Cs emissions.
- Measure the flue gas velocities and $O_2$.
- Compare the particulate flow in the flue gas channel to the particulate flow in the filter pilot plant to determine if the sampling to the filter plant is (at least by the mass) representative for the duct.
- Measure the fuel consumption and boiler efficiency indirectly by measuring steam and flue gas parameters

The largest share of air for the combustion comes from primary air (under fired air). Secondary air is provided near the fuel injection to support the flame.

*Table 1.1 Main parameters of boiler (as given by the sawmill staff)*

| | |
|---|---|
| Type | TAMPELLA (Finland) |
| Wood fuel moisture content | 60% |
| Wood fuel consumption (bulk volume) | 11 $m^3$/h |
| Size of fuel fractions | >30 mm (1-2%); 20-30 mm (10%)<br>10-20 mm (60%); <10 mm (30%) |
| Temperature in furnace | 1150$^oC$ |
| Excess air coefficient | 3.5* |
| Boiler heat area total | 300 $m^2$ |
| Steam pressure | 10 bar |
| Steam productivity | 9 ton/h |
| Steam temperature | 230$^oC$ |
| Economiser heat area | 511 $m^2$ |
| Economiser outlet water | 188$^oC$ |
| Economiser inlet water | 100$^oC$ |
| Flue gas temperature after economiser | 140$^oC$ |
| Bottom slag flow | 65-70 kg/h |
| Fly ash flow | 30-35 kg/h |
| Main design features | Fixed grate furnace of 13.5 $m^2$ -grate with 342 bars;<br>Vertical water-tubes boiler;<br>4 circulation tubes of 83 mm of diameter each;<br>176 boiling tubes of 83 mm in diameter each;<br>Boiler steam collector of 230 mm in diameter;<br>110 economiser tubes of 115 mm in diameter;<br>858 air-heater tubes of 70 mm in diameter;<br>Main centrifugal air fan of 20,100 $m^3$/hr;<br>Additional centrifugal air fan of 5,220 $m^3$/hr;<br>No flue gas treatment system |

** It should be noted that the Excess Air Coefficient, as given by the sawmill staff, is at variance with other related parameters.*

The fuel handling system consists of fuel receipt and transportation to fuel bunker near the boiler. Preplanning for this test included provisions to ensure that the fuel prepared from this test was not mixed with other fuel in the feed system, that the fuel could be accurately sampled, and that the fuel feed rate was as consistent and controlled as possible. The following observations and provisions were made:

1. The fuel received the latest is on the top of the cone of the fuel dropped in the fuel storage. When fuel is taken from the storage for transportation to the boiler, it is taken from the bottom of the cone. This limits the mixing with ”left over” fuel in the storage. However, some mixing is inevitable.
2. We considered to take the fuel samples at the conveyer belt, as this is usually where the most representative samples are taken. However, in this case it would not be easy both because the belt was constantly moving and the distance for transportation of the fuel between the storage and the boiler was very long. This would cause a long time delay. Therefore it was decided to take the fuel samples from the chute, immediately before the fuel is fed into the boiler.
3. There was significant concern regarding constant fuel feeding. The two primary concerns were manually operated, intermittently feeding onto the grate and no constant ash removal process. Both of these features create variations in combustion conditions. Plant personnel committed to devise means of providing fuel feeding conditions as uniform as possible.

The feeding system consisted of a chute filled with fuel, see Figure 1.3. When more fuel was needed the chute was opened, the moving/flowing of the chips and wood stickers was helped by manually pushing the fuel further, so it fell from the sludge to the grate, which was positioned approximately

1,5 metres below the exit of the chute. The combustion air was supposed to be closed off when feeding of the fuel took place, as a safety issue, but we did not notice that it took place.

*Figure 1.1 Wood chips on the grate right after fuel addition.*

*Figure 1.2 Burning wood chips on the grate.*

The pyrometer measurement positions in the boiler at the tests were approximately 2 and 5 metres above the grate, respectively. The lowest position is referred to as the ground level and the highest position is referred to as the 1st floor, because this was where we were working in the building to make the measurements.

Concerning the operation of the boiler there was a lack of control equipment apart from measurements of the steam pressure and steam flow. However as to the Rechitza plant, the purpose of the boiler was to get rid of the woody by-product from the sawmill, and to produce steam. The purpose has never been to produce flue gas at dedicated conditions for scientists. Therefore optimisation of the combustion has not been an issue in the boiler operation e.g. monitored by an $O_2$ measurement in the

flue gas, and therefore it took some time before the operation staff fully understood our needs/demands and how to satisfy these the best.

During the test more than three different fuels were used, as there were not sufficient amounts of one type purchased for the test available. The change between the different fuels caused operational problems for the operators, as the fuels had different combustion characteristics.

*Figure 1.3 The photo shows the chute where the fuel is stored right before feeding into the boiler.*

**Baghouse Design**

To secure low emission values a baghouse fitted with filter bags working according to the surface filtration principle.

The 2-stage aerosol capture system includes one inert-type cyclone filter coupled with two bag filters. The baghouse filter installation was designed and produced by "GIPRO-GasoOchistka" Public Corporation in co-operation with IPEP and Minsk Research & Design Institute of Thermal/Energy Facility Adjustment. A cyclone was installed before the baghouse in order to reduce the dust mass load to the last stage and eliminate possible access of sparkles to bag material. The system is designed to treat 2800-3000 $Nm^3$ of flue gas per hour.

This system is mounted in a by-pass circuit incorporated into the boiler flue gas outlet duct, thus treating about 15% of the total flue gas flow. The system is equipped with one induced fan with a productivity of 6000 $Nm^3\ h^{-1}$ and a pressure head of 5kPa. The baghouse has a filter regeneration system with pulse cleaning by air pressure jets. A warning alarm system was also installed. This was activated when the temperature and pressure drops in the baghouse exceed 200$^oC$ and 3 kPa respectively. The overall view of the installation is shown in Figure 1.4.

*Figure 1.4 Baghouse built over the underground flue gas duct. The boiler building to the left and the stack to the right.*

The functional scheme of the system is shown in Figure 1.5 and 1.6. Approximately 15% of exhaust gas are iso-kinetically taken from the flue gas outlet duct and directed to the by-pass circuit where the capture system is installed, first entering the cyclone.

The gas then leaves the cyclone and enters the filtration section and is evenly distributed among two separate modules assembled in parallel. A module has a number of filter bags each made in the form of cage (cartridge) which is fixed to a cell plate on the top of module. In each module the flue gas crosses the bags from outside to inside, and the aerosols deposit on the external surface of the bags.

Then the cleaned flue gas leaves the filtration section, returning back downstream of the boiler flue gas outlet duct, and ejects from the boiler stack. The flue gas flow along the by-pass circuit is controlled by the baghouse induced fan and gate-type slide valve (SG4, see Fig. 1.5).

The design of a baghouse filter includes the counter flow compressed air injection from the top cells through injection nozzles to clean the bags. The compressed air is provided from a manifold placed between the cell plate and top platform. This rapidly pulsing counter flow air injected into each bag, escapes it through the outer side thus shaking off the filter cake and blowing off the dust retained in pores of filter material. The cleaning cycle is provided without withholding filtering process. The frequency of cleaning cycles is governed for both modules by the relevant control device, setting up the time interval between the compressed air injections and the pressure drop.

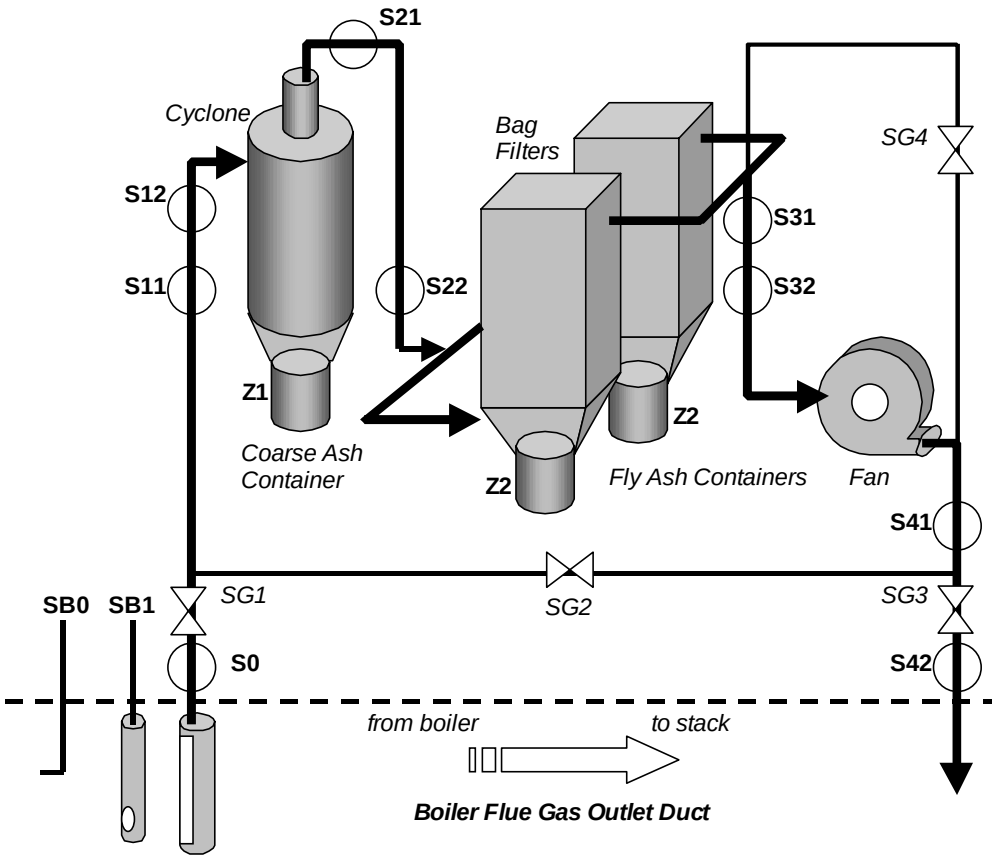


*Figure 1.5 Functional scheme of the by-pass circuit with test facility and sampling positions SB/S0/S1/S2/S3/S4:*

- **SB0, SB1** – Sampling probes positioned in the underground duct, see also Figure 1.6.
- **S**i – Sampling ports in the piping sections of the baghouse filter for extraction of total dust and size fractionated samples.
- **Z**i – Sampling ports for sampling of cyclone ashes (Z1) and filter ashes (Z2)
- **SG**i **–** Sliding gates for control of main flow and by-pass flow.

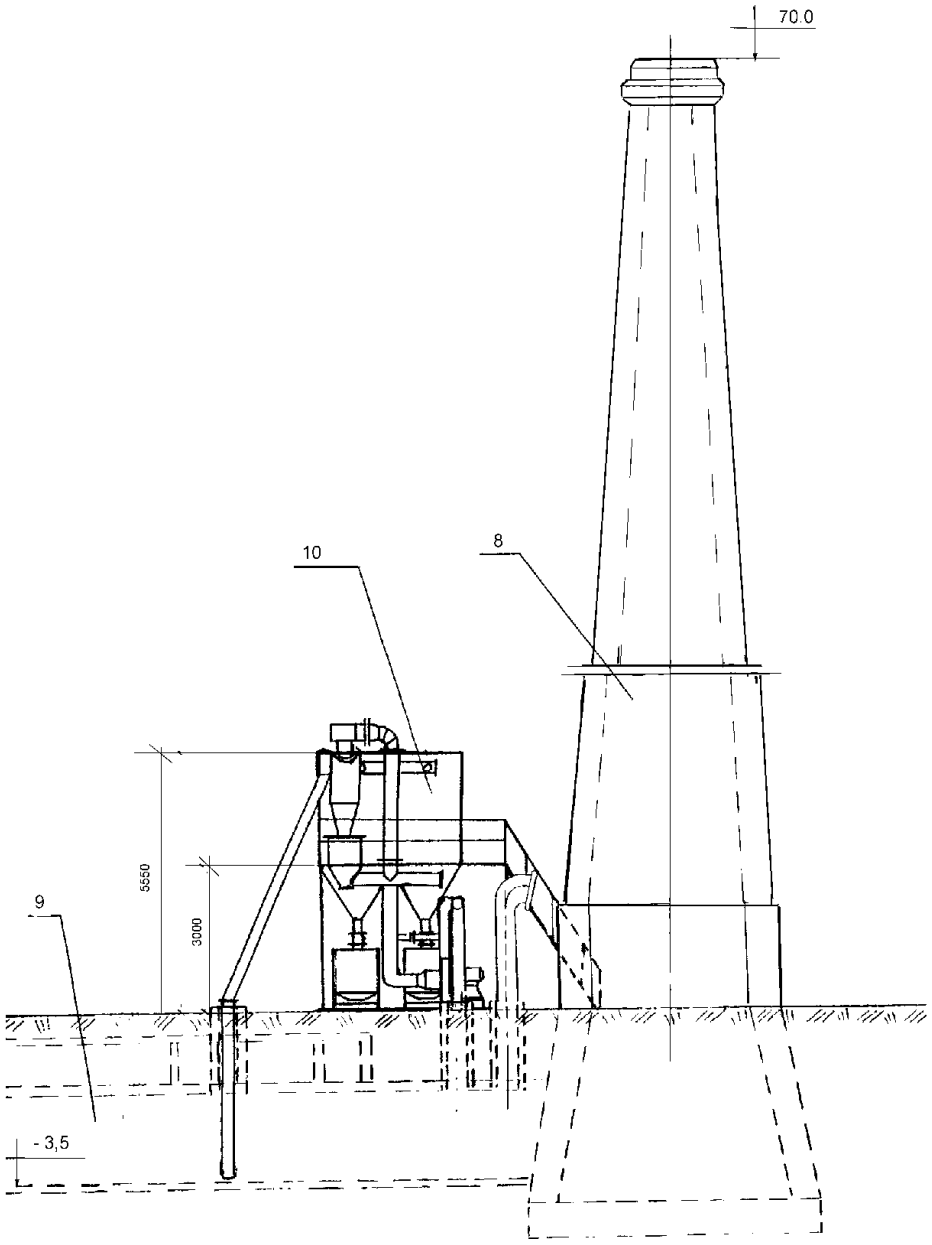


*Figure 1.6 Diagram of the filter test facility constructed at the Rechitza Drew sawmill. The main duct leading the flue gas to the stack is positioned underground. In the left side the inlet pipe from the underground duct leads the flue gas in to the cyclone. The cyclone can be seen in front of the two baghouses.*

# 2 Boiler Characteristics

## 2.1 Methods Applied

Peak combustor temperatures were determined using a suction pyrometer equipped with a type R thermocouple (Figure 2.1). A suction pyrometer is designed to measure gas temperatures with minimal heat radiation losses. Continuous temperature measurements were recorded over two intervals of about one hour each during the test. These temperatures were measured at two points above the combustor bed, as near to the flame as was possible given the limited access.

Combustor gas composition measurements were planned for the facility but could not be completed due to an instrument failure early in the test. However, IPEP recorded flue gas compositions from which some inferences can be made regarding combustor gas compositions.

The measurements in the duct (Figure 2.2) included (1) gas velocity, (2) oxygen content, and (3) fly ash loading. All measurements were made between the boiler and the bag house slipstream (position SB1, Figure 1.5). These measurements were made at several locations across the duct to determine spatial variations.

The velocities were determined using a calibrated Pitot tube. Gas samples were extracted to determine gas composition. Particle loading was determined by extractive sampling of particles on a ceramic fibre filter. All measurements were made at four horizontal and six vertical positions across the duct, for a total of 24 sampling locations. The gas velocity and composition measurements were made once during the three-day test. The particle loading measurements were made twice.

Steam temperature, pressure and flow rate and feed water temperature and pressure were determined three times during the last two days of the three-day test. In addition, the combustion air temperature and flue gas temperature and flow rate were determined. These measurements form the basis of the boiler efficiency and fuel feed rate determinations. Each of the three measurement campaigns lasted for more than 2 hours.

## 2.2 Results Achieved

The results are discussed in the following order

- Results from measurements in the boiler
- Results from measurements in the duct
- Indirect estimation of the boiler efficiency and the fuel consumption

*Figure 2.1 Measurement of the combustion temperature in the boiler using a suction pyrometer.*

*Figure 2.2 Measurement of the flow field and oxygen distribution in the duct. A similar method is used for sampling fly ash from the duct*

**Results from Measurements in the Boiler**

The following figures (Figures 2.3 and 2.4) show the temperature in the boiler measured at two different positions.

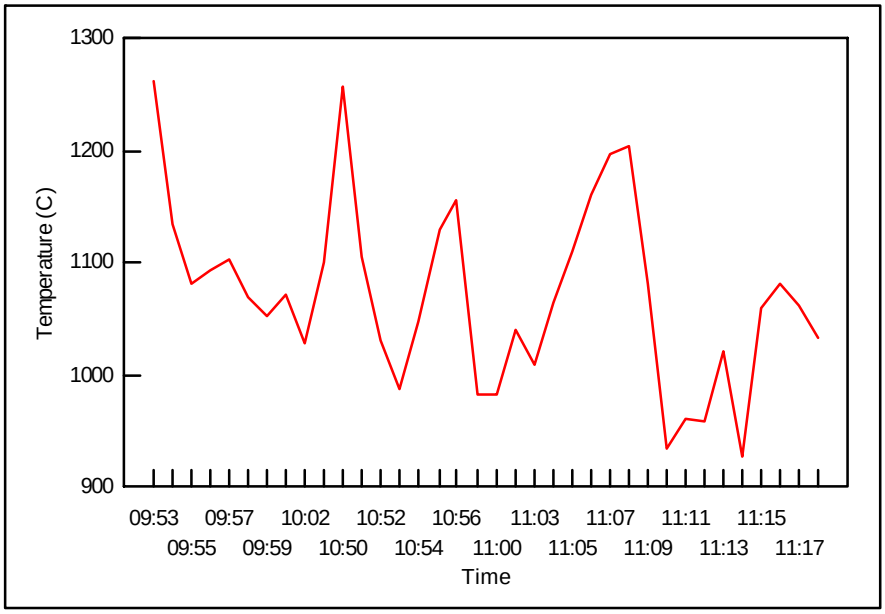


*Figure 2.3 Pyrometer measurement ground level, date 1999.06.18.*

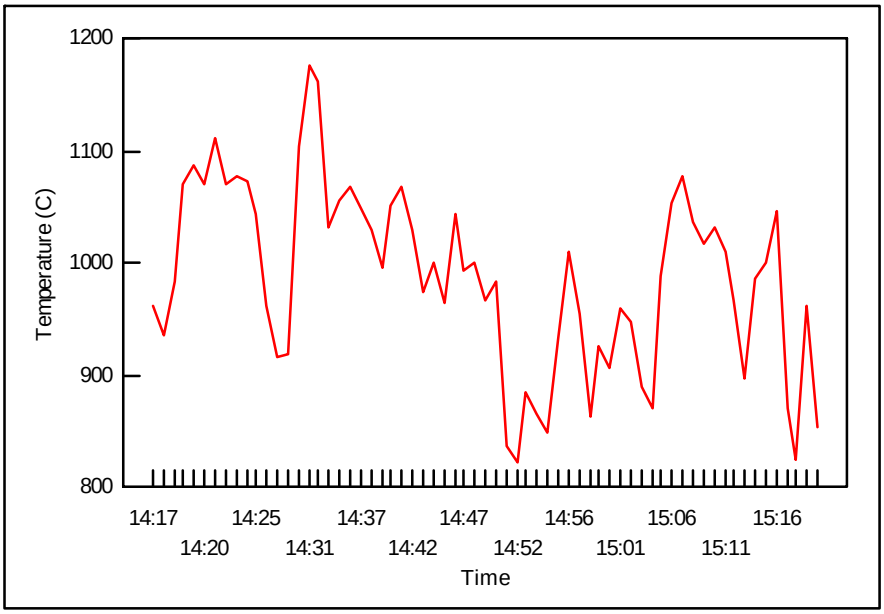


*Figure 2.4 Pyrometer measurement 1. floor, date 1999.06.18.*

**Results from Measurements in the Duct**

The parameters measured in the ducts were (1) the oxygen content, (2) the flow field, and (3) a representative sampling of fly ash. The results achieved are presented in the following, Figures 2.5 - 2.7 and Table 2.1.

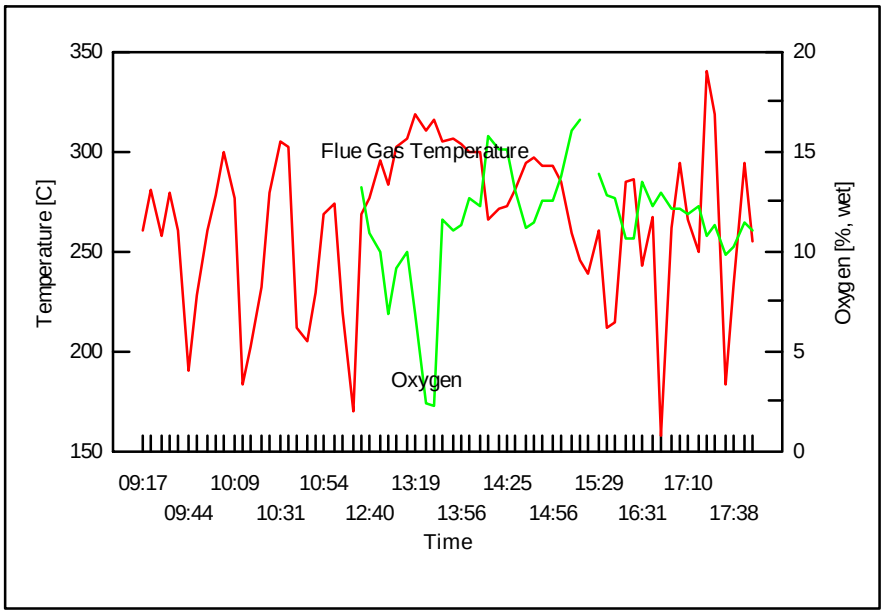


*Figure 2.5 Flue Gas temperature and Flue Gas oxygen content, date 1999.06.17*

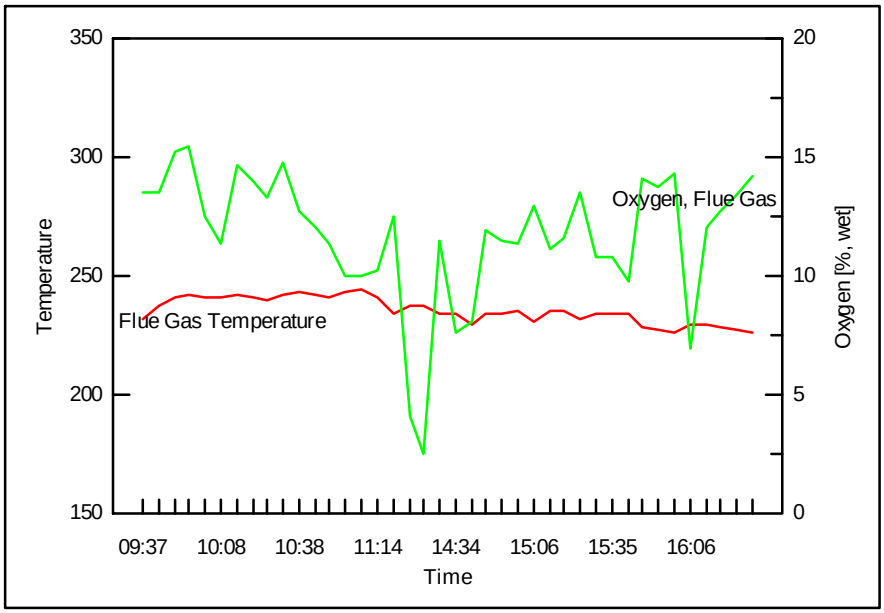


*Figure 2.6 Flue Gas temperature and Flue Gas oxygen content, date 1999.06.18*

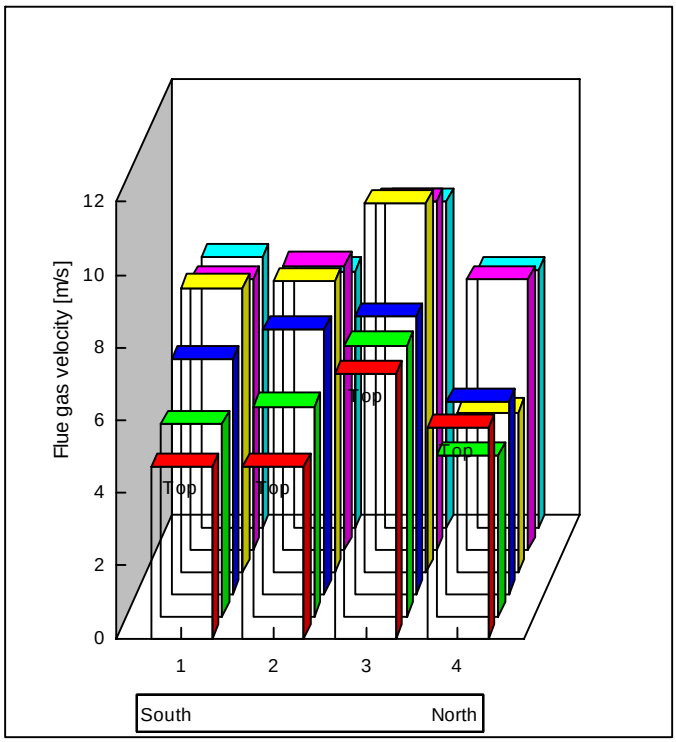


*Figure 2.7 Flue Gas velocity distribution in underground duct. diagrams.*

*Table 2.1 Result of dust measurement in underground duct.*

| Dust Measurement in underground duct. | | | |
|---|---|---|---|
| Date | | 1999.06.17 | 1999.06.17 |
| Time | | 09.17 – 11.07 | 16.30 – 17.40 |
| Flue Gas velocity, avg | [m/s] | 7,32 | 7,33 |
| Flue Gas flow, wet | [$Nm^3/h$] | 30663 | 30080 |
| Flue Gas flow, dry | [$Nm^3/h$] | 24266 | 25311 |
| Dust collected | [g] | 1,073 | 0,4761 |
| Dust concentration, wet | [$mg/Nm^3$] | 365 | 658 |
| Dust concentration, dry | [$mg/Nm^3$] | 461 | 783 |
| Dust flow in duct | [kg/h] | 11 | 20 |
| Isokinetic ratio | [%] | 14,3 | 10,9 |

**Indirect Estimation of the Boiler Efficiency and the Fuel Consumption**

The boiler efficiency is the ratio of energy in the steam to energy in the fuel and is a fundamental measure of boiler performance. The boiler efficiency may be determined either directly (based on fuel flow rate and steam flow rate) or indirectly. Since measurement of the solid fuel flow is often not very precise, the boiler efficiency is often most accurately determined by the indirect method. With this method the losses from the boiler are found and the efficiency is determined by difference. The largest losses from a boiler are generally, in order of decreasing importance, sensible heat in the flue gases, heat losses from the boiler, unburned carbon, and sensible heat losses associated with ash removal.

To determine the boiler efficiency by the indirect method, the following measurements are required: Flue gas flow rate, temperature and composition ($O_2$ and CO); combustion air temperature; fly ash carbon content; and parasitic losses from the boiler and ancillary equipment. Heat losses from the boiler were not directly measured but were determined using standard values for boiler of this size, type and fuel type.

Having found the boiler efficiency, the fuel flow may be calculated based on the known rate of steam production (Fig. 2.8 – 2.10). The results of evaluation of boiler efficiency are presented in Tables 2.2 – 2.4).

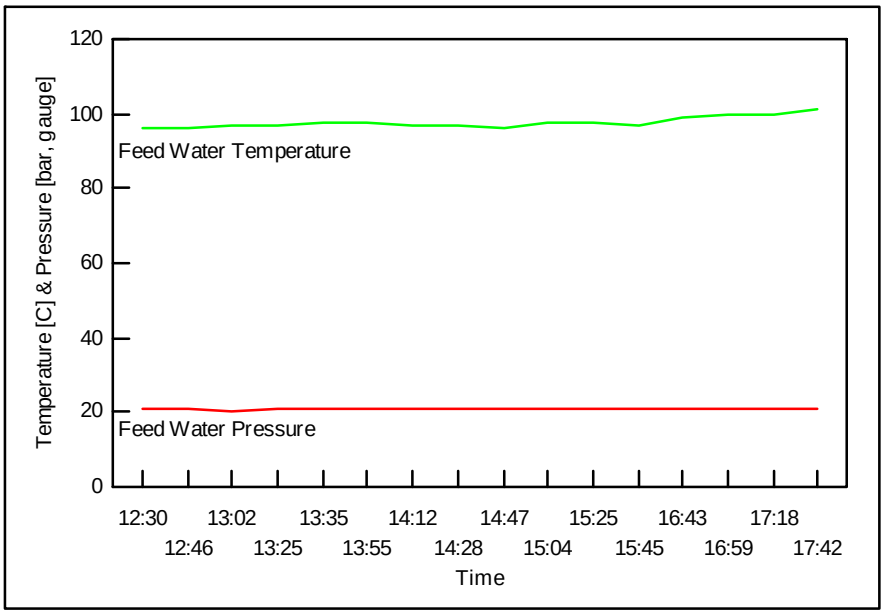


*Figure 2.8 Steam data from 1999.06.17.*

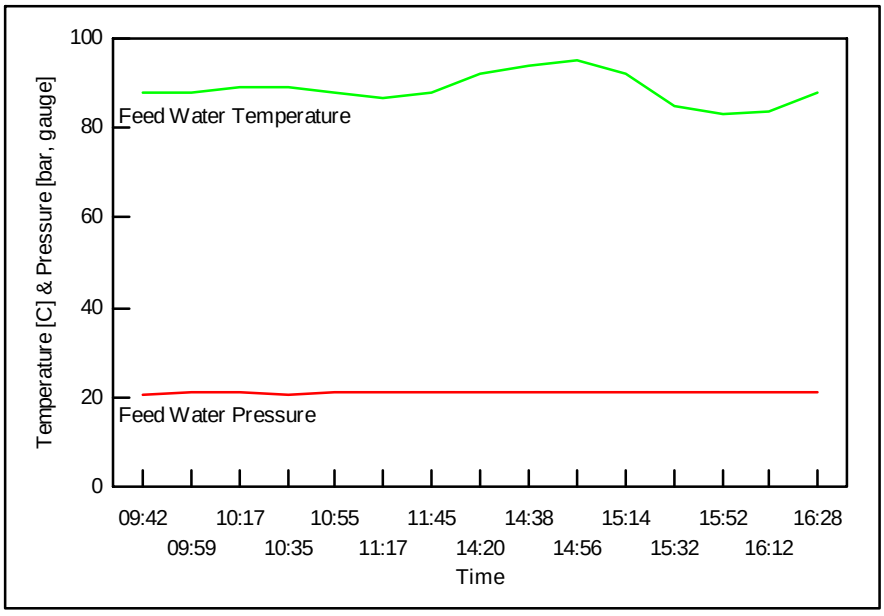


*Figure 2.9 Feed Water temperature and Feed Water pressure, date 1999.06.18.*

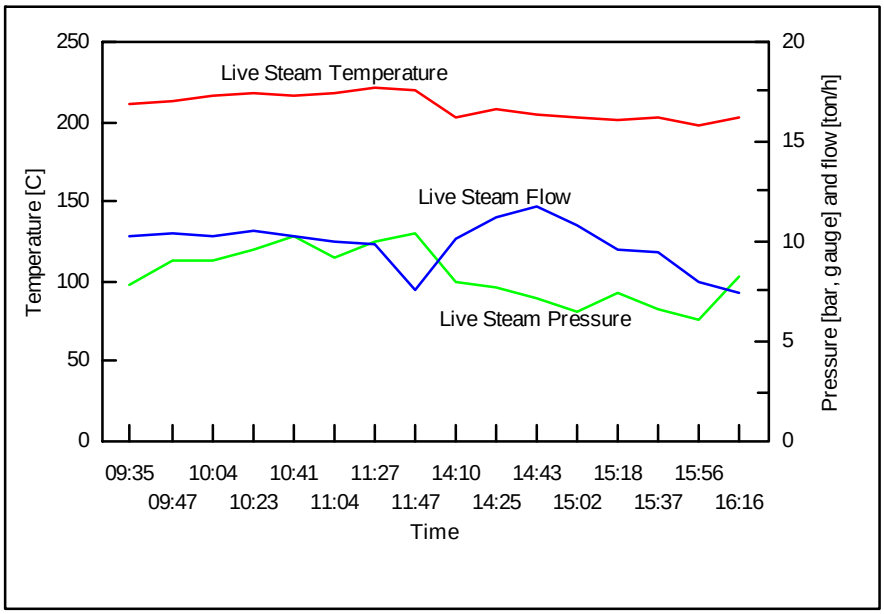


*Figure 2.10 Steam data from 1999.06.18.*

*Table 2.2 Results of boiler efficiency measurements on 1999.06.17 during the time interval 12.25-17.50.*

| **Fuel analysis** | | | **Specific air / flue gas quantity** | | | | |
|---|---|---|---|---|---|---|---|
| Hu | MJ/kg | 10,21 | Air, lhamda = 1 | kg/kg | 3,51 | Nm³/kg | 2,71 |
| C | | 29,3% | Air, lhamda > 1 | kg/kg | 9,56 | Nm³/kg | 7,40 |
| S | | -0,0% | Flue gas, dry, lhamda = 1 | kg/kg | 3,78 | Nm³/kg | 2,70 |
| H | | 3,1% | Flue gas, lhamda > 1 | kg/kg | 9,83 | Nm³/kg | 7,38 |
| N | | 0,6% | **Flue gas analysis** | | | | |
| O | | 22,2% | | **O2** | **CO2** | **H2O** | **N2** |
| W | | 43,1% | % Mass, wet | 13,1 | 10,0 | 8,5 | 67,2 |
| A | | 1,7% | % Mass, dry | 14,3 | 10,9 | 0,0 | 73,4 |
| Cl | | 0,0% | %Volume, wet | 11,5 | 6,4 | 13,3 | 68,7 |
| Total | | 100,0% | %Volume, dry | 13,3 | 7,4 | 0,0 | 79,2 |

| **Flue Gas / Air data:** | | | | | |
|---|---|---|---|---|---|
| Flue gas temperature | °C | 275,3 | Enthalpy flue gas | kJ/kg | 273,4 |
| Reference temperature | °C | 25 | Air temperature | °C | 35 |
| Lhamda | | 2,73 | Enthalpy Air | kJ/kg | 10,2 |
| Density, flue gas, wet | kg/Nm³ | 1,262 | Water content, Air | kg/kg dry air | 0,0207 |

| **Energy Balance** | | | | | | |
|---|---|---|---|---|---|---|
| Boiler effency | | 67,9% | | O2-% Air Preheater inlet | | 11,5% |
| Steam production | MJ/s | 7,0 | | O2-% Air Preheater outlet | | 11,5% |
| Energy, supplied | MJ/s | 10,3 | | Air Preheater leak | | -0,0% |
| Energy supplied (fuel) | MJ/s | 10,3 | | Air flow | kg/s | 9,6 |
| Energy supplied (other) | MJ/s | 0 | | Air flow | Nm³/s | 7,5 |
| Flue gas loss | MJ/s | 2,882 | 28,0% | Flue gas, wet | kg/s | 10,5 |
| Radiation | MJ/s | 0,086 | 0,8% | Flue gas, wet | Nm³/s | 8,4 |
| Slag | MJ/s | 0,228 | 2,2% | Flue gas, wet | m³/s | 16,8 |
| Fly ash | MJ/s | 0,108 | 1,0% | Fuel, gasified | kg/s | 0,981 |
| Total loss | MJ/s | 3,304 | 32,1% | Fuel, supplied | kg/s | 0,999 |
| Difference | | 0,000 | | | | |

| **Ash Balance:** | | | | | |
|---|---|---|---|---|---|
| Fly ash share | | 5,0% | Slag, water | | 0,0% |
| Slag share | | 95,0% | Slag, dry | kg/s | 0,022 |
| Unburnt, fly ash | | 80,0% | Slag, wet | kg/s | 0,022 |
| Unburnt slag | | 30,0% | Fly ash | kg/s | 0,004 |
| Slag temperature | °C | 500 | | | |

*Table 2.3 Results of boiler efficiency measurements on 1999.06.18 during the time interval 09.30-11.45.*

| **Fuel analysis** | | | **Specific air / flue gas quantity** | | | | |
|---|---|---|---|---|---|---|---|
| Hu | MJ/kg | 9,90 | Air, lhamda = 1 | kg/kg | 3,42 | Nm³/kg | 2,64 |
| C | | 28,6% | Air, lhamda > 1 | kg/kg | 11,15 | Nm³/kg | 8,62 |
| S | | -0,0% | Flue gas, dry, lhamda = 1 | kg/kg | 3,68 | Nm³/kg | 2,63 |
| H | | 3,1% | Flue gas, lhamda > 1 | kg/kg | 11,41 | Nm³/kg | 8,61 |
| N | | 0,5% | **Flue gas analysis** | | | | |
| O | | 21,6% | | **O2** | **CO2** | **H2O** | **N2** |
| W | | 44,5% | % Mass, wet | 14,5 | 8,5 | 7,7 | 68,1 |
| A | | 1,7% | % Mass, dry | 15,7 | 9,2 | 0,0 | 73,7 |
| Cl | | 0,0% | %Volume, wet | 12,8 | 5,4 | 12,1 | 69,6 |
| Total | | 100,0% | %Volume, dry | 14,6 | 6,2 | 0,0 | 79,2 |

| **Flue Gas / Air data:** | | | | | | |
|---|---|---|---|---|---|---|
| Flue gas temperature | °C | 240,9 | Enthalpy flue gas | | kJ/kg | 233,6 |
| Reference temperature | °C | 25 | Air temperature | | °C | 35 |
| Lhamda | | 3,26 | Enthalpy Air | | kJ/kg | 10,2 |
| Density, flue gas, wet | kg/Nm³ | 1,263 | Water content, Air | | kg/kg dry air | 0,0207 |
| **Energy Balance** | | | | | | |
| Boiler effency | | 67,6% | O2-% Air Preheater inlet | | | 12,8% |
| Steam production | MJ/s | 7,0 | O2-% Air Preheater outlet | | | 12,8% |
| Energy, supplied | MJ/s | 10,4 | Air Preheater leak | | | -0,0% |
| Energy supplied (fuel) | MJ/s | 10,4 | Air flow | | kg/s | 11,6 |
| Energy supplied (other) | MJ/s | 0 | Air flow | | Nm³/s | 9,1 |
| Flue gas loss | MJ/s | 2,956 28,3% | Flue gas, wet | | kg/s | 12,7 |
| Radiation | MJ/s | 0,086 0,8% | Flue gas, wet | | Nm³/s | 10,0 |
| Slag | MJ/s | 0,232 2,2% | Flue gas, wet | | m³/s | 18,9 |
| Fly ash | MJ/s | 0,110 1,1% | Fuel, gasified | | kg/s | 1,023 |
| Total loss | MJ/s | 3,384 32,4% | Fuel, supplied | | kg/s | 1,042 |
| Difference | | 0,000 | | | | |
| **Ash Balance:** | | | | | | |
| Fly ash share | | 5,0% | Slag, water | | 0,0% | |
| Slag share | | 95,0% | Slag, dry | kg/s | 0,022 | |
| Unburnt, fly ash | | 80,0% | Slag, wet | kg/s | 0,022 | |
| Unburnt slag | | 30,0% | Fly ash | kg/s | 0,004 | |
| Slag temperature | °C | 500 | | | | |

*Table 2.4 Results of boiler efficiency measurements on 1999.06.18 during the time interval 14.10-16.15.*

| **Fuel analysis** | | | **Specific air / flue gas quantity** | | | | | |
|---|---|---|---|---|---|---|---|---|
| Hu | MJ/kg | 10,39 | Air, lhamda = 1 | kg/kg | 3,56 | Nm³/kg | 2,75 |
| C | | 29,7% | Air, lhamda > 1 | kg/kg | 9,03 | Nm³/kg | 6,98 |
| S | | -0,0% | Flue gas, dry, lhamda = 1 | kg/kg | 3,83 | Nm³/kg | 2,73 |
| H | | 3,2% | Flue gas, lhamda > 1 | kg/kg | 9,31 | Nm³/kg | 6,97 |
| N | | 0,6% | **Flue gas analysis** | | | | |
| O | | 22,5% | | **O2** | **CO2** | **H2O** | **N2** |
| W | | 42,3% | % Mass, wet | 12,5 | 10,7 | 8,8 | 66,8 |
| A | | 1,7% | % Mass, dry | 13,7 | 11,7 | 0,0 | 73,3 |
| Cl | | 0,0% | %Volume, wet | 11,0 | 6,9 | 13,8 | 68,3 |
| Total | | 100,0% | %Volume, dry | 12,7 | 8,0 | 0,0 | 79,2 |

| **Flue Gas / Air data:** | | | | | | |
|---|---|---|---|---|---|---|
| Flue gas temperature | °C | 232,2 | Enthalpy flue gas | | kJ/kg | 225,8 |
| Reference temperature | °C | 25 | Air temperature | | °C | 35 |
| Lhamda | | 2,54 | Enthalpy Air | | kJ/kg | 10,2 |
| Density, flue gas, wet | kg/Nm³ | 1,262 | Water content, Air | | kg/kg dry air | 0,0207 |

| **Energy Balance** | | | | | | | |
|---|---|---|---|---|---|---|---|
| Boiler effency | | 74,2% | | O2-% Air Preheater inlet | | | 11,0% |
| Steam production | MJ/s | 6,9 | | O2-% Air Preheater outlet | | | 11,0% |
| Energy, supplied | MJ/s | 9,3 | | Air Preheater leak | | | -0,0% |
| Energy supplied (fuel) | MJ/s | 9,3 | | Air flow | | kg/s | 8,1 |
| Energy supplied (other) | MJ/s | 0 | | Air flow | | Nm³/s | 6,3 |
| Flue gas loss | MJ/s | 2,009 | 21,6% | Flue gas, wet | | kg/s | 8,9 |
| Radiation | MJ/s | 0,085 | 0,9% | Flue gas, wet | | Nm³/s | 7,0 |
| Slag | MJ/s | 0,206 | 2,2% | Flue gas, wet | | m³/s | 13,0 |
| Fly ash | MJ/s | 0,097 | 1,0% | Fuel, gasified | | kg/s | 0,872 |
| Total loss | MJ/s | 2,396 | 25,8% | Fuel, supplied | | kg/s | 0,888 |
| Difference | | 0,000 | | | | | |

| **Ash Balance:** | | | | | |
|---|---|---|---|---|---|
| Fly ash share | | 5,0% | Slag, water | | 0,0% |
| Slag share | | 95,0% | Slag, dry | kg/s | 0,020 |
| Unburnt, fly ash | | 80,0% | Slag, wet | kg/s | 0,020 |
| Unburnt slag | | 30,0% | Fly ash | kg/s | 0,004 |
| Slag temperature | °C | 500 | | | |

**Discussion**

Concerning the characterisation of the combustion conditions it is clear, that the combustion conditions were very unsteady, which is probably impossible to avoid when batch firing. The visual impression, that the smoke emitted were frequently very dark (black), suggests that there were frequently at least locally and probably globally reducing conditions in the boiler. During the investigation, the $O_2$ concentrations in the duct varied from 2% to 19%. During periods of relatively steady operation the $O_2$ was 12-14%. There is significant air leakage in this furnace (as is common with this style of furnace), making the estimation of furnace oxygen content difficult. However, stack opacity became high due to a sooty plume whenever the duct oxygen content dropped below 6-8 percent. The stack opacity was high every 10-25 minutes and remained high for 3-15 minutes or longer. Such heavy soothing is almost certainly associated with nearly globally reducing conditions in the furnace.

The varying stoichiometry of the furnace complicates data analysis for several reasons. First, the total concentration of particulate and especially of small particulate is heavily impacted by soot. The amount of soot produced from the transient reducing conditions almost certainly exceeds the amount of inorganic aerosol by orders of magnitude. Since we are interested in the caesium activity in the fly ash and especially in the aerosol, the varying amounts of soot have a large impact on the measurements. This can be partially corrected by correcting the aerosol activity measurements to a carbon-free basis.

A second impact of the varying stoichiometry is the impact on caesium chemistry. Reducing conditions generally promote the formation of volatile forms of alkali (caesium, potassium, and sodium). Therefore, the amount of caesium found in the aerosol was varying quite widely during the test, making data interpretation difficult. This is best corrected by limiting data evaluation to periods of time during which the combustion conditions were relatively constant and known. However, none of the samples sampled after the baghouse and few of those sampled before it were collected during periods of sufficiently constant operating conditions.

Finally, the varying conditions lead to significant changes in temperature and flow patterns in the boiler. Volatilisation of caesium is highly temperature dependent and formation of aerosol from vapour condenses depends on time. Therefore, the amount and size of the aerosol formed during the test could be expected to vary with combustion conditions. These trends will be difficult to unambiguously sort out of the data.

The measurements in the duct showed that the flue gas flow velocity was relatively constant, despite the variations in combustion conditions. The flue gas velocity in this boiler is determined almost entirely by the size of the stack and the temperature of the gases in it. Combustion conditions are relatively unimportant. Since the stack height is constant and the gas temperature is nearly constant, the velocities are also nearly constant.

The particulate flow in the flue gas duct was measured by the mass of the collected fly ash. The fly ash in the flue gas before the filter was measured in two separate tests to be 461 mg $Nm^{-3}$ (dry) and 783 mg $Nm^{-3}$ (dry). We do not have a quantitative measure of fly ash carbon content, but the visual indication is that it was very high. The fly ash was dark black, whereas fly ash from non-soothing boilers is grey. Comparisons of fly ash concentrations measured in the duct with those measured in the bag house inlet are not yet complete.

The boiler efficiency and fuel consumption were determined at three points during the test. The boiler thermal efficiencies (percentage of fuel energy absorbed by the steam) were 67,9%, 67,6% and 74,2%. These values are relatively constant, but significantly lower than commonly measured for western boilers, the latter varying from 85-92%. All efficiencies are determined on a lower heating value basis (as is the custom in Europe but not in the US). The lower efficiencies are associated with the older boiler design, significant air in leakage, high stack oxygen concentrations, and carbon losses in the form of unburned carbon in the fly ash. They are not particularly surprising for this style of boiler under these operating conditions. The average fuel consumptions during the three measurements were 0,999 kg/s, 1,042 kg/s and 0,888 kg/s, although these numbers are not particularly meaningful since the boiler was intermittently fed.

## 2.3 Evaluation of Stability Regimes

In order identify main sources of error and to find the time spans were the boiler was operating under reasonably stable conditions, suitable for data analysis, the main parameters of the boiler operation have been studied. The goal was to find time spans where different measurements could be compared.

The composition of flue gas (e.g. $O_2$ and CO content) was changing in a wide range that was caused by inconstancy of fuel load. Elsamprojekt and IPEP separately measured the oxygen concentration in different positions. Figure 2.11 compares the two data sets measured in the neighbouring ports SB0 and SB1. There is a good agreement between the data, especially during the more stable period on the 18/6, and both sets show considerable scatter.

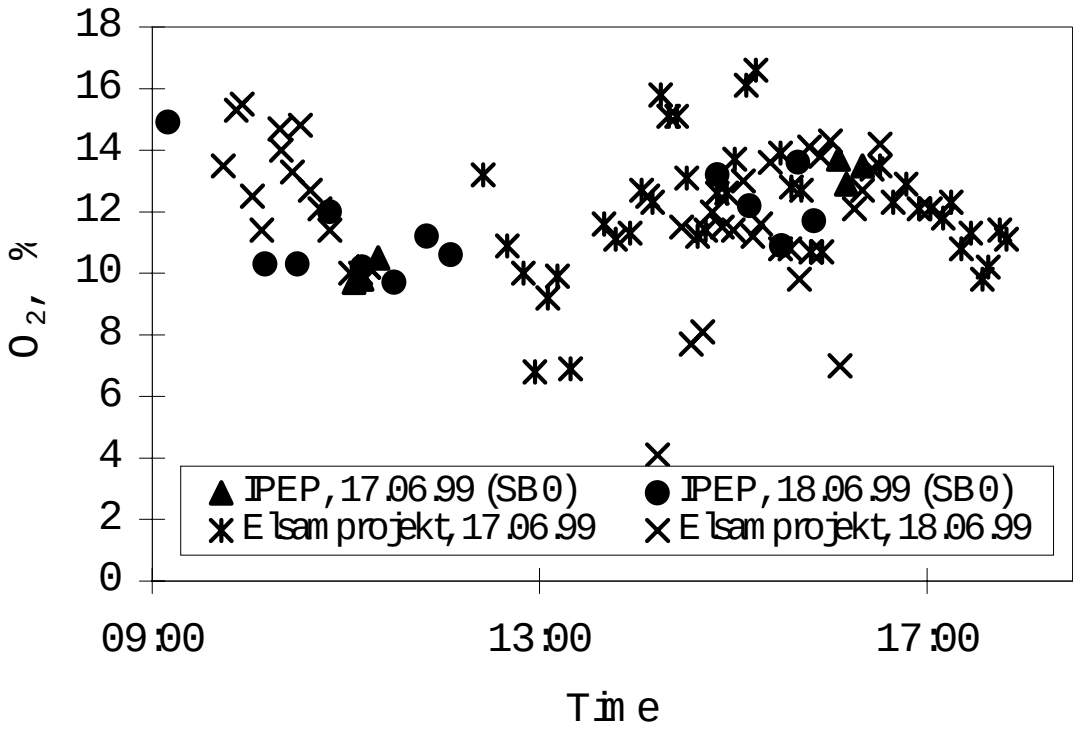


*Figure 2.11 $O_2$ measurements in the ports SB0 (IPEP) and SB1 (Elsamprojekt)*

It can be seen in Figure 2.12 that the oxygen concentration in flue gas at the point SB0 in the main duct right after furnace is lower than that at the capture system leaving point S42 located downstream. The difference is a factor of 1.3 - 1.4 that hardly belongs to measurement errors since the data obtained with different methods by Elsamprojekt and IPEP from close sampling points are in a good agreement (see Figure 2.11 above). This deviation is probably caused by a significant inflow of ambient air due to leaks in the furnace and underground flue gas duct. Some leaking would also occur during exchange of sampling probes in the pilot facility at the sampling port before S41. This is another error source and it clearly indicates that the dust samples obtained in the baghouse filter plant are not quantitatively correct for the exhaust conditions.

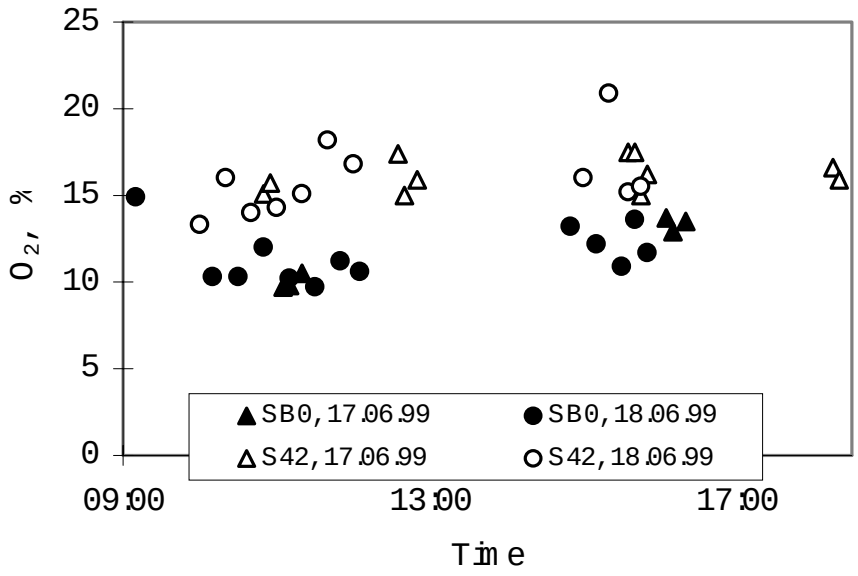


*Figure 2.12 $O_2$ Concentration in Different Sampling Ports measured by IPEP.*

The ratio between $O_2$ and CO illustrates the effect of the bulk firing together with the lack of control with the combustion air supply. The under-burning conditions lead to the complete oxidizing illustrated by the inverse relationship between the two gases seen in Figure 2.13.

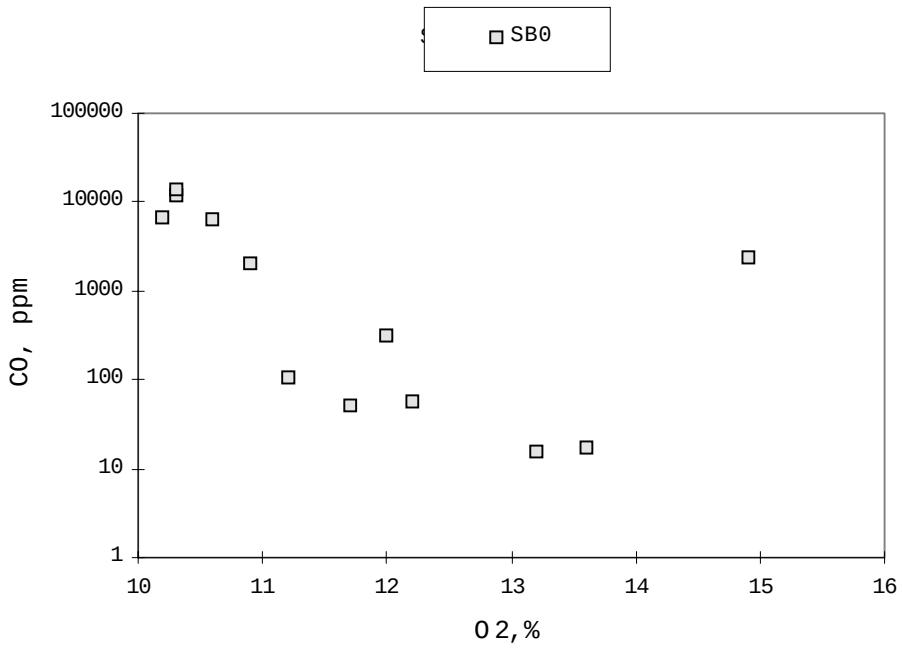


*Figure 2.13 $CO/O_2$ Ratio measured by IPEP.*

**Temperature in the Furnace Chamber**

The non-continuous fuel supply also caused of temperature variation in the furnace (from 800 to 1250°C) within short time intervals (Figure 2.14). We do not have this data from the entire measuring period and we can just conclude that the combustion conditions was very variable regarding temperature when we discuss the behaviour of Cs-137.

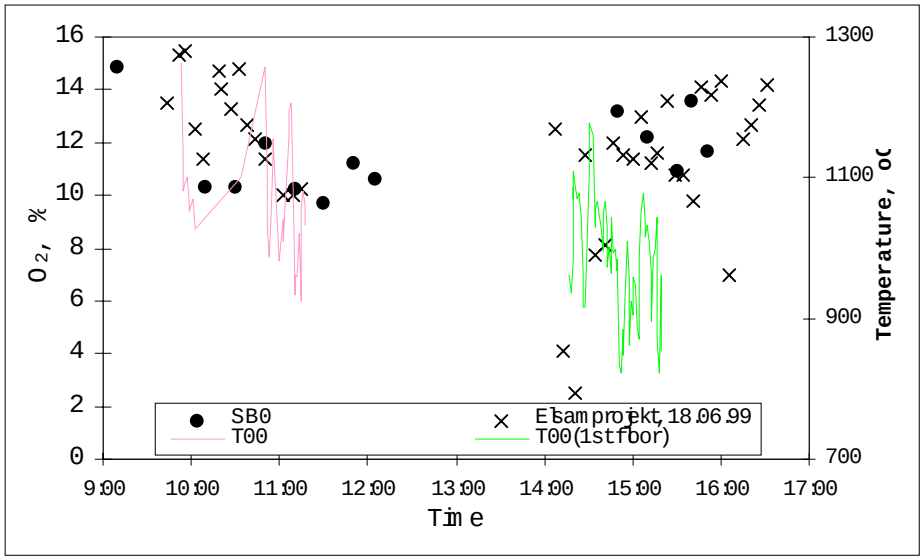


*Figure 2.14 Furnace Bed Temperature (T00) and $O_2$ Concentration in Flue Gas. 18.06.99*

The live steam output also reflected the variations in combustion conditions as illustrated in Figure 2.15 to Figure 2.17. Apparently the boiler was run at fuel load during 16/6, whereas it was running at reduced power during 17/6 and 18/6.

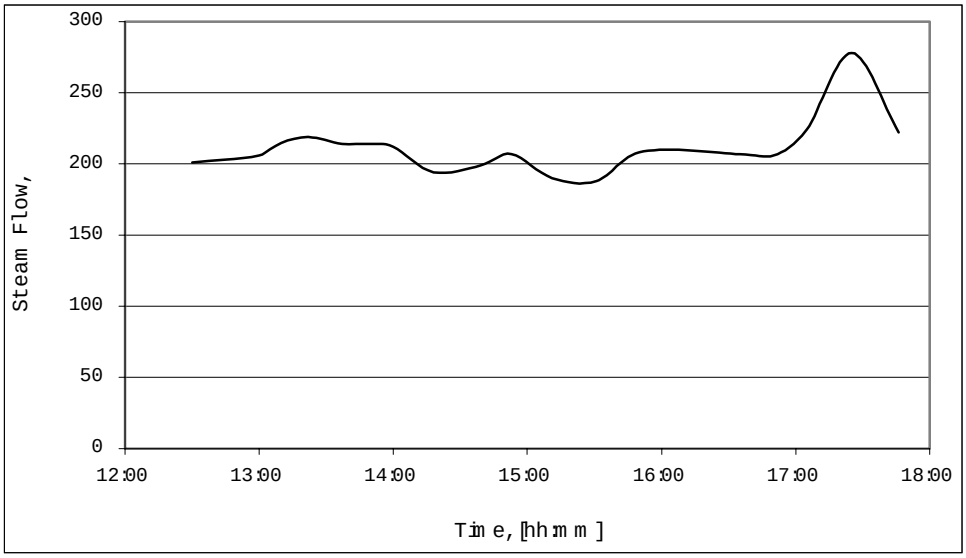


*Figure 2.15 Boiler Live Steam Flow (16.06.99)*

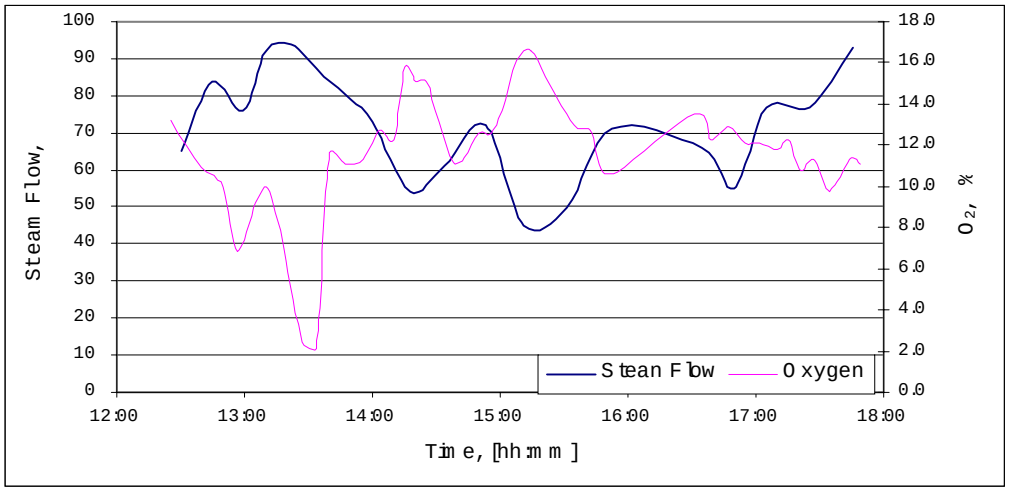


*Figure 2.16 Boiler Live Steam Flow and Flue Gas Oxygen Content (17.06.99)*

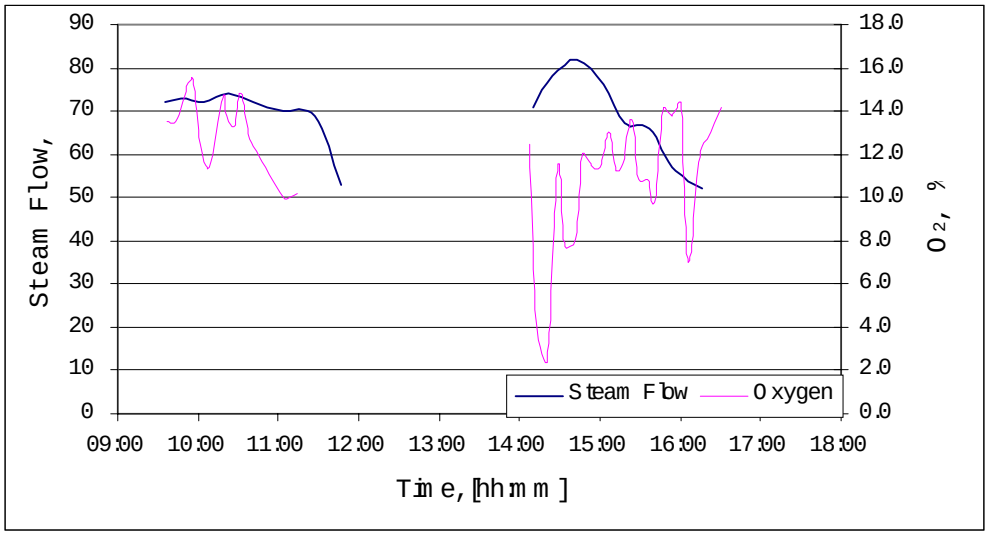


*Figure 2.17 Boiler Live Steam Flow and Flue Gas Oxygen Content (18.06.99)*

**Flue Gas Flow in Test Facility Duct**

The dynamic characteristics of flue gas flow between furnace and stack are mainly defined by the stack height, therefore the flue gas flow rate did not vary much, only within some 4%. However, as it follows from the results of traversing, the air velocity profile along the duct height is non-uniform. The flow velocity in the lower part of the duct channel, where the dust gravity is likely to be highest, is 40% higher than that in the upper part.

As for flue gas flow parameters inside the capture facility, they varied within a larger range (see Figure 2.18, Figure 2.19 and Figure 2.20). This was caused by periodic changes in the settings controlling the flow rate and alteration of intervals between the baghouse cleaning cycles.

Both these two circumstances lead to problems when trying to extract a iso-kinetic flue gas stream from the underground duct into the bag house facility. It can be concluded that over all the obtained data from the test facility is not representative for the exhaust flue gas. Single parameters, such as specific activity of sub-micron aerosol, will still be valid.

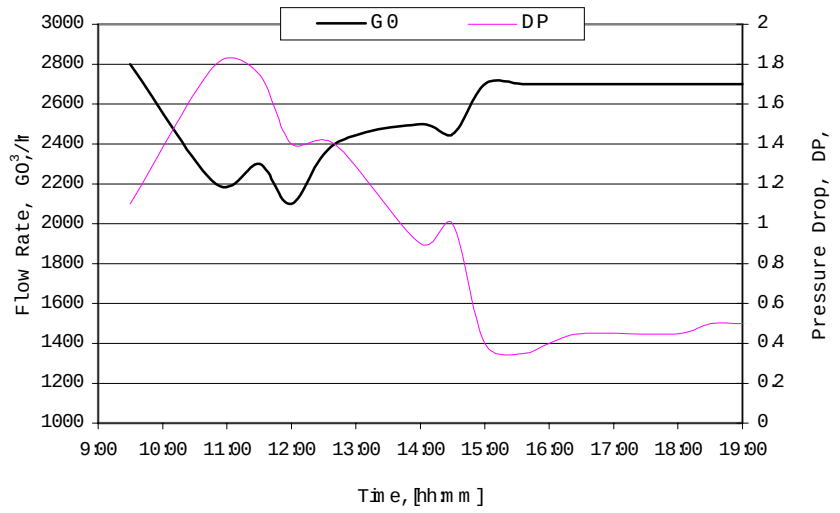


*Figure 2.18 Flue gas flow rate and pressure drop in test facility 16.06.99.*

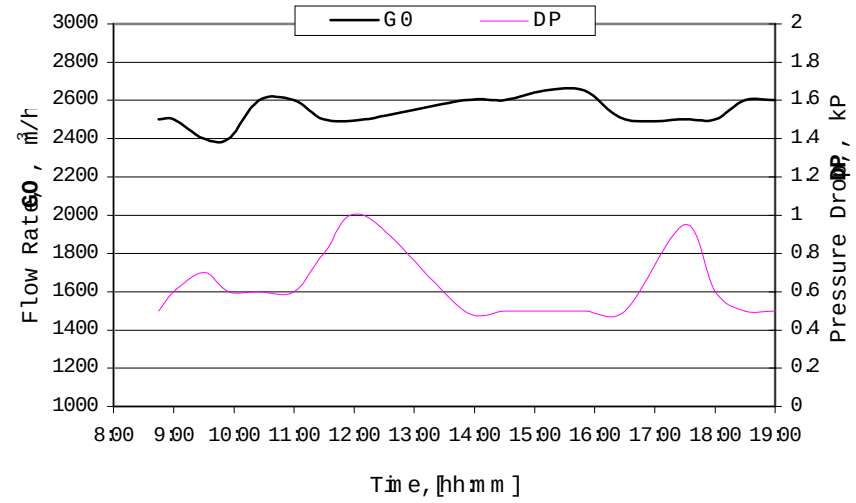


*Figure 2.19 Flue gas flow rate and pressure drop in test facility 17.06.99.*

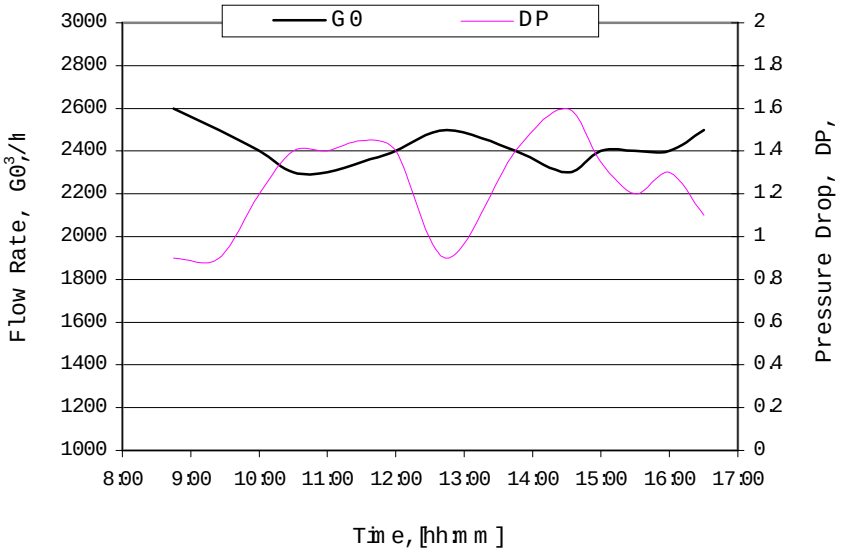


*Figure 2.20 Flue Gas flow rate and pressure drop in the test facility 18.06.99.*

**Conclusion on Stable Time Regimes**

From the above review of the test regimes and combustion conditions, one can make the following resume:

- Several time intervals can be singled out, within which the results of aerosol measurements and the samples taken from the duct can be referred to a conditionally stable regime of combustion. They are as follows:
- 12:00 to 13:30, 15:30 to 17:00, and 18:00 to 19:00
- 9:30 to 12:30, 14:00 to 16:30, and 17:00 to 19:00
- 9:30 to 11:30, and 15:00 to 18:00
- Uneven distribution of the flue gas velocity in the main duct does not allow us to consider the extraction of gas flow to the capture facility as sampling attributed to isokinetic conditions.
- The evident variations of oxidising conditions and inequality of fuel should cause sufficient differences of data on aerosols. First of all, it concerns the data on radioactivity since chemistry and volatility of caesium and its species are mainly defined by conditions in a furnace.

Instability of oxidising conditions was also a main reason of periodic sooting (every 5-10 minutes) and thus, was a source of the lesser-contaminated fine dust containing carbon. The latter distorts the picture of aerosol formation.

# 3 Baghouse Measurements

In order to test the capture efficiency of the baghouse facility a number of different measurements were carried out. Size specific number concentrations were measured together with total mass concentration and size distribution according to mass.

These measurements were made at different locations. The schematic position of the sampling ports fitted into the pipes is shown in figure 1.5. Based on these measurements it is possible to evaluate the performance of the cyclone and the baghouse filter as a function of particle size.

The first day of the test was spent preparing and testing equipment. Next day, Tuesday the 15/6, there were no measurements done at the baghouse due to problems with the fan. A full test programme was carried out over the last three days of the week.

## 3.1 Test Facility Run Procedure

The baghouse test facility was only operated during daytime and it had to be restarted every morning.

The by-pass circuit with filters was preheated prior to the actual test in order to exceed the dew point and avoid the condensation of flue gas moisture on filter bags. This is achieved by running the circulation fan with the SG2 sliding gate open and the SG1 / SG3 sliding gates closed (see Fig. 1.5). The idling circulation along the by-pass circuit is maintained until the temperature of air in the system exceeds 40$^{o}$C (app. 1 hour run).

Then the idling circulation flow is stopped by closing the SG2 sliding gate, and the SG1 / SG3 sliding gates are opened simultaneously. A fraction of the boiler flue gas stream (approx. 2,900 m$^3$ per hour) is iso-kinetically taken from the boiler outlet duct and enters the test facility.

In Table 3.1 an example of temperature parameters at three main points along the by-pass circuit during a start-up is given. For the log numbers of temperature measurement positions see Fig. 3.1.

*Table 3.1 Temperature variations along the duct of the test facility during the start-up procedure.*

| Procedure | Time | T11, °C | T12, °C | T13, °C |
|---|---|---|---|---|
| Idling circulation | 6:10 (start) | 20 | 20 | 20 |
| | 8:00 | 42 | 40 | 36 |
| Actual run | 8:22 (start) | 55 | 40 | 36 |
| | 8:25 | 68 | 53 | 50 |
| | 8:28 | 195 | 110 | 68 |
| | 8:30 | 198 | 127 | 75 |
| | 8:45 | 200 | 135 | 95 |

In the cyclone the coarse fly ash particles are selected from fine aerosols and accumulated in a hopper (container Z1, see Fig. 1.5) equipped with special sliding gate opening/damming the dust flow down to the container. The coarse dust from the container is manually emptied by the end of each day into the plastic bag for further analysis. Every day, during each test run, several samples were taken from a port positioned between the sliding gate and the container by a special sampling device for time-dependent characterisation of the ash.

After the cyclone, the flue gas enters the baghouse and the flue gas stream is evenly divided among the two modules. In the baghouse the fine dust is captured on the surface and pores of filter material, and the dust cake is then shaken off into two containers Z2 (see Fig. 1.5) by means of bypass cleaning cycles. The removed fine dust is collected in a container (one container for each module), and each container is emptied manually by the end of each day into a plastic bag for further analysis. Likewise the coarse dust sampling from a cyclone, during each day of the test, several samples were also taken by a special sampling device from a sampling port positioned between the sliding gate and the container.

After the baghouse, the clean flue gas returns back into the boiler outlet duct through a baghouse fan. The fan is equipped with a short circuit with a gate-type slide valve (SG4, see Fig. 1.5) in order to adjust the flow regime of the filter system to that of the boiler outlet duct thus providing a stable flue gas flow rate through the whole by-pass circuit.

When the test is completed the SG1 / SG3 sliding gates (see Fig. 1.5) are closed and the SG2 sliding gate is opened. The baghouse fan blowing with air for half an hour cleans out the by-pass circuit.

For characterisation of the test parameters and collection of data several ports for positioning the probes and measuring tools are arranged as shown in the schematic diagrams (Fig. 1.5 and Fig. 3.1).

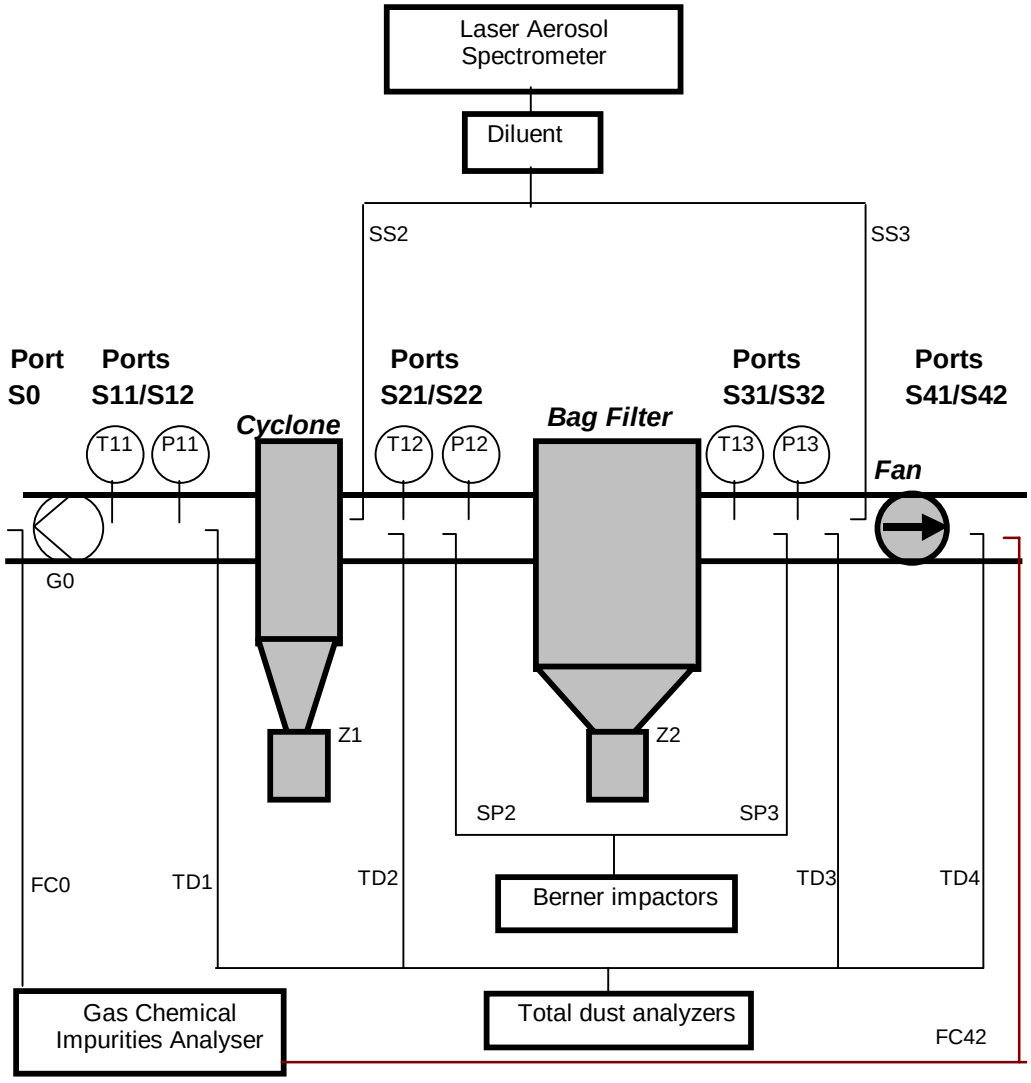


*Figure 3.1 Functional scheme of sampling and measurements at the baghouse test facility.*

**Plan for the Baghouse Test**

For detailed characterisation of the target mass flows the following measurements and samplings were provided by IPEP and RISØ, as listed in Tables 3.2 and 3.3 below.

*Table 3.2 List of the objects / parameters sampled / measured by IPEP*

| Log No | Target object | Sampling procedure in situ | Parameters to be analysed | Measurement procedure ↻ - in situ; 💻 - in lab |
|---|---|---|---|---|
| TD1<br>TD2<br>TD4<br>AD1<br>AD2<br>AD4 | Aerosols | From the S12/S21/S41 ports by iso-kinetic probes | Total Dust content before and after the cyclone, Total dust content after the baghouse, Activity of Dust samples | 💻<br>Dust mass flow, Elemental analysis, Granulometry, Radiological measurements of different fractions |
| SS2<br>SS3 | Aerosols | From the S22/S31 ports by iso-kinetic probe | Spectrum of particulate Size in micron and sub-micron diapason | ↻<br>On-line laser spectrum analysis of aerosols fractions |
| FCB0<br>FC0<br>FC42 | Flue gas | Performed by IPEP from the SB0/S0/S42 ports | Flue gas Chemistry ($O_2$, $CO_2$, CO, $NO_X$, $SO_X$) and moisture | ↻<br>On-line direct analysis of different gases and chemical impurities |
| ED0<br>ED1<br>ED2<br>ED3 | Radioactive exposure | | Exposure Dose rate from different compartments of the facility | ↻<br>Direct measurements of exposure dose rate by dosimeter |

*Table 3.3 List of the objects / parameters sampled / measured by RISØ*

| Log No | Target object | Sampling procedure in situ | Parameters to be fixed | Measurement procedure ↻ - in situ; 💻 - in lab |
|---|---|---|---|---|
| TD1<br>TD2<br>TD3<br>AD1<br>AD2<br>AD3 | Aerosols | From the S11/S22/S32 sampling points by iso-kinetic probe | Total Dust content before and after the cyclone, Total dust content after the baghouse, Activity of Dust samples | ↻<br>Dust mass flow<br>💻<br>Radiological measurements of fractions |
| SP1<br>SP2<br>SP3<br>AP1<br>AP2<br>AP3 | Aerosols | From the S11/S22/S31 sampling points by Berner impactor | Size distribution of Particulate in sub-micron diapason, Activity of each Particulate fraction | ↻<br>Mass fraction of particulate of different size<br>💻<br>Elemental analysis of different frac-tions, Radiological measurements of fractions, NAA analysis |

The general physical parameters of flue gas (flow rate, pressure, pressure drop, and temperature) that characterise the conditions of test performance in different positions of test facility are presented in Annex A.

## 3.2 Laser Measurements

The aerosol laser spectrometry was carried out continuously of flue gas iso-kinetically sampled from two ports (S22 and S31). These measurements made it possible to evaluate the variations with time in the content of fine aerosols in flue gas. It was found that the aerosol concentration varied significantly even within relatively short time intervals. This ties in with the visual impression of the intensity of smoke escaping from the stack. The smoke generally changed with 5-10 minutes intervals between being very dark and thick and being transparent. Therefore, representative measurements/samplings were performed only in a few test intervals when dust load variations were comparatively small. These results are presented in Tables 3.4 and 3.5. More detailed results of the laser spectrometer measurements are given in Appendix B.

Based on the measurements before and after the filter, filter efficiencies have been calculated as a function of particle size. These figures are presented in the bottom of the Tables 3.4 and 3.5. No distinct variation with particle size could be observed. It should be noted that the concentrations above 0.4 µm are based on relatively few counted particles and there is thus a significant uncertainty associated with these figures.

*Table 3.4 Particle number size distribution measured by consecutive aerosol laser spectrometry. Results are presented from two ports - before and after the baghouse filter. Data is from 17/6.*

| Time | 0,2-0,25 µm | 0,25-0,3 µm | 0,3-0,4 µm | 0,4-0,5 µm | 0,5-0,7 µm | 0,7-1,0 µm | 1,0-2,0 µm | Comments |
|---|---|---|---|---|---|---|---|---|
| **17.06.99, Port log. # S22**, $N_2$ dilution ratio = 135; Volume of probe = 50 $cm^3$ | | | | | | | | |
| 9:49 | 96660 | 34965 | 11475 | 7020 | 945 | 675 | 0 | Gray smoke |
| 9:51 | 108405 | 38340 | 12555 | 7965 | 405 | 405 | 270 | |
| 9:52 | 88560 | 31995 | 13905 | 8370 | 1215 | 675 | 270 | |
| 9:53 | 110160 | 33075 | 13230 | 11475 | 1080 | 540 | 0 | |
| **Avrg.** | **100946** | **34594** | **12791** | **8708** | **911** | **574** | **135** | |
| **17.06.99, Port log. # S31**, $N_2$ dilution ratio = 4.5; Volume of probe = 50 $cm^3$ | | | | | | | | |
| 10:12 | 6935 | 2421 | 743 | 369 | 41 | 59 | 36 | Gray smoke |
| 10:15 | 6597 | 1994 | 594 | 203 | 9 | 0 | 9 | |
| 10:16 | 6512 | 2034 | 657 | 324 | 14 | 27 | 9 | |
| 10:17 | 6804 | 2462 | 639 | 338 | 36 | 23 | 14 | |
| **Avrg.** | **6712** | **2228** | **658** | **309** | **25** | **27** | **17** | |
| **Filter eff.** | **93,4%** | **93,6%** | **94,9%** | **96,5%** | **97,3%** | **95.3%** | **87.4%** | |

*Table 3.5 Particle number size distribution measured by consecutive aerosol laser spectrometry. Results are presented from two ports - before and after the baghouse filter. Data from is from 18/6.*

| Time | 0,2-0,25 µm | 0,25-0,3 µm | 0,3-0,4 µm | 0,4-0,5 µm | 0,5-0,7 µm | 0,7-1,0 µm | 1,0-2,0 µm | Comments |
|---|---|---|---|---|---|---|---|---|
| **18.06.99, Port log. # S31**, $N_2$ dilution ratio = 4.5; Volume of probe = 50 $cm^3$ | | | | | | | | |
| 12:53 | 927 | 68 | 23 | 5 | 5 | 5 | 0 | Smoke is |
| 12:54 | 635 | 36 | 9 | 9 | 0 | 0 | 0 | almost |
| 12:56 | 450 | 14 | 5 | 0 | 0 | 0 | 0 | transparent |
| 12:57 | 1040 | 131 | 18 | 14 | 5 | 0 | 0 | |
| **Avrg.** | **763** | **62** | **14** | **7** | **3** | **1** | **0** | |
| **18.06.99, Port log. # S22**, $N_2$ dilution ratio = 9.0; Volume of probe = 50 $cm^3$ | | | | | | | | |
| 13:02 | 144000 | 8235 | 1773 | 1404 | 369 | 414 | 99 | Smoke is |
| 13:04 | 179703 | 8136 | 1782 | 1836 | 594 | 441 | 117 | almost |
| 13:05 | 183483 | 8307 | 2079 | 1953 | 387 | 279 | 36 | transparent |
| 13:06 | 241857 | 9252 | 2223 | 2250 | 423 | 432 | 135 | |
| **Avrg.** | **187261** | **8483** | **1964** | **1861** | **443** | **392** | **97** | |
| **Filter efficiency** | **99,6%** | **99,3%** | **99,3%** | **99,6%** | **99,3%** | **99,7%** | **100%** | |

## 3.3 Total Dust Measurements by Risø

### Measuring Equipment

Risoe has assembled a portable system for total dust measurements according to the German standard VDI 2066 part 7. Figure 3.2 below shows the complete system for the sampling excluding the measuring head, which is shown in Figure 3.3. From the inlet the system features a cooling spiral, a water separator, a drying column, a pump with a bypass valve for flow control, a flow meter, a gas meter and a thermometer mounted with the gas meter for correction to normal cubic metres sampled. The measuring head for 'in-pipe' sampling uses 5-cm Ø quartz fibre filter paper for filtration. The nozzle is exchangeable with inlet diameters from 6 mm to 20 mm. This enables a coarse regulation of the inlet flow. The fine-tuning, ensuring iso-kinetic sampling is done by regulation of the bypass valve at the suction pump.

This system had prior to the test in Belarus been tested at Danish power plants, with good results both concerning durability and quality of results. That is, two systems are available for simultaneous sampling at two locations, e.g. before and after a filter.

*Figure 3.2 Complete mount for total dust measurements. On the left the cooling circuit with a water separator underneath. In the centre a drying column.*

*Figure 3.3 Measuring head/filter holder for total dust measurements. The filter holder uses 5 cm Ø quartz fibre filters. The sampling aperture can be adjusted by exchanging the front end of the filter house*

**Results of the Dust Measurements**

In total 29 total dust measurements were made. The details of the measurements are listed in Table 3.7 together with the results of the mass and $^{137}$Cs activity analysis. Measuring locations:

- S1 Before the cyclone
- S2 After the cyclone before the baghouse
- S3 After the baghouse

Hereafter, the suffixes 'L' or 'R' indicate that samples were taken from the left or right port. 'LR' means that traversing was performed in both ports.

All TD mass concentration results are stated for dry air at 20 $^{o}$C, but they are not corrected for oxygen content.

The first measurement on Monday 14/6 was an initial test. There were no measurements on Tuesday the 15/6.

Due to the very unstable flue gas conditions traversing was stopped on 18/6 and thus only one sampling port is listed as a position for sampling carried out on this day. This simplification enabled us to increase the number of measurements done this day. In general, larger variation in TD was observed

making it very difficult to compare consecutive measurements and undermining any positive benefit of traversing.

In general there were big variations in both mass and activity concentrations. This was also observed in the data on particulate concentration obtained with laser spectrometry. The mass concentration varied on a small time scale - an order of magnitude in 10 minutes. The variations in the activity concentration were smaller, but it is unfortunate that the highest activities were achieved early during the test period where fewer measurements were made.

*Table 3.6 Review of the Total Dust measurements made by Risø. All mass and activity concentrations are given for a temperature of 20 $^{o}$C and dry air.*

| | | | Duration | Mass | Volume | Mass /volume | Activity | | Activity /mass | Activity /volume |
|---|---|---|---|---|---|---|---|---|---|---|
| ID | Position | Start time | [minutes] | [mg] | [m$^3$] | [mg/m$^3$] | [Bq] | ``+/- | [Bq/g] | [Bq/m$^3$] |
| TD01 | S2-L | 14.06-17:30 | 5 | 33.53 | 0.085 | 396 | 0.20 | 0.013 | 6 | 2.39 |
| TD02 | S2-L | 16.06-10:17 | 4 | 46.34 | 0.097 | 480 | 0.29 | 0.013 | 6 | 2.99 |
| TD03 | S1-LR | 16.06-12:12 | 8 | 48.84 | 0.061 | 795 | 0.53 | 0.024 | 11 | 8.71 |
| TD04 | S2-LR | 16.06-12:13 | 8 | 56.33 | 0.104 | 538 | 0.72 | 0.029 | 13 | 6.83 |
| TD05 | S3-LR | 16.06-14:36 | 240 | 2.60 | 1.966 | 1.3 | 0.066 | 0.009 | 25 | 0.033 |
| TD07 | S2-L | 16.06-15:09 | 8 | 7.16 | 0.131 | 54.5 | 0.26 | 0.017 | 36 | 1.95 |
| TD08 | S2-R | 16.06-16:49 | 16 | 7.88 | 0.278 | 28.3 | 0.38 | 0.021 | 48 | 1.36 |
| TD09 | S1-LR | 17.06-09:59 | 4 | 21.97 | 0.067 | 327 | 0.18 | 0.010 | 8 | 2.67 |
| TD10 | S3-LR | 17.06-08:37 | 240 | 1.67 | 3.410 | 0.49 | 0.029 | 0.008 | 17 | 0.01 |
| TD11 | S2-LR | 17.06-10:03 | 8 | 3.62 | 0.185 | 19.6 | 0.12 | 0.014 | 32 | 0.63 |
| TD12 | S2-LR | 17.06-12:01 | 4 | 13.68 | 0.065 | 211 | 0.10 | 0.014 | 7 | 1.55 |
| TD13 | S2-LR | 17.06-15:14 | 8 | 4.48 | 0.151 | 29.7 | 0.24 | 0.019 | 55 | 1.62 |
| TD14 | S3-LR | 17.06-14:13 | 180 | 2.53 | 2.922 | 0.87 | 0.061 | 0.009 | 24 | 0.021 |
| TD15 | S1-LR | 17.06-16:29 | 8 | 17.02 | 0.133 | 128 | 0.20 | 0.014 | 12 | 1.53 |
| TD16 | S2-LR | 17.06-17:30 | 4 | 29.37 | 0.096 | 308 | 0.25 | 0.014 | 8 | 2.58 |
| TD17 | S1-L | 18.06-09:05 | 4 | 2.79 | 0.067 | 42 | 0.099 | 0.0098 | 35 | 1.47 |
| TD18 | S2-L | 18.06-09:05 | 4 | 2.70 | 0.064 | 42 | 0.120 | 0.012 | 44 | 1.89 |
| TD19 | S2-L | 18.06-11:35 | 8 | 9.69 | 0.132 | 74 | 0.20 | 0.016 | 20 | 1.48 |
| TD20 | S1-L | 18.06-09:40 | 4 | 7.06 | 0.067 | 106 | 0.083 | 0.014 | 12 | 1.24 |
| TD21 | S1-L | 18.06-10:05 | 5 | 19.60 | 0.064 | 304 | 0.12 | 0.016 | 6 | 1.93 |
| TD22 | S1-L | 18.06-10:23 | 20 | 57.62 | 0.364 | 158 | 0.44 | 0.04 | 8 | 1.19 |
| TD23 | S1-L | 18.06-11:35 | 8 | 8.14 | 0.130 | 63 | 0.157 | 0.0194 | 19 | 1.21 |
| TD24 | S2-L | 18.06-15:22 | 12 | 17.67 | 0.174 | 102 | 0.26 | 0.0189 | 15 | 1.49 |
| TD26 | S3-L | 18.06-14:36 | 120 | 0.32 | 1.802 | 0.18 | 0.017 | 0.0051 | 51 | 0.01 |
| TD27 | S2 | 18.06-14:46 | 12 | 16.81 | 0.1835 | 91.6 | 0.269 | 0.0166 | 16 | 1.47 |
| TD28 | S2-L | 18.06-15:45 | 12 | 6.47 | 0.1958 | 33.0 | 0.321 | 0.0181 | 50 | 1.64 |
| TD29 | S2-L | 18.06-16:14 | 12 | 7.32 | 0.1954 | 37.5 | 0.42 | 0.0224 | 57 | 2.15 |

When TD measurements made at the same time before and after the cyclone (TD17 *vs*. TD18, and TD19 *vs*. TD23) are compared an increase in mass load is observed. This is of course peculiar. However, the increase is not significant. But it repeats itself for the activity measurements that show a 15 to 29 % increase after the cyclone. This is an increase of three standard deviations on the activity measurements. Another set of measurements shows a reduction of 32% (TD03 *vs*. TD04). This is in better agreement with the amount of ashes collected at the cyclone and below the baghouse filters. Here the reduction is similar for the $^{137}$Cs activity measurements as well.

By comparing the samples made at positions S1 and S2 with the samples from S3 some estimates can be made of the filter efficiency. These calculations are presented in Table 3.7. Please note that Ratio2 and Ratio3 are based on measurements both before and after the cyclone, whereas Ratio1 and Ratio4 give the 'pure' filter efficiency. It can be seen that Ratio1 gives a comparatively low filter efficiency. The explanation could simply be that the two samples taken before the filter are not representative for the input as they only cover 10 % of the sampling time after the filter. In addition, both the TD07 and TD08 measurements were performed within the time interval of very unstable combustion

conditions in the furnace. In general, the filter efficiency calculation gave a stable result both when based on mass and activity measurements.

*Table 3.7 Calculations of filter efficiency for four sets of filter samples. The second and third columns show the ID of the after filter sample and the pre-filter samples, respectively. The fourth column shows the total sample collection time before and after the filter in minutes.*

| ID | After filter sample | Before filter Samples | Fraction covered | Filter efficiency, % | |
|---|---|---|---|---|---|
| | | | | Mass | Activity |
| Ratio1 | TD05 | TD07, TD08; both from S2 | 24/240 | 96.4 | 97.9 |
| Ratio2 | TD10 | TD09 (from S1), TD11, TD12; both S2 | 16/240 | 99.7 | 99.5 |
| Ratio3 | TD14 | TD13 (S2), TD15(S1), TD16(S2) | 20/180 | 99.4 | 99.6 |
| Ratio4 | TD26 | TD24, TD27, TD28, TD29; all S2 | 48/120 | 99.7 | 99.4 |

As it was realised already during the tests that the dust concentrations were very variable, longer sample times before the filter were applied on the last day of the tests. Ratio4 probably gives the best estimate of the filter efficiency as the sampling before the filter covers 40 % of the after filter sampling time. The dust levels before and after the filter are illustrated in Figure 3.5. Between the TD measurements before the filter a number of impactor measurements were made. These are included in a new figure in the section dealing with the impactor measurements.

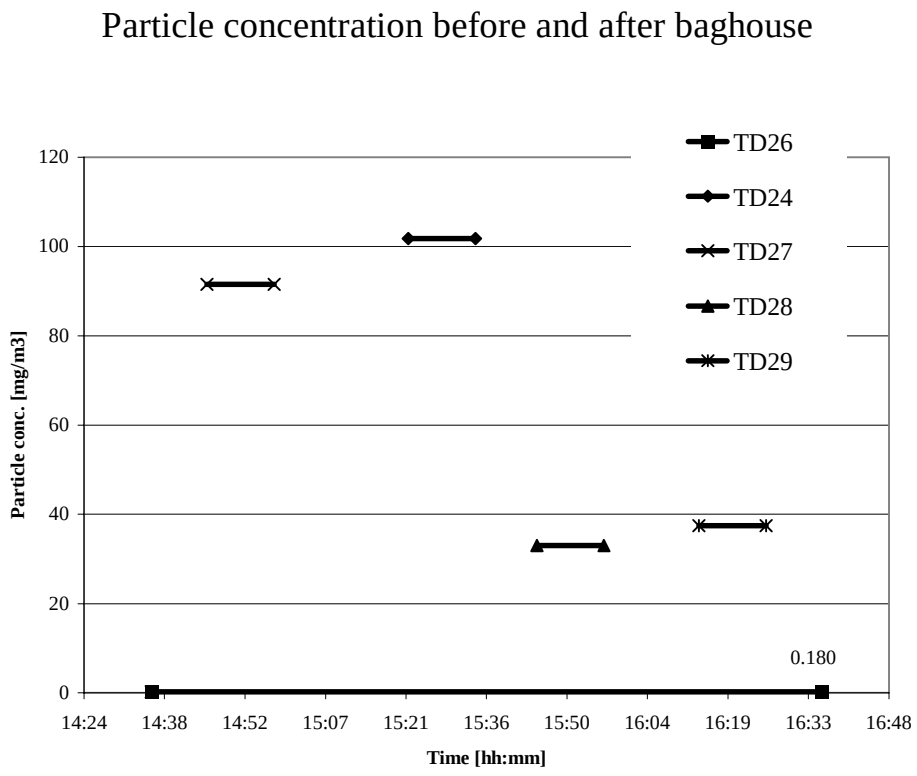


*Figure 3.4 Four TD measurements before the baghouse are shown together with one TD measurement after the baghouse (TD26).*

## 3.4 Dust Measurements by IPEP

The total dust content was determined by the exterior filtration method. A certain volume of flue gas was iso-kinetically taken from the identified ports (S12, S21 and S41) and pumped through the cascade impactors where the aerosols were entrapped. The filters were weighed, and the results are presented in Table 3.9.

*Table 3.9. Total dust content in flue gas*

| ID | Date | Time | Sampling duration Minutes | Volume $Nm^3$ | Mass Collected g | Dust Content $g/m^3$ | Smoke |
|---|---|---|---|---|---|---|---|
| TD1 | 17.06.99 | 9:15 | 2 | 0,036 | 0,1010 | 2,8 | Thick black smoke |
| TD2 | 17.06.99 | 9:15 | 5 | 0,038 | 0,0431 | 1,13 | Thick black smoke |
| TD4 | 17.06.99 | 12:28 | 332 | 43,68 | 0,2289 | 0,005 | |
| TD1 | 17.06.99 | 14:50 | 8 | 0,17 | 0,0257 | 0,15 | Almost transparent |
| TD2 | 17.06.99 | 15:04 | 13 | 0,17 | 0,007 | 0,04 | Almost transparent |
| TD1 | 17.06.99 | 16:10 | 10 | 0,21 | 0,0274 | 0,13 | Almost transparent |
| TD4 | 18.06.99 | 10:00 | 405 | 65,6 | 0,0871 | 0,0013 | |
| TD1 | 18.06.99 | 10:25 | 4 | 0,09 | 0,0363 | 0,41 | Dark gray smoke |
| TD2 | 18.06.99 | 10:47 | 5 | 0,042 | 0,0140 | 0,33 | Dark gray smoke |
| TD1 | 18.06.99 | 14:41 | 19 | 0,35 | 0,0171 | 0,05 | Light gray smoke |
| TD2 | 18.06.99 | 16:05 | 25 | 0,39 | 0,0081 | 0,021 | Light gray smoke |

These results are subject to the same problems as described above. It was impossible to run the boiler steadily enough to be in agreement with quality of data anticipated and the high precision instrumentation used. The boiler personnel tried to stoke the fire-box steadily, but the main reason is that the boiler has a fixed grate. The heap of chips in furnace did not move along the grate, but was growing until it subsided down from time to time. Nevertheless, the average picture can be obtained from the above results. In Table 3.10, the efficiency of different elements of the test capture system is presented as calculated on the basis of the above data.

*Table 3.10. Average efficiency of capture system. These efficiencies are comparable to those achieved by ESP filters (Electro Static Precipitators), but at least one order of magnitude lower than those achieved by common bag house filter installations.*

| Date | Average dust content | | | Capture efficiency, % | | |
|---|---|---|---|---|---|---|
| | Before cyclone $mg\ m^{-3}$ | Before baghouse $mg\ m^{-3}$ | After baghouse $mg\ m^{-3}$ | Cyclone % | Bag house % | Total system % |
| 17.06.99 | 1.03 | 0.585 | 0.005 | 43 | 99.1 | 99.5 |
| 18.06.99 | 0.23 | 0.18 | 0.0013 | 22 | 99.3 | 99.4 |
| Average | 0.708 | 0.38 | 0.00315 | 46 | 99.2 | 99.6 |

## 3.5 Impactor Measurements

**Equipment**

For the impactor measurements two identical Berner low-pressure impactors (BLPI) from Hauke GmbH were used. These have 10 stages and cut-off diameters from 30 nm up to 16 μm. They were calibrated by Hillamo and Kaupinen, 1991. As the pipe diameters at the filter test plant are relatively narrow, 200 mm, compared to the impactor dimension, 110 mm diameter, a gas stream was iso-kinetically extracted. The dimension of the measuring head was determined after measurement of the flow rate on the first day of the test. To avoid condensation of vapour in the impactors they were pre-

heated and placed in insulation material before they were mounted in the set-up. Figure 3.5 shows a diagram illustrating the mounting of the impactor. The 4" fitting was screwed into the thread in the sampling port. The insulated impactor could be moved back and forth through the fitting enabling traversing.

A set-up with a pre-filtration system was prepared for sampling before the cyclone in case of an overload with big particles. However, the first measurements showed that the fine mode aerosol below one micrometer dominated the particle size distribution. Therefore it was not necessary to have the pre-filtration cyclone installed in the sampling line before the impactor.

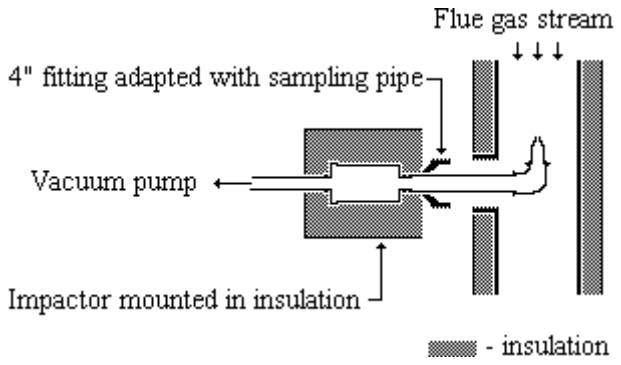


*Figure 3.5 Principle diagram of the impactor mounting on the side of the main bag house duct.*

The impactor results have been corrected to dry air at 0 $^{o}$C . Also the impactor flow rate was corrected, according to the paper by Valmari et al. (1998). The mass flow rate declines with the square root of the relative temperature increase when doing in-stack measurements.

A total of 22 impactor measurements were made. 21 of these gave useful results. All impactor samples have been weighed and all the mass size distributions can be seen in Appendix A. A total of 5 impactor $^{137}$Cs size distributions have been measured.

*Table 3.11 Review of impactor measurements. 'ID' is the sample batch identification. 'Pos.' is the measurement position code. 'Imp' is the identity of the impactor used. 'Qual' is a subjective judgement of the quality of the sample. Three types of collector surface were used: 'Alu-g' is an aluminium foil coated with vacuum grease, 'Alu-ng' is the same without grease and the third was a teflon foil. All concentrations are given for dry air at 0 $^oC$.*

| ID | Pos. | Imp. | Collector surface | Foil numbers | Start time | Duration [minutes] | Volume [$m^3$] | Total collected [mg] | [$mg/m^3$] |
|---|---|---|---|---|---|---|---|---|---|
| IMP-1 | S1 | 25-43 | Alu-g | 402-411 | 16.06-15:05 | 8 | 0.206 | | |
| IMP-2 | S2L | 25-22 | Alu-g | 442-451 | 16.06-18:05 | 8 | 1.549 | 41.41 | 26.7 |
| IMP-3 | S3 | 25-43 | Alu-ng | 412-421 | 16:06-14:32 | 240 | 6.168 | 11.08 | 1.80 |
| IMP-4 | S3 | 25-43 | Alu-ng | 352-361 | 17.06-08:45 | 240 | 6.168 | 6.03 | 0.98 |
| IMP-5 | S1 | 25-22 | Alu-g | 422-431 | 17.06-09:00 | 2 | 0.051 | 22.56 | 3.66 |
| IMP-6 | S2 | 25-22 | Alu-g | 392-401 | 17.06-10:06 | 4 | 0.102 | 13.46 | 132.5 |
| IMP-7 | S2 | 25-22 | Teflon | 242-251 | 17.06-12:16 | 1.33 | 0.034 | 2.12 | 62.5 |
| IMP-8 | S3 | 25-22 | Alu-g | 452-461 | 17.06-14:45 | 180 | 4.572 | 3.92 | 0.86 |
| IMP-9 | S2 | 25-43 | Alu-g | 462-471 | 17.06-15:33 | 1.33 | 0.034 | 1.17 | 34.3 |
| IMP-10 | S1 | 25-43 | Teflon | 252-261 | 17.06-16:30 | 1.33 | 0.034 | 1.66 | 48.5 |
| IMP-11 | S2 | 25-22 | Alu-ng | 362-371 | 17.06-18:20 | 1 | 0.025 | 0.47 | 18.7 |
| IMP-12 | S1L | 25-22 | Alu-g | 472-481 | 18.06-09:29 | 1 | 0.025 | 4.19 | 165.0 |
| IMP-13 | S2L | 25-43 | Alu-g | 432-441 | 18.06-09:29 | 1 | 0.026 | 3.64 | 141.4 |
| IMP-14 | S1L | 25-22 | Teflon | 272-281 | 18.06-11:05 | 1 | 0.025 | 6.62 | 260.8 |
| IMP-15 | S2 | 25-43 | Teflon | 262-271 | 18.06-11:05 | 1 | 0.026 | 6.11 | 237.7 |
| IMP-16 | S2 | 25-43 | Teflon | 282-291 | 18.06-14:00 | 0.75 | 0.019 | 9.37 | 485.9 |
| IMP-17 | S2 | 25-22 | Alu-ng | 342-351 | 18.06-14:00 | 0.75 | 0.019 | 11.43 | 600.0 |
| IMP-18 | S3T | 25-22 | Teflon | 292-301 | 18.06-14:36 | 120 | 3.048 | 1.95 | 0.64 |
| IMP-19 | S2L | 25-43 | Alu-ng | 372-381 | 18.06-15:05 | 1 | 0.026 | 7.60 | 295.5 |
| IMP-20 | S2L | 25-43 | Teflon | 302-311 | 18.06-16:02 | 0.5 | 0.013 | 0.76 | 0.25 |
| IMP-21 | S2L | 25-43 | Alu-ng | 382-391 | 18.06-17:36 | 1 | 0.026 | 0.80 | 30.9 |
| IMP-22 | S2L | 25-22 | Alu-g | 482-491 | 18.06-17:36 | 1 | 0.025 | 0.73 | 28.7 |

Figure 3.6 shows the effect of the cyclone by comparing IMP-12 and IMP-13. The impactor only samples relatively small particles, with its top size being approximately 16 micron. Particles of this size or smaller are inefficiently collected in the cyclone, as indicated by the relatively small change in the mass loading illustrated in the figure. However, the total dust did not show any significant reduction in the level before and after the cyclone.

Another example of the particle size distribution after the filter is given in Figure 3.7. These data were collected on the same day and should be nominal duplications of the after cyclone data illustrated in Figure 3.6. As is evident, the distributions differ substantially in both shape and magnitude. These differences are likely to be associated with shifts from sooting to non-sooting conditions in the furnace. The bulk of the sample illustrated in Figure 3.8 may be soot rather than fly ash.

In Figure 3.8 a size distribution measured after the filter is shown. It is a relatively flat distribution, but with an indicated maximum at about 0.2 microns. The concentration is about two orders of magnitude below the pre-filter data indicating capture efficiencies of approximately 99% at all sizes in the bag house filter. Such capture efficiencies are high in absolute terms, but are low compared to what is expected from filters of this quality. Elemental analyses of these samples, that have yet to be completed, will allow us to more precisely determine the fractions of soot in the sample.

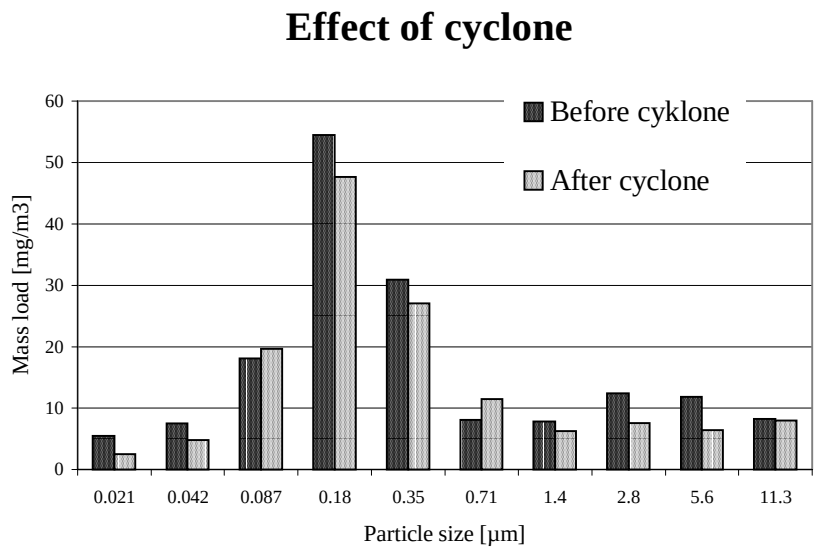


*Figure 3.6 Particle size distribution measured 18/6 before and after the cyclone. Results are from impactor measurements IMP-12 and IMP-13.*

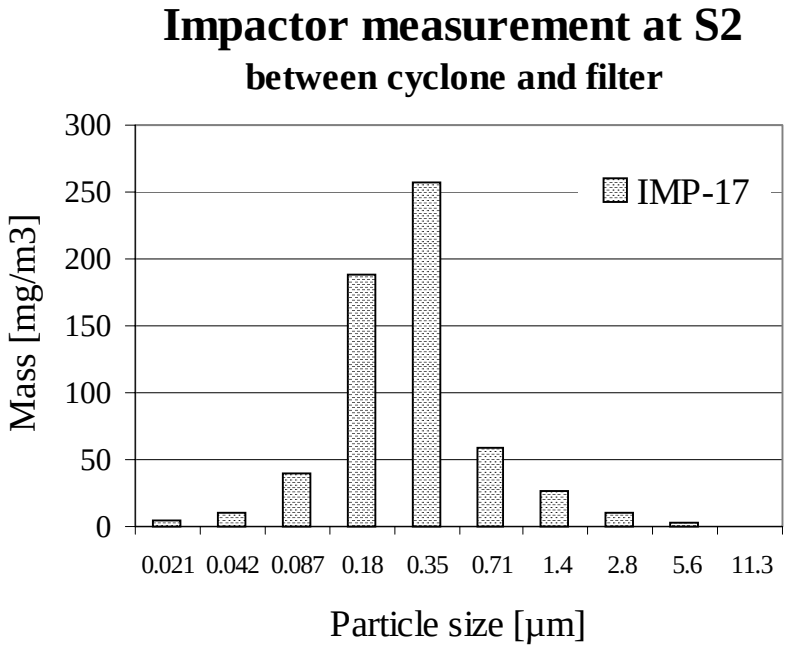


*Figure 3.7 Impactor measurement IMP-17 taken at S2 18/6 1999.*

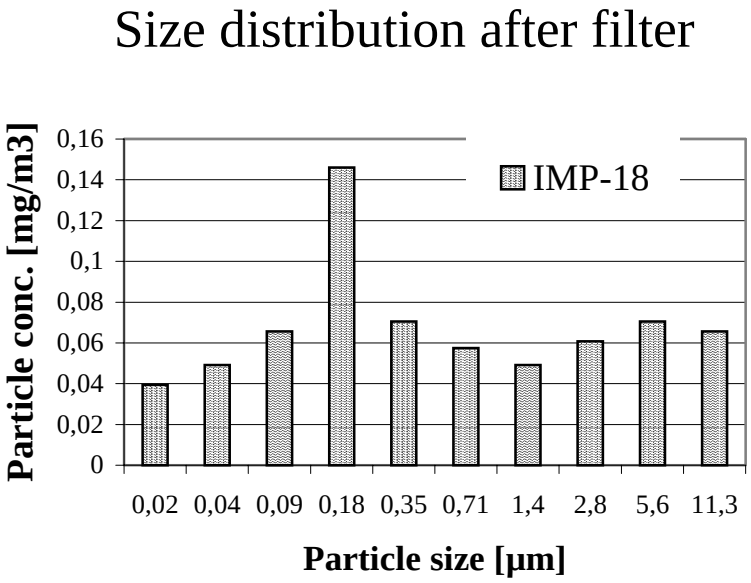


*Figure 3.8 Particle size distribution after the filter.*

**Cs-137 Measurements for Impactor Samples**

A number of impactor samples were selected for activity measurements. A 65 % Germanium detector was used for the measurements. In order to have sufficient material for the analysis only series were more than 3 mg was deposition in total on the 10 collectors was analysed. preferably 10 mg. The activity size distributions are all shown in Appendix C. A discussion of the activity measurements is given in Chapter 4.

*Table 3.8 Review of Cs-137 measurements on impactor samples.*

| Measure-ment | Measure-ment | **Sub micron** | | | **Supra micron** | | |
|---|---|---|---|---|---|---|---|
| | | Mass | Activity | Specific activity | Mass | Activity | Specific act. |
| ID | Position | [mg] | [Bq] | [Bq/g] | [mg] | [Bq] | [Bq/g] |
| IMP 3 | S3 | 4.1 | 0.123 | 30 | 7.0 | 0.045 | 6 |
| IMP 4 | S3 | 3.9 | 0.0656 | 17 | 2.2 | 0.034 | 16 |
| IMP 5 | S1 | 20.8 | 0.179 | 9 | 1.7 | 0.034 | 20 |
| IMP 6 | S2 | 6.7 | 0.2791 | 42 | 6.8 | 0.150 | 22 |
| IMP 12 | S1 | 3.2 | 0.085 | 27 | 1.0 | 0.023 | 23 |
| IMP 13 | S2 | 2.9 | 0.058 | 20 | 0.7 | 0.023 | 31 |
| IMP 17 | S2 | 10.7 | 0.012 | 1 | | BDL* | |

*BDL - Below Detection Limit

In Figure 3.9 an activity size distribution is shown together with a mass size distribution. The activity has a distinct maximum for the fine mode aerosol whereas the mass distribution is bimodal by nature. This pattern can arise from nucleation and aerosol formation of the radionuclides themselves, condensation of radionuclides on small particles, or generation of fine radionuclide particles during combustion. Elemental analyses of the samples should allow these various mechanisms to be distinguished.

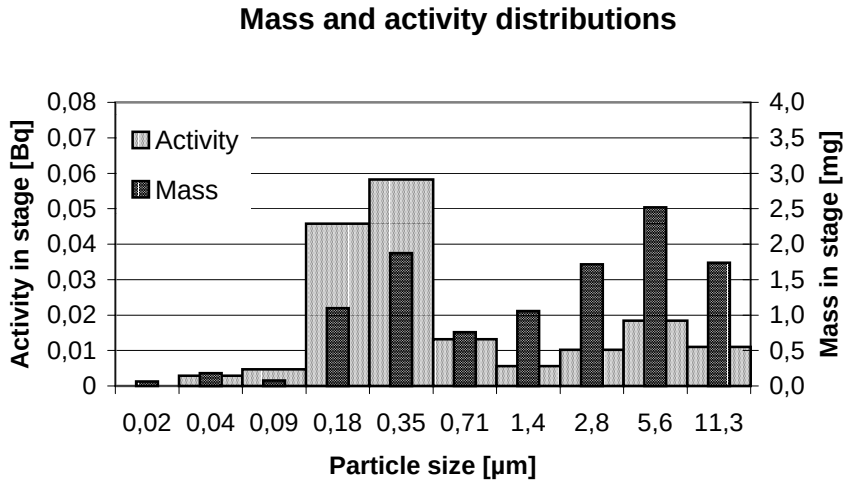


*Figure 3.9 Mass and activity (IMP4)*

## 3.6 Discussion of Dust Measurements

Comparison between the various data is difficult due to the large time variations in the aerosol load. In general IPEP achieved higher values, but the relationship they found between before and after the filter was in good agreement with Risø measurements. Risø impactor measurements and total dust measurements was also in good agreement.

In order to make a more systematic comparison and evaluation of the results a number of data sets have been selected for the stable periods during each of the three days of the actual test.

**Data Selection**

The measurements of dust content were carried out with different methods in the four main sampling points of the test facility (boiler outlet, before cyclone, before baghouse, after baghouse) by all three groups of researchers (IPEP, RISØ, and Elsamprojekt). The review of data is given in the charts below (Figure 3.10, Figure 3.11 and Figure 3.12. In these charts, the data on oxygen variations are also shown. The black bars show the dust content at the boiler outlet and before the cyclone. The red and green (blue) ones indicate the data on dust content before and after the filter correspondingly. Prefix "IMP" denotes the data obtained by impactor measurements.

The time intervals of unstable regimes are marked in abscissa (time argument) by the black segments. As can be seen, a part of the results does not fit into the time intervals of stable regimes, and these results are not analysed further.

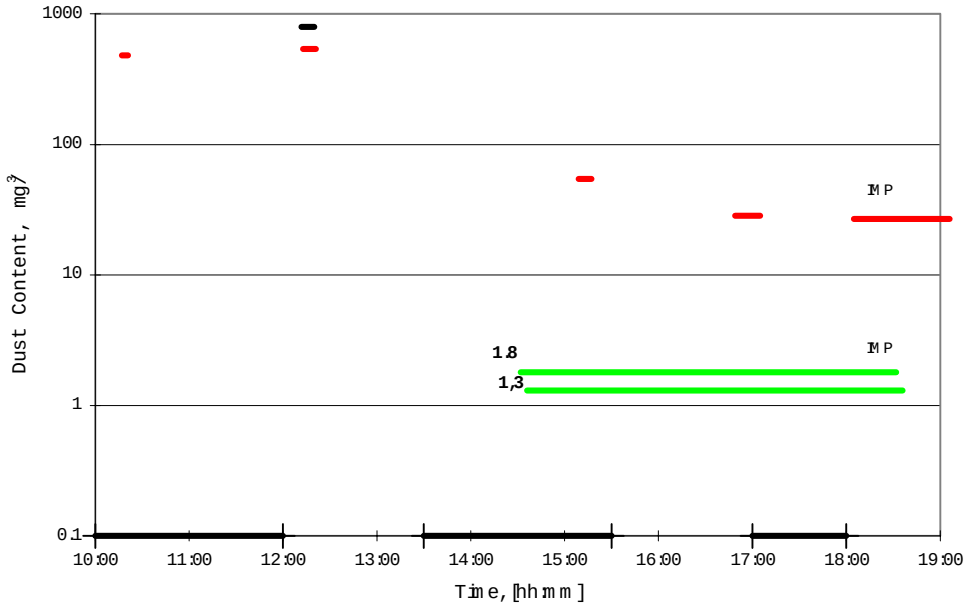


*Figure 3.10 Results of total dust measurements by RISØ, 16.06.99.*

Not many measurements were performed on the 16th of June, the first day of actual test. It follows from Figure 3.10 that only one set of data can be chosen, taking into account also the fact that the error for the impactor measurements may be high due to the rather long duration of measurements after the filter, half of which are associated with unstable regimes. The chosen series of 16/06/99 is shown in Table 3.9.

*Table 3.9 Data selected from 16/06/99.*

| Series ID | Date | Time interval | Sampling point | Sample ID |
|---|---|---|---|---|
| TD-C/1-16** | 16.06 99 | 12:12 – 12:20 | Before cyclone, S11 | TD03 |
| | 16.06.99 | 12:13 – 12:21 | After cyclone, S22 | TD04 |

** - RISØ

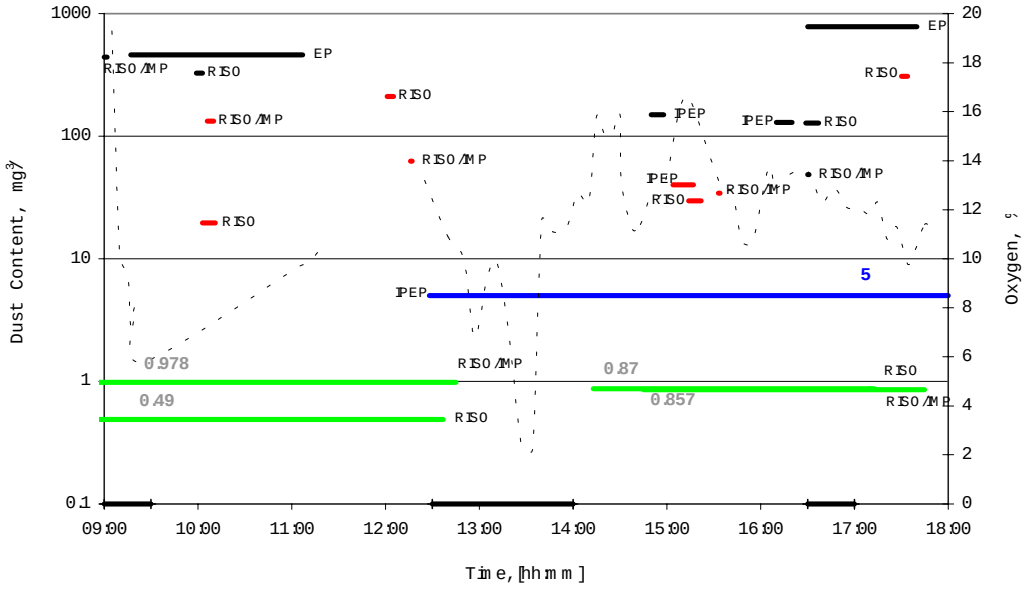


*Figure 3.11 Results of dust measurements by IPEP, Elsamprojekt, RISØ 17.06.99. Dot line shows oxygen concentration.*

The Figure 3.11 draws the attention to a large difference between the data on dust concentration before cyclone obtained by Elsamprojekt at the point SB1 (the boiler duct) and those obtained by other groups at the point S11 (the test facility inlet duct). The lower content detected at the point S11 indicates an extent of non-isokinetic extraction of flue gas from the boiler duct to the capture system, as it was also assumed from analysis in section 2.3.

There is a large difference between the results obtained by IPEP and RISØ after the baghouse filter. There may be two likely explanations for this. First of all, in the IPEP measurements, a significant fraction of the measurement time was during unstable conditions. Secondly, since IPEP's sampling point (S41) was located far downstream from RISØ's point (S31/S32), the influence of duct non-compactness could be sufficiently high to detect some extraneous fine dust from the surface air around the facility. In any case, IPEP's results after the filter should not be considered.

The data on dust concentration for sample TD11 before the filter are set too low compared, e.g., to the data of IMP-6 obtained at the same time from the neighbouring port. Here we almost certainly have a fatal experimental error (i.e. accidental loss of mass). Therefore, the series listed in *Table 3.10* was chosen for the further evaluation:

*Table 3.10 Data selected from 1706/99.*

| Series ID | Date | Time interval | Sampling point | Sample ID |
|---|---|---|---|---|
| IMP-F/4-17** | 17.06 99 | 10:06 – 10:10 | Before filter, S22 | IMP-6 |
| | 17.06.99 | 8:45 – 12:45 | After filter, S31 | IMP-4 |
| TD-F/5-17** | 17.06 99 | 12:01 – 12:05 | Before filter, S22 | TD12 |
| | 17.06.99 | 8:37 – 12:37 | After filter, S32 | TD10 |
| IMP-F/6-17** | 17.06 99 | 12:16 – 12:18 | Before filter, S22 | IMP-7 |
| | 17.06.99 | 8:45 – 12:45 | After filter, S31 | IMP-4 |
| TD-C/2-17* | 17.06 99 | 14:50 – 14:58 | Before cyclone, S12 | |
| | 17.06.99 | 15:04 – 15:17 | After cyclone, S21 | |
| TD-F/7-17** | 17.06 99 | 15:14 – 15:22 | Before filter, S22 | TD13 |
| | 17.06.99 | 14:13 – 17:13 | After filter, S32 | TD14 |
| IMP-F/8-17** | 17.06 99 | 15:33 – 15:35 | Before filter, S22 | IMP-9 |
| | 17.06.99 | 14:45 – 17:45 | After filter, S31 | IMP-8 |
| TD-F/9-17** | 17.06 99 | 17:30 – 17:34 | Before filter, S22 | TD16 |
| | 17.06.99 | 14:13 – 17:13 | After filter, S32 | TD14 |

* - IPEP

** - RISØ

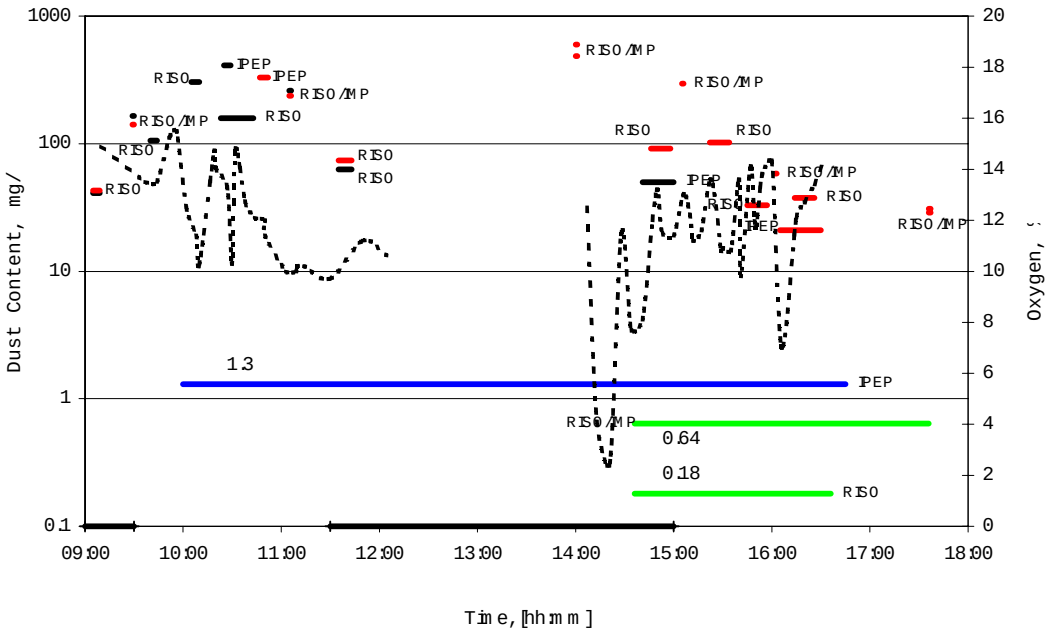


*Figure 3.12 Results of dust measurements by IPEP and RISØ, 18.06.99. Dot line shows oxygen concentration*

On 18.06.99 (Figure 3.12), there were longer periods of stable operation of the furnace compared to the previous dates. The results are in better agreement. Nevertheless, the comment related to IPEP's measurements in the point S41 should be the same as that given above. The second discrepancy, which is difficult to explain, is the negative difference between the dust content detected by Risø before and after the cyclone between 11:35 and 11:43.

Based on analysis, the data listed in Table 3.12 were selected to further evaluate the filter efficiency.

*Table 3.11 Data selected from 18/06/99*

| Series ID | Date | Time interval | Sampling point | Sample ID |
|---|---|---|---|---|
| IMP-C/1-18** | 18.06 99 | 9:29 – 9:30 | Before cyclone, S11 | IMP-12 |
| | 18.06 99 | 9:29 – 9:30 | After cyclone, S22 | IMP-13 |
| TD-C/2-18* | 18.06 99 | 10:25 – 10:29 | Before cyclone, S12 | |
| | 18.06 99 | 10:47 – 10:52 | After cyclone, S21 | |
| IMP-C/3-18** | 18.06 99 | 11:05 – 11:06 | Before cyclone, S11 | IMP-14 |
| | 18.06 99 | 11:05 – 11:06 | After cyclone, S22 | IMP-15 |
| IMP-F/2-18** | 18.06 99 | 15:05 – 15:06 | Before filter, S22 | IMP-19 |
| | 18.06 99 | 14:36 – 17:36 | After filter, S31 | IMP-18 |
| TD-F/3-18** | 18.06 99 | 15:22 – 15:34 | Before filter, S22 | TD24 |
| | 18.06 99 | 14:36 – 16:36 | After filter, S32 | TD26 |
| TD-F/4-18** | 18.06 99 | 15:45 – 15:57 | Before filter, S22 | TD28 |
| | 18.06 99 | 14:36 – 16:36 | After filter, S32 | TD26 |
| TD-F/5-18** | 18.06 99 | 16:14 – 16:26 | Before filter, S22 | TD29 |
| | 18.06 99 | 14:36 – 16:36 | After filter, S32 | TD26 |
| IMP-F/6-18** | 18.06 99 | 16:02 – 16:03 | Before filter, S22 | IMP-20 |
| | 18.06 99 | 14:36 – 17:36 | After filter, S31 | IMP-18 |
| IMP-F/7-18** | 18.06 99 | 17:36 – 17:37 | Before filter, S22 | IMP-21 |
| | 18.06 99 | 14:36 – 17:36 | After filter, S31 | IMP-18 |
| IMP-F/8-18** | 18.06 99 | 17:36 – 17:37 | Before filter, S22 | IMP-22 |
| | 18.06 99 | 14:36 – 17:36 | After filter, S31 | IMP-18 |

* - IPEP

** - RISØ

An interesting pattern is observed when analysing the dust concentration after the baghouse (Figure 3.13). The filter efficiency was improving during the test as the filter material was covered with dust.

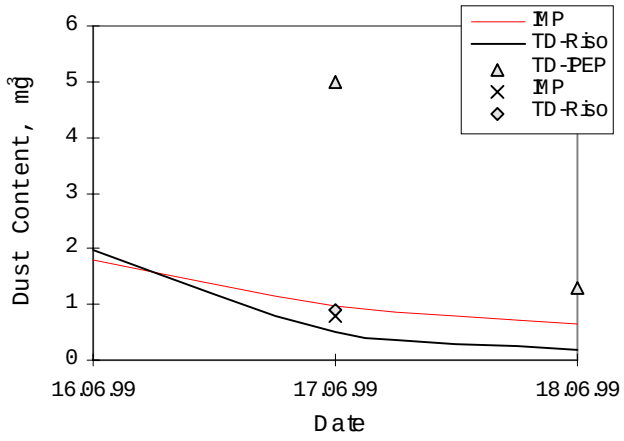


*Figure 3.13 Concentration of dust in air after the baghouse plotted as function of time. Total dust (TD) and impactor (IMP) measurements made by different teams.*

### Cyclone Capture Efficiency from Dust Concentration Data

The cyclone capture efficiency, as calculated on a basis of selected series, is presented in Figure 3.14. The deviation is large due to non-coincident intervals of time of measurements in some series (e.g.,

TD-C/2-17). Overall the cyclone efficiency was low. This is also confirmed by the amount of ash collected in the cyclone and baghouse catches. The former contained much less mass of ash compared to the baghouse container. The reason for this is that the flue gas mainly consisted of relatively small particles with diameters below the cyclone capture efficiency curve.

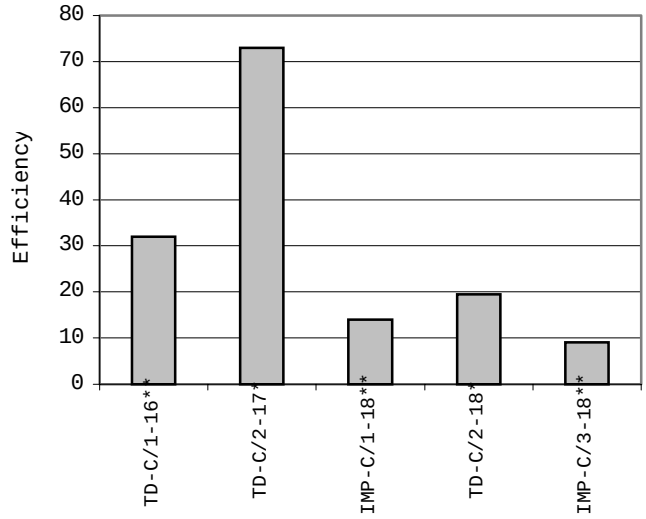


*Figure 3.14 Efficiency of Cyclone (in %) based on five data sets from stable periods of operation.*

**Baghouse Capture Efficiency from Dust Concentration Data**

In Figure 3.15, the calculated filter capture efficiencies are shown, as calculated on the basis of the series chosen. As expected, the results of impactor measurements correspond to a lower efficiency than total filter measurements. The impactor does not reflect the total picture of dust content in the flow before baghouse. After the baghouse, both methods gave practically identical results.

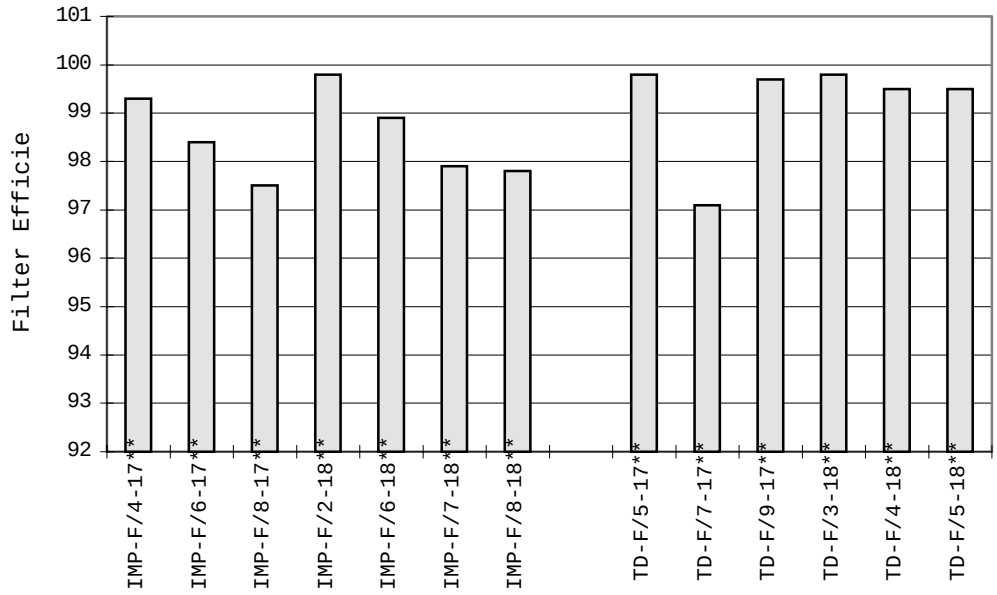


*Figure 3.15 Efficiency of Baghouse Filter based on thirteen selected data sets from periods of stable operation.*

Based on the selected data, the average values listed in Table 3.12 for the baghouse filter efficiency were obtained.

*Table 3.12 Summary of filter efficiency measurements*

| Method | Average efficiency, % | Min/Max, % |
|---|---|---|
| Total dust measurements | 99.2 | 97.1 / 99.8 |
| Impactor measurements | 98.5 | 97.5 / 99.8 |
| Laser spectrometry | 91.7 | 83.6 / 99.6 |

**Filter Efficiency as a Function of Particle Size**

In Figure 3.16 and Figure 3.17 the baghouse filter efficiency for different aerosol fractions is presented. Like the aerosol laser spectrometry data (see section 3.2), these results do not disclose the dependence of filter efficiency on aerosol fractions, at least within the investigated range of particle size.

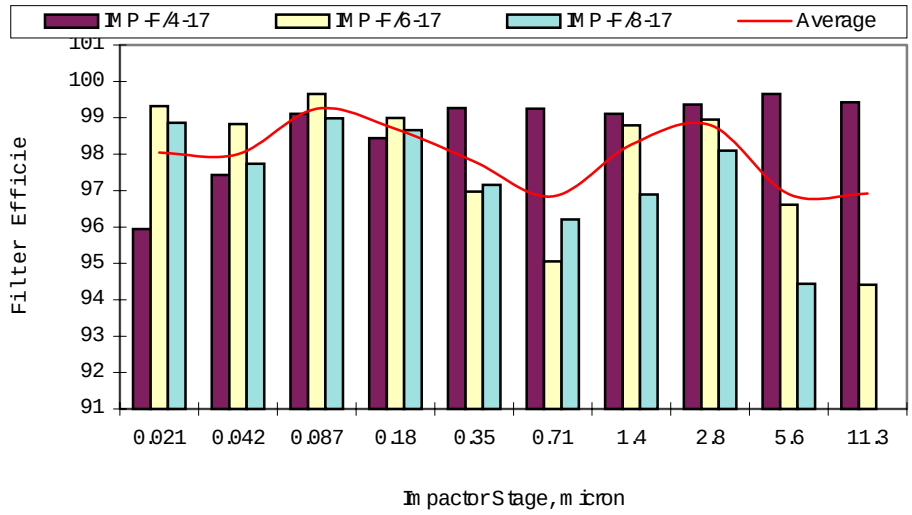


*Figure 3.16 Filter efficiency according to different impactor stages, 17.06.99.*

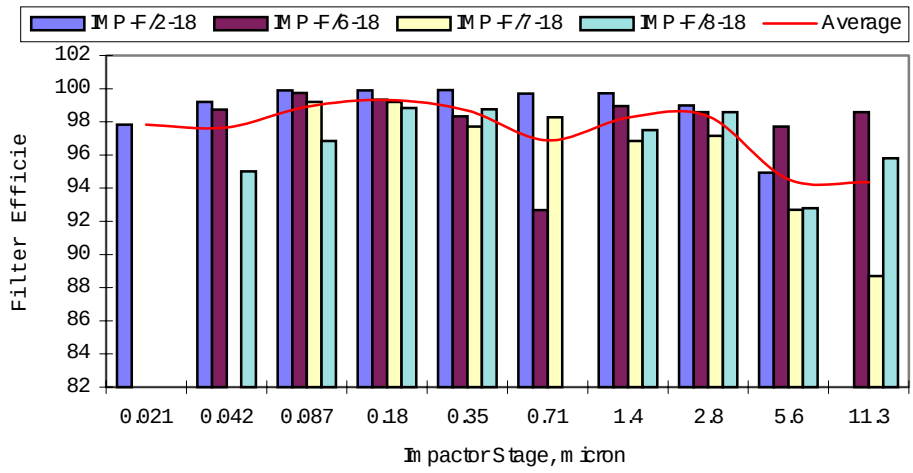


*Figure 3.17 Filter Efficiency According to Different Impactor Stages (18.06.99)*

# 4 Activity Measurements

## 4.1 Fuel, Ash and Slag Analysis

During the test, several samples of fly ash and bottom ash were taken from the designated ports and placed in plastic flasks. In addition, the ashes collected in the containers under the cyclone and filters (Z1, Z2) were manually poured into plastic bags by the end of each day.

The samples of slag and bottom ash were taken from the furnace chamber after the entire test burn had been carried out and combustion in furnace had been extinguished. All samples were transported to IPEP for further analysis and distribution among other participants. The time of sampling and volume of samples are summarised in Table 4.1.

The samples of wood fuel were collected manually from the feed conveyer right before entering the feed hopper of the combustor chamber. A description of these samples is given in Table 4.2.

*Table 4.1 Description of ash samples*

| Time of sampling | **Port Z1** | | **Port Z2(1)** | | **Port Z2(2)** | | **Port Z0, slag and bottom ash** |
|---|---|---|---|---|---|---|---|
| | Volume, $cm^3$ | Mass, g | Volume, $cm^3$ | Mass, g | Volume, $cm^3$ | Mass, g | |
| **15.06.99** | | | | | | | |
| 19:00-20:00 | 12 | | | | | | |
| **16.06.99** | | | | | | | |
| 15:10-16:10 | 7 | | 13 | | 10 | | |
| 9:30-19:00 | | ≈200 | | ≈200 | | ≈200 | |
| **17.06.99** | | | | | | | |
| 9:45-11:00 | | | 13 | | | 0,39 | |
| 11:15-12:15 | | 0,34 | | 0,28 | - | - | |
| 12:30-13:30 | - | - | 1,5 | 0,16 | | 0,13 | |
| 14:00-15:00 | - | - | 4 | | - | - | |
| 15:20-16:20 | 4 | | 8 | | | 0,026 | |
| 16:30-17:30 | - | - | - | - | - | - | |
| 17:45-18:45 | 5 | | 7,5 | | - | - | |
| 8:30-19:00 | | ≈500 | | ≈1000 | | ≈1000 | |
| **18.06.99** | | | | | | | |
| 8:50-9:50 | | 0,086 | | 0,18 | | 0,02 | |
| 10:10-11:10 | 1 | 0,44 | 1 | 0,13 | | 0,015 | |
| 11:20-12:20 | | 0,14 | - | - | - | - | |
| 12:35-13:35 | | 0,46 | 3 | 0,22 | - | - | |
| 14:00-15:00 | | 0,06 | 20 | | - | - | |
| 15:10-16:10 | - | - | 1 | 0,12 | - | - | |
| 16:20-17:20 | 5 | | 15 | | 22 | | |
| 8:15-17:20 | | 100 | | 500 | | 500 | |
| **20.06.99** | | | | | | | |
| 10:00 | | | | | | | 80 litres |
| **18.06.99** | | | | | | | |
| 10:00-16:45 | | | Moisture condensate from flue gas from the **S41 port**, total volume = 0.4 litre | | | | |

*Table 4.2 Description of fuel samples*

| Time of sampling | *Log. # of sample: W1* | | |
|---|---|---|---|
| | Type of fuel | Approximate weight, kg | Moisture content [%] |
| **16.06.99** | | | |
| 15:30 | Sawdust and shavings | 1 | 35.7 |
| **17.06.99** | | | |
| 9:35 | Sawdust, shavings and chips | 2 | 37.3 |
| 10:35 | Sawdust, shavings and chips | 2 | 40.6 |
| 11:35 | Sawdust, shavings and chips | 3 | 37.8 |
| 12:35 | Sawdust, shavings and chips | 2 | 35.5 |
| 13:35 | Sawdust, shavings and chips | 2 | 55.6 |
| 14:35 | Chips | 3 | 48.7 |
| 15:35 | Chips | 3 | 47.1 |
| 16:35 | Chips | 2 | 40.2 |
| 17:35 | Chips | 3 | 31.2 |
| 18:35 | Chips | 3 | 34.7 |
| **18.06.99** | | | |
| 8:40 | Shavings and chips | 2.5 | 55.6 |
| 9:40 | Shavings and chips | 3 | 32.2 |
| 10:40 | Shavings and chips | 3 | 45.8 |
| 15:40 | Shavings and chips | 2 | 42.0 |
| 16:40 | Shavings and chips | 3 | 42.6 |

The probe preparation and following radiological measurements for biomass samples were provided in accordance with the guidance "Determination of Content and Forms of Artificial Radionuclides in Environmental Objects", Up-to-Date Methods of Separation and Determination of Radioactive Elements, Moscow, 1989. Total $^{137}Cs$ content in wood fuel samples after drying at 105°C and coarse grinding (until approx. 1 mm x 1 mm) was determined in a three-dimensional geometry by the gamma-gay spectrometry. The samples had a volume of approx. 103.7 $cm^3$.

The $^{137}Cs$ specific activity of ashes was measured by the gamma-spectrometer in three-dimensional geometry. The samples subjected to radiological analysis had a volume of approx. 13.7 $cm^3$.

The small content of $^{137}Cs$ in the total dust samples was measured using a low-background spectrometer with Ge(Li) detector system and a guard annulus NaI(Tl) detector to provide gamma-ray spectrometry of the small samples with low activity level. The method is based on the anti-coincidence mode that gives the sensitivity of 0.1 Bq/probe in case of two-dimensional geometry, the counting time being 7,200 seconds or less. The detector was calibrated with different container dimensions and sample densities. The detecting time varied from 2-3 hours to 30-50 hours depending on the mass of the sample. All equipment has been verified (certificate No. BY/112.02.2.0.0464, of 18.05.98). The results are shown in Appendix D.

As can be seen by comparing the results in Appendix D with Table 4.3, the results of the ash and slag contamination analyses performed at IPEP are in good agreement with corresponding results from analyses performed at Risø. The results is discussed further in the next section and summarised in Table 4.4.

The Risø results were obtained from measurement of 200 $cm^3$ samples in Risø standard geometry on a high purity Ge detector. The Canberra Genie software system was applied for the data treatment. The analyses were density corrected, and in sample preparation, precautions were made to eliminate the influence of static electricity. Loss on ignition (indicating the principally combustible part of the ash samples) was determined by heating to 550°C for 2 hours. As can be seen, the cyclone ash, which is rich on large particles, has a comparatively lower loss on ignition than does the fly ash, consisting of small particles with large surface-to-mass relationship, to which gas will have condensed. Practically no loss on ignition was detected for the slag samples.

*Table 4.3 Specific activity of ash and slag samples measured at Risø.*

| ID | Sample | Date | Loss on ignition | Bq $^{137}$Cs activity [Bq g$^{-1}$] |
|---|---|---|---|---|
| A | Cyclone ash | 16/6. 99 | 39.8 % | 3.0 ± 0.1 |
| B | Fly ash 1 | 16/6. 99 | 72.6 % | 11.9 ± 0.3 |
| C | Fly ash 2 | 16/6. 99 | 77.7 % | 10.7 ± 0.3 |
| D | Cyclone ash | 17/6. 99 | 38.0 % | 4.4 ± 0.1 |
| E | Fly ash 1 | 17/6. 99 | 79.0 % | 10.3 ± 0.3 |
| F | Fly ash 2 | 17/6. 99 | 82.4 % | 9.4 ± 0.2 |
| G | Slag < 2mm | All week | ~0 | 1.6 ± 0.05 |
| H | Slag > 2mm | All week | ~0 | 1.8 ± 0.05 |

## 4.2 Discussion of Cs-137 in Aerosols and Ashes

**Radioactivity of Samples from Facility Compartments**

The results of daily measurements of $^{137}$Cs content in ashes sampled from different ports are shown in Fig. 4.1 - 4.3. The analysis of the samples taken from the catches of two baghouse modules (Fig. 4.3) gave differing data on specific activity. The fly ash captured in the right module Z2(2) has lower activity than that in the left module Z2(1). One can derive two reasons. The baghouse design may have some elements, which could result in inertial separation of ash particles. In this case, the right module might collect larger number of bigger particles of dust (soot) that has low activity. The likely reason is that the right baghouse module has lower efficiency in the sub-micron diapason (probably resulting from certain defects in a filter bag).

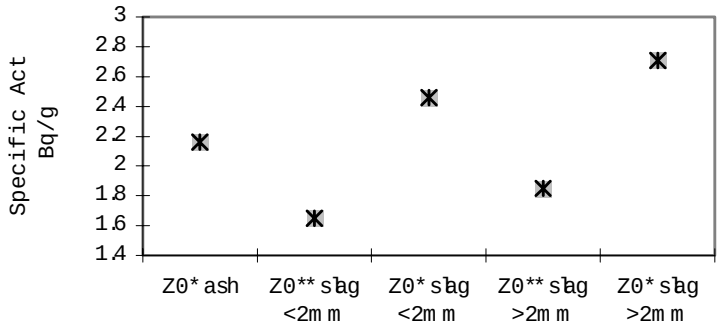


*Figure 4.1 Specific Activity of Bottom Ash and Slag (* - IPEP; ** - RISØ)*

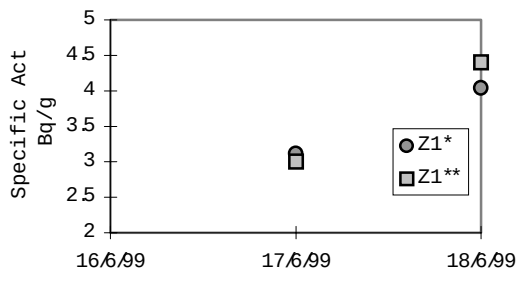


*Figure 4.2 Specific Activity of Cyclone Ash*

(* - IPEP; ** - RISØ)

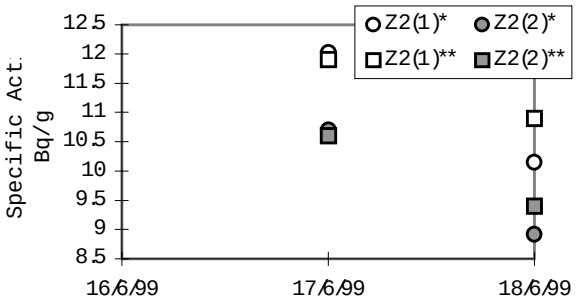


*Figure 4.3 Specific Activity of Baghouse Ash*

(* - IPEP; ** - RISØ)

Some samples of fly ash were taken from special ports several times during a day. The results of their analysis are given in Fig. 4.4 and 4.5. These data are in a good agreement with the averaged activity of the samples ($Z1_{cont}$ $Z2_{cont}$) taken at the end of each day from the catches (see Fig. 4.2 and 4.3).

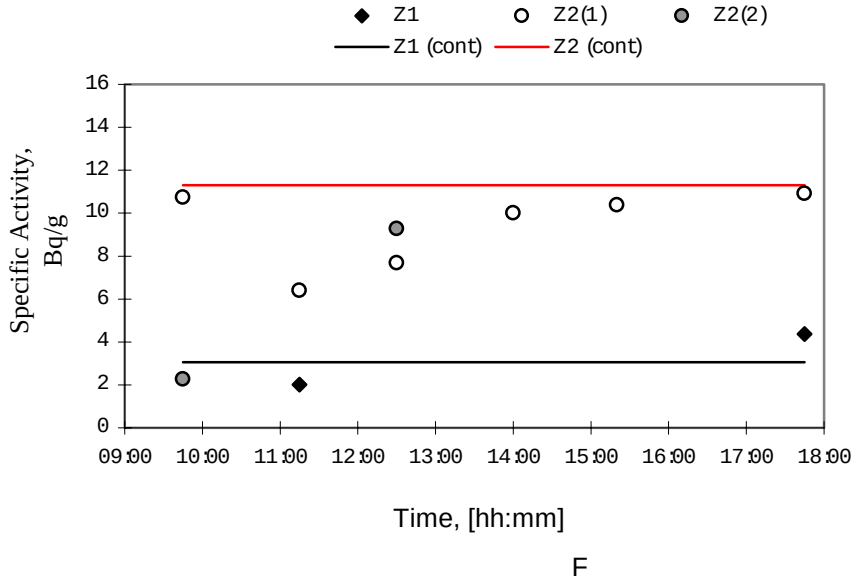


F

*Figure 4.4 Specific Activity of Time-dependent Ash Samples (17.06.99)*

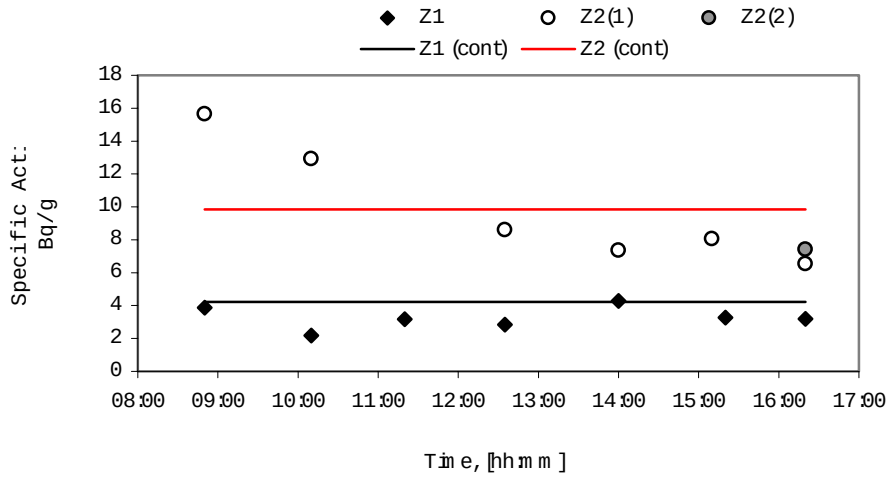


*Figure 4.5 Specific Activity of Time-dependent Ash Samples (18.06.99)*

From the above data, the following averaged values of the $^{137}Cs$ content in ashes sampled from furnace, cyclone and baghouse can be derived:

*Table 4.4 Summary of specific activities for slag and fly ashes.*

| Material | Date | Specific activity [Bq/g] | Max/Min [Bq/g] |
|---|---|---|---|
| Bottom ash and slag (Z0) | 18.06.99 | 2.1 | 2.7 / 1.6 |
| Coarse ash from cyclone (Z1) | 17.06.99 | 3.1 | 4.4 / 2.0 |
| | 18.06.99 | 3.5 | 4.4 / 2.2 |
| Fine fly ash from baghouse (Z2) | 17.06.99 | 9.4 | 12.0 / 3.0 |
| | 18.06.99 | 9.6 | 6.5 / 15.6 |

**Radioactivity of Samples Collected by Total Filter and Impactor**

As was noted in Chapter 2, the unstable oxidizing conditions in furnace led to periodical heavy sooting. This resulted in a wide fluctuation in the content of low-active organic dust (carbon particles) in the flue gas flow. The higher number of such particles, the higher total dust content, and the lower the specific activity of dust.

In Figure 4.6 and Figure 4.7, the dependence of the specific activity of the samples entrapped by total filters and impactor foils in three sampling points (S1, S2, and S3) is plotted as a function of the inverse value of dust concentration measured using the same filters and foils. These graphs confirm the above assumption.

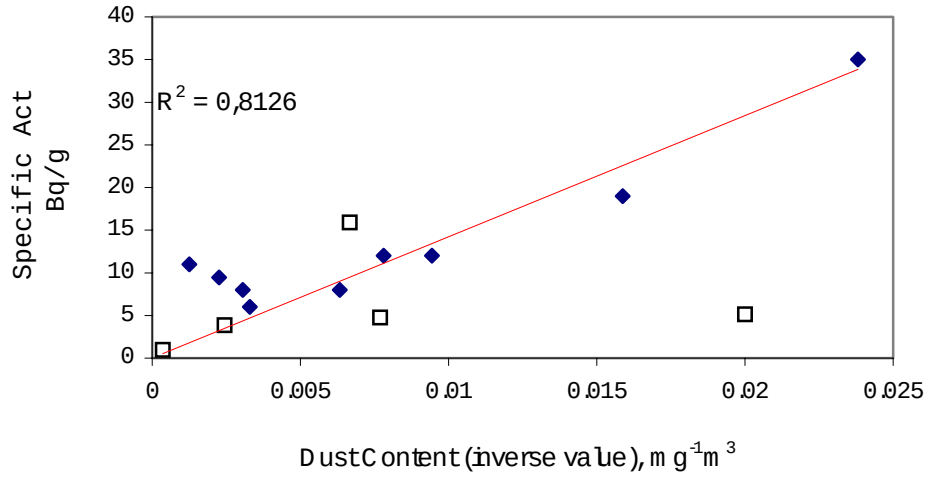


*Figure 4.6 Specific Activity of Aerosols* vs. *Inverse Dust Content measured at port S1 ( before the baghouse cyclone)*

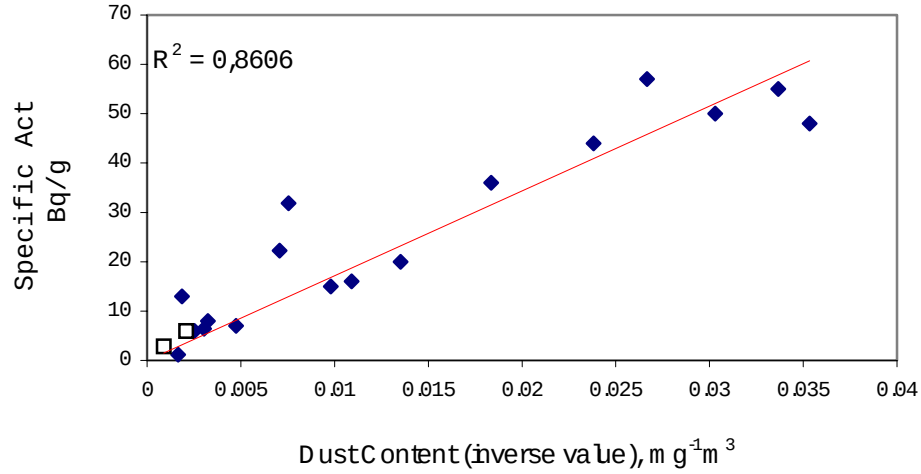


*Figure 4.7 Specific Activity of Aerosols* vs. *Inverse Dust Content measured at port S2 (before the baghouse filter)*

In this correlation, the proportionality coefficient is related to the value of the $^{137}$Cs content in a unit volume of flue gas, which is mostly defined by (i) the rate of vapour formation of $^{137}$Cs and its species, (ii) the absorption/condensation/nucleation characteristics of $^{137}$Cs, and (iii) the number of the $^{137}$Cs-containing aerosol particles. In the case of presence of non-contaminated aerosols, this value (volumetric activity) has a slight dependence on the total dust concentration (see Fig. 4.8 and 4.9).

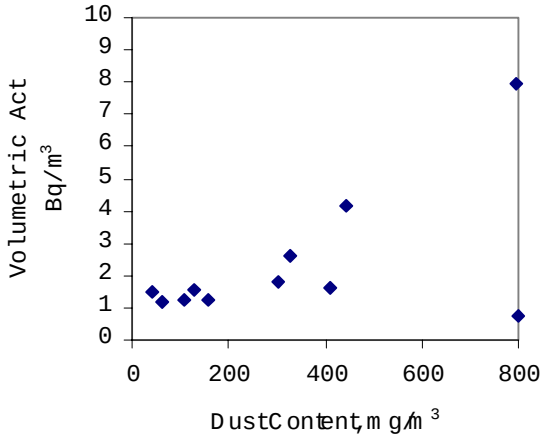


*Figure 4.8 Volumetric Activity at S1*

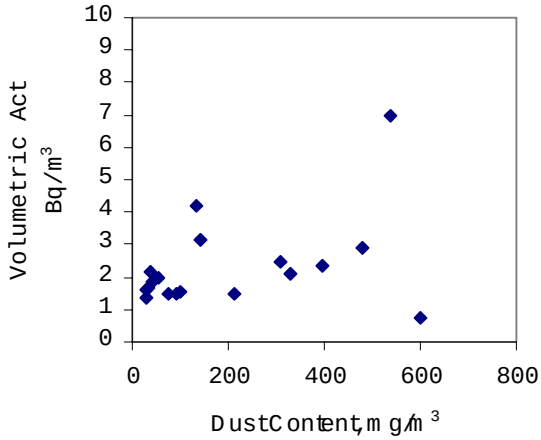


*Figure 4.9 Volumetric Activity before filter at S2*

A somewhat different picture would be expected for the specific values of aerosol activity after the baghouse filter. Here, the mass specific activity should not depend on the dust content, since in the after-filter flow, the submicron aerosols dominate, carrying the major part of the activity. In fact, it was the case in this test (see Fig. 4.10). As for the volumetric activity, it depends proportionally on the amount of dust per unit volume, since this dust mostly consists of the contaminated particulate (Fig. 4.11).

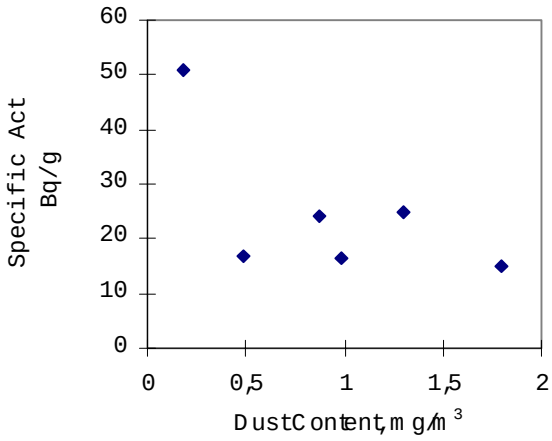


*Figure 4.10 Specific Activity (after filter, S3)*

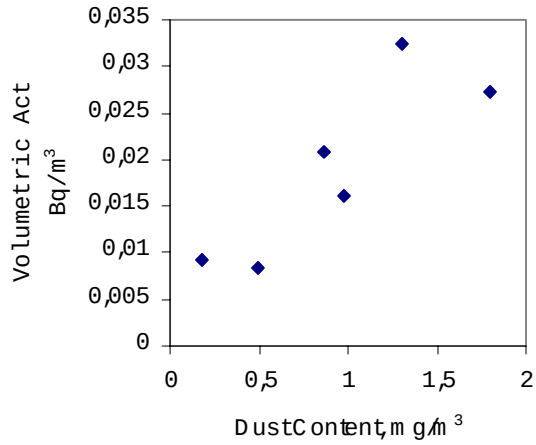


*Figure 4.11 Volumetric Activity (after filter, S3)*

**Activity of Different Fractions According to Impactor Data**

Due to the relatively low radioactivity level in the fuel and small amount of material collected on the impactor foils the $^{137}Cs$ content was mostly below the detection limit of the applied gamma spectrometer. At Risø, six samples were analysed for which the data on radioactivity of aerosols entrapped on the impactor foils of 10 stages were obtained.

It is difficult to make any comprehensive evaluation or modelling on this background. Some results received from the same sampling point and under similar conditions differ significantly (see *Figure 4.12* and *Figure 4.13*).

| Specific Activity of Samples: | Surface Activity of Samples: |
|---|---|
| IMP-3, Port S3 | IMP-3, Port S3 |
| 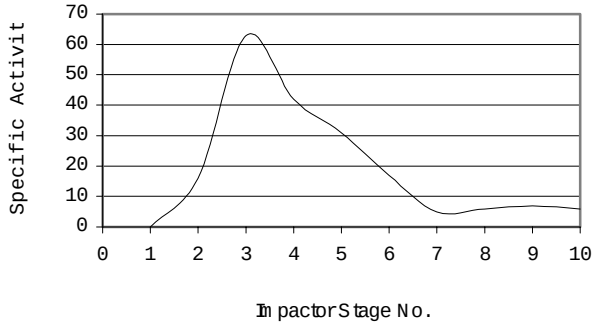 | 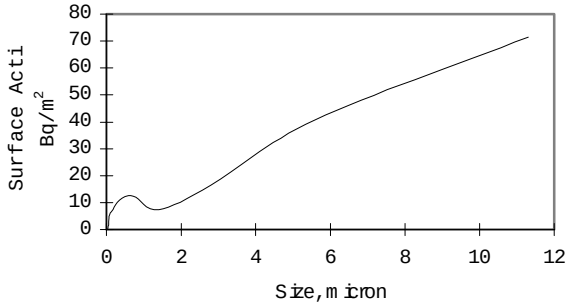 |
| IMP-4, Port S3 | IMP-4, Port S3 |
| 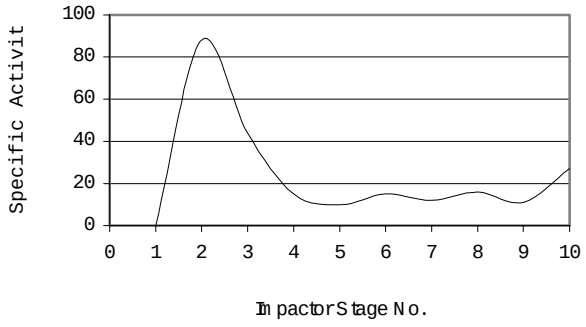 | 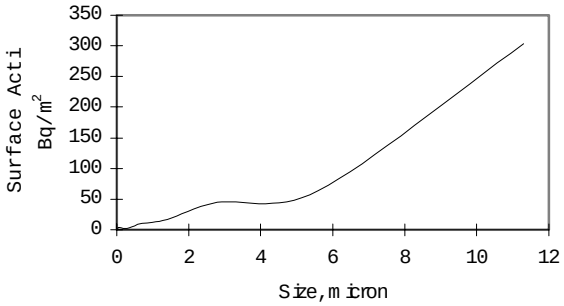 |
| IMP-5, Port S1 | IMP-5, Port S1 |
|  | 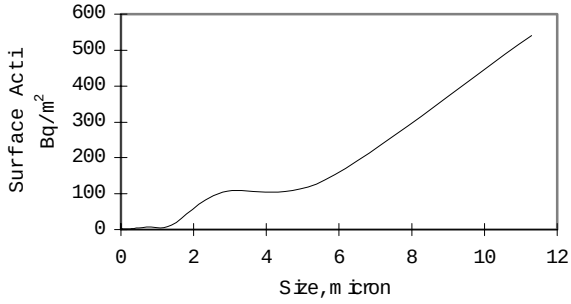 |
| IMP-12, Port S1 | IMP-12, Port S1 |
| 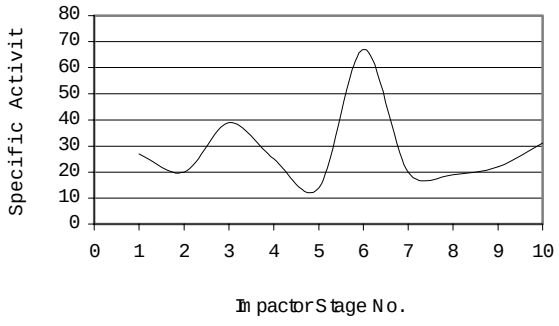 | 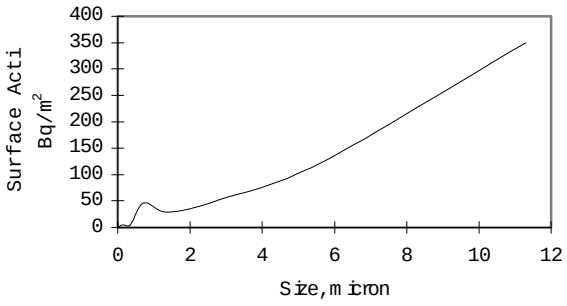 |

Continued on the next page

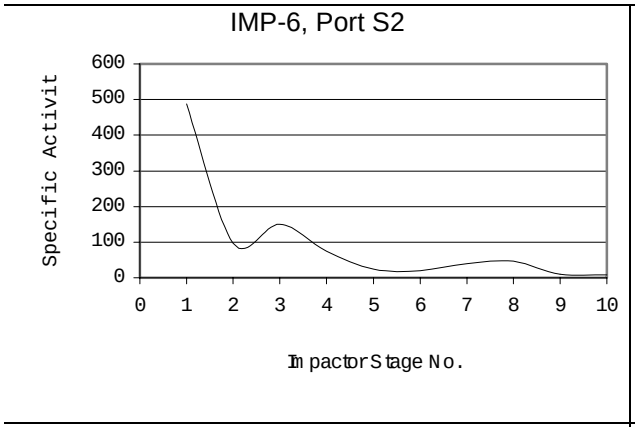


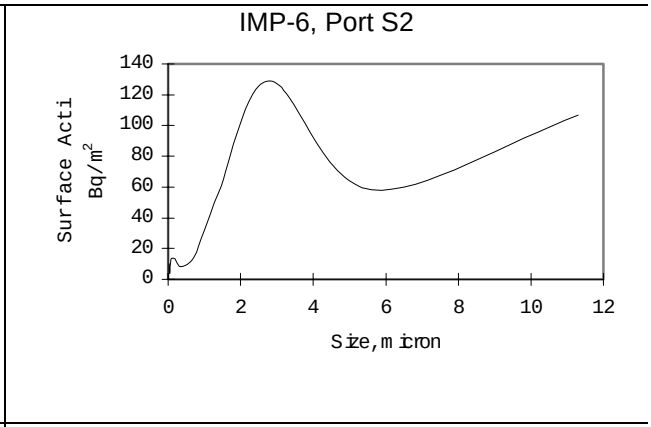


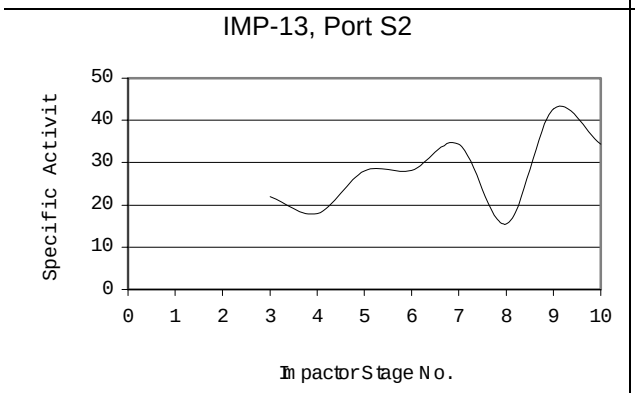


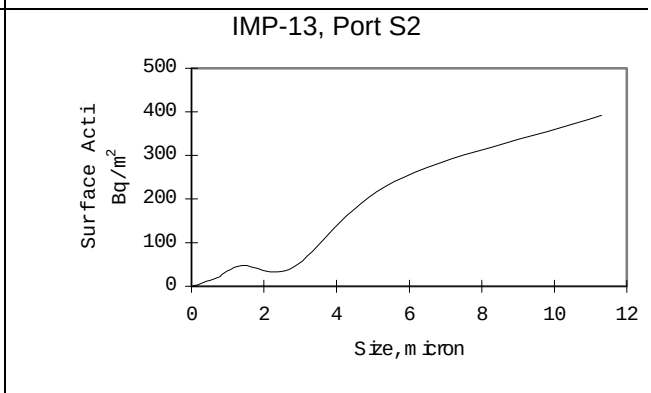


*Figure 4.12 Specific Activity of Samples*

*Figure 4.13. Surface Activity of Samples*

**Efficiency of Cyclone and Baghouse with Regard to Radioactivity**

It follows from the generalisation of measurements of the $^{137}Cs$ content in ash samples (Chapter 4.2) that the volumetric activity of aerosols in the sampling points S1, S2 and S3 has the mean values shown in Table 4.5.

*Table 4.5 Mean volumetric activities in the baghouse facility.*

| Sampling point | Volumetric activity, Bq/m$^3$ | Standard deviation, Bq/m$^3$ |
|---|---|---|
| Before cyclone (S1) | 2.33 | 0.96 |
| Before baghouse (S2) | 2.30 | 0.77 |
| After baghouse (S3) | 0.019 | 0.01 |

From these data, the capture efficiency of the cyclone and filter can be estimated with regard to radioactivity. This is shown in Table 4.6.

*Table 4.6 Capture efficiencies for Cs-137 based on all results.*

| System | Capture efficiency, % | Max / Min, % |
|---|---|---|
| Cyclone | 1.3 | 53.5 / -124 |
| Baghouse | 99.2 | 99.7 / 98.1 |

The above values are calculated on the basis of generalisation of the results of all measurements. At the same time, by analogy with the dust capture efficiency, it is possible to make an assessment of efficiency within each measurement series chosen (see Chapter 3.1). The results of such an estimation are presented below in Fig. 4.14 and 4.15 and Table 4.7.

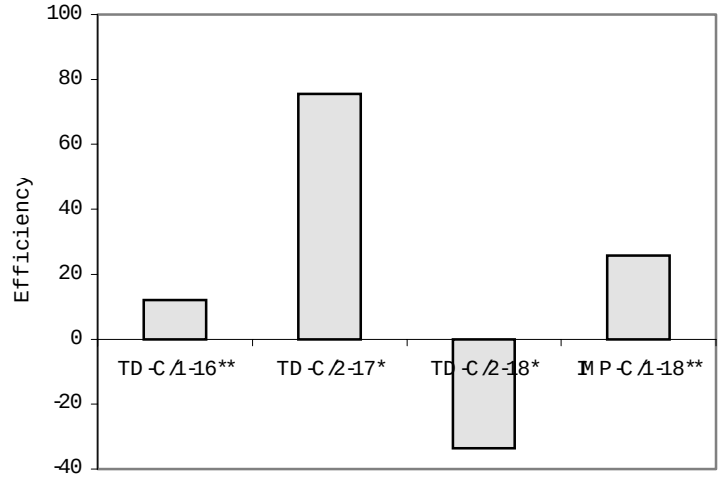


*Figure 4.14 Radioactivity Capture Efficiency of Cyclone*

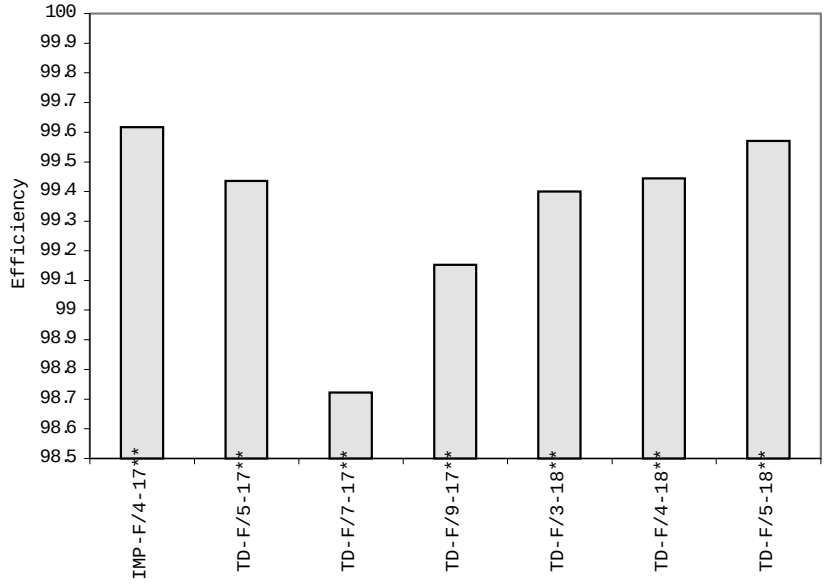


*Figure 4.15 Radioactivity Capture Efficiency of Baghouse Filter.*

*Table 4.7 Capture efficiencies for Cs-137 based on selected results.*

| System | Capture efficiency, % | Max / Min, % |
|---|---|---|
| Cyclone | 4.8 | 25.8 / -33.5 |
| Baghouse | 99.3 | 99.6 / 98.7 |

The results in Table 4.7 do not differ from the previous ones in Table 4.6, but the deviations are smaller.

As can be seen from comparison of the results, in almost all cases the baghouse efficiency of capture of dust is lower than that of radioactivity. As for the capture efficiency of the cyclone, the opposite is the case, i.e. the efficiency of dust treatment is higher. These results are in line with the fact that $^{137}$Cs is carried mainly by fine aerosol fractions.

# 5 Conclusions

A series of in situ tests has been conducted in Belarus to examine the fate of radiocaesium in the process of energy production in a boiler system fired with contaminated biomass from the Belarussian forests contaminated by the Chernobyl accident. Of particular interest in this context is the emission to the atmosphere of radiocaesium from the stack of the bio-energy plant.

Aerosol laser spectrometry measurements before and after the filter system at the test plant show that the impact on particles in the range between ca. 0.2 µm and 2.0µm is rather homogeneous and highly significant. Impactor measurements confirm this and show that the cyclone before the filter as expected generally has a great effect on the super micron particles. The size distribution of particles between the cyclone and the filter exhibits a nice Gaussian-like shape with a GMD of about 250 nm. The coarse particles have here been removed from the flue gas stream.

The smaller particles are efficiently filtered in the baghouse filter mounted at the plant. Total dust measurements show that the radiocaesium contaminant capture efficiency of the cyclone is slightly less than a factor of 2. However, after the exhaust air has passed through the baghouse filter only ca. 0.3 to 0.6 % of the caesium remains. This result was observed by two independent measuring teams.

Overall, laser measurements, total dust measurements and impactor measurements gave a filter efficiency of about 99.5 % for the entire baghouse construction.

In the preliminary assessment of the potential consequences of radiocaesium stack releases from a power plant fired with contaminated biomass, as reported in the final report of Phase 1a of the project, it was assumed that 10 % of the radiocaesium in the fuel would be released from the stack. This estimate was considered to be 'probably conservative'. The results of the tests described in the present report demonstrate that this assumption must in fact be considered highly conservative. If the in situ findings in Belarus were applied in the preliminary stack release consequence analysis from the Phase 1a report, it would thus reduce the number of expected fatal cancers by a factor of ca. 20. The estimate would then be that there would be less than one case of fatal cancer from 100 years operation of power plants fired with an annual total of 1,000,000 tonnes of biomass. It should however be stressed that a proper and fully covering consequence analysis in relation to the construction of any specific biomass-fired power plant would demand the incorporation of site- and case-specific data.

The test in Belarus also provided a unique opportunity to study the factor by which the radiocaesium in the fuel is concentrated in the various types of ash produced in the plant. As expected, the organic content in the slag was negligible, increasing in the cyclone ash, and greatest in the fly ash (72-82 %). The specific radiocaesium activity was found to increase in the order slag - cyclone ash - fly ash. Relative to the fuel content the radiocaesium concentration factor was about 15 in the slag, 30 in the cyclone ash and 90 in the fly ash. Although these figures tie in with the general observations of Hedvall et al. (1996), who examined the ash concentration of radiocaesium in 13 Swedish biomass fired power plants, the absolute values of the concentration factors are critically dependent on process-specific parameters, and may be associated with significant variations. For instance, Hedvall et al. in a few cases recorded higher concentration factors for bottom ash than for fly ash.

Fuel rich (reducing) conditions in the furnace significantly alter the chemical transformations and volatility of caesium. Such conditions occurred frequently during these investigations. Reducing conditions enhance the volatility of caesium in every major component in the furnace, including particles, deposits, grate ash, and slag.

Definitive field data on the fate of caesium during combustion require better control and characterisation of combustion conditions than was achieved during this test.

# 6 Acknowledgement

The work reported here received funding from Wheelabrator Environmental Systems, Inc., USA, USA Department of Energy's Initiatives for Proliferation Prevention (IPP) programme and Energistyrelsen, Danish Ministry of Environment and Energy.

We are grateful to the support provided by each of these institutions.

# 7 References

Steven G. Buckley, Melissa M. Lunden, Allen L. Robinson, David C. Allen, Albert Sandoval, Alexandre grebenkov, and Larry Baxter: ”Fate of Sr and Cs in Biomass Combustion”.

DIN 1942. Abnahmeversuche an Dampferzeugern (VDI-Dampferzeugerregeln). Deutsche Norm, Februar 1994.

Alexandre J. Grebenkov: ”Baghouse Filter for Pilot-Scale Facilities. Field Test Results. IPEP’s contribution to the Joint Test at Rechitza Drev Sawmill”, October 1999.

Hedvall, R., Erlandsson, B. and Matsson, S., Cs-137 in fuels and ash products from biofuel power plants in Sweden, J. Environ. Radioactivity 31, no. 1, pp. 103-117, 1996.

Hillamo, R.E. and E.I. Kauppinen, On the Performance of the Berner Low Pressure Impactor, Aerosol Science and Technology, Vol. 14, pp. 33-47, 1991.

Helle Junker, Jens-Martin Jensen, Henrik Boye Jørgensen, Jørn Roed, Kasper Andersson, Pieter D. Kofman, Ebbe Bøllehuus, Larry Baxter, Alexandre Grebenkov: “Chernobyl Bioenergy Project. Power Production from Radioactively Contaminated Biomass and Forest Litter in Belarus. Final Report, Phase 1”, September 1998.

Valmari, Tuomas; Esko I. Kauppinen, Juha Kurkela, Jorma K. Jokiniemi, George Sfiris and Hannu Revitzer; Fly ash formation and depotion during fluidized bed combustion of willow, J. of Aerosol Science, Vol. 29, no. 4, pp. 445 - 459, 1998.

# Appendix A

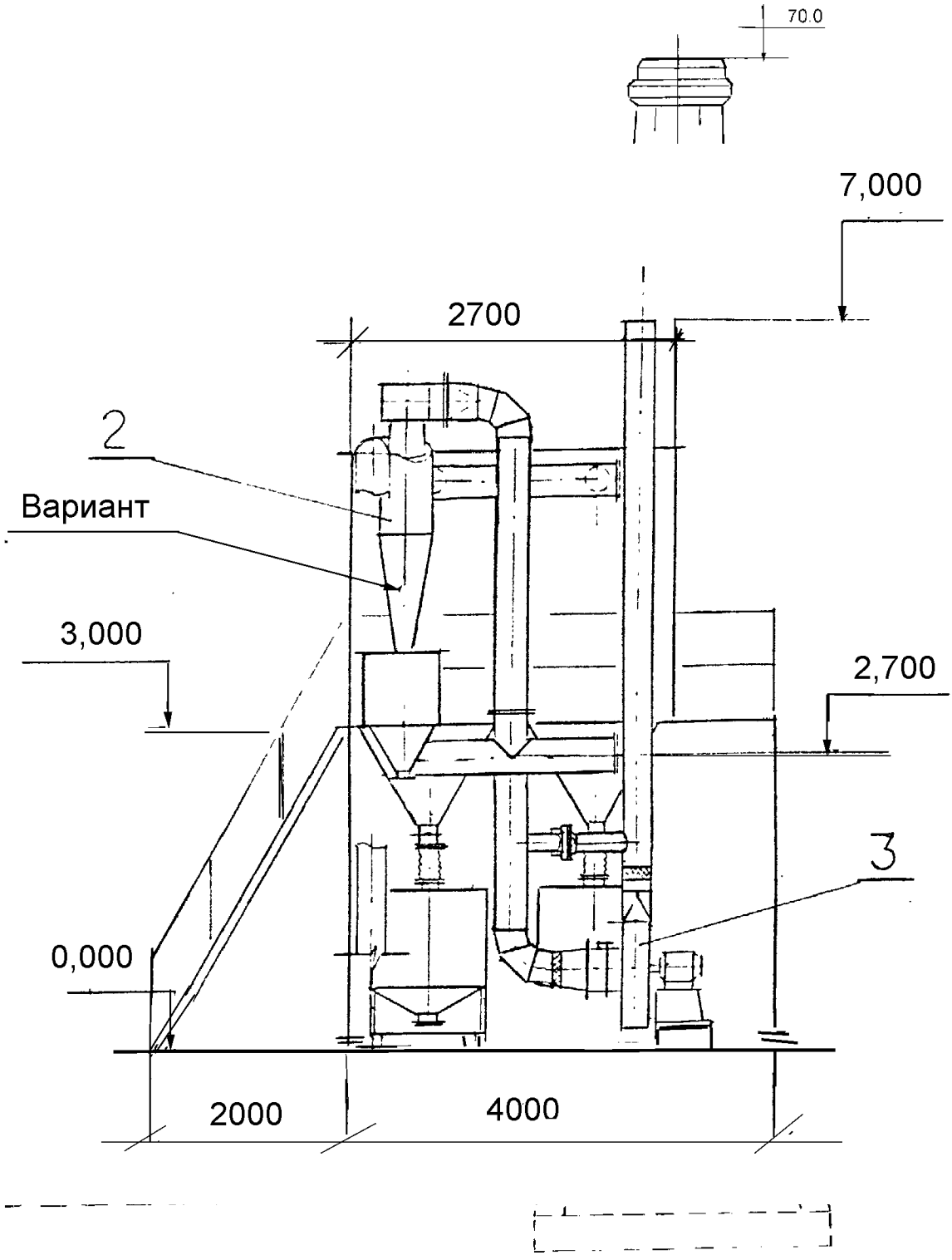


*Figure A.1 Baghouse assembling at the Rechitza Drew Sawmill boiler. Front-site view.*

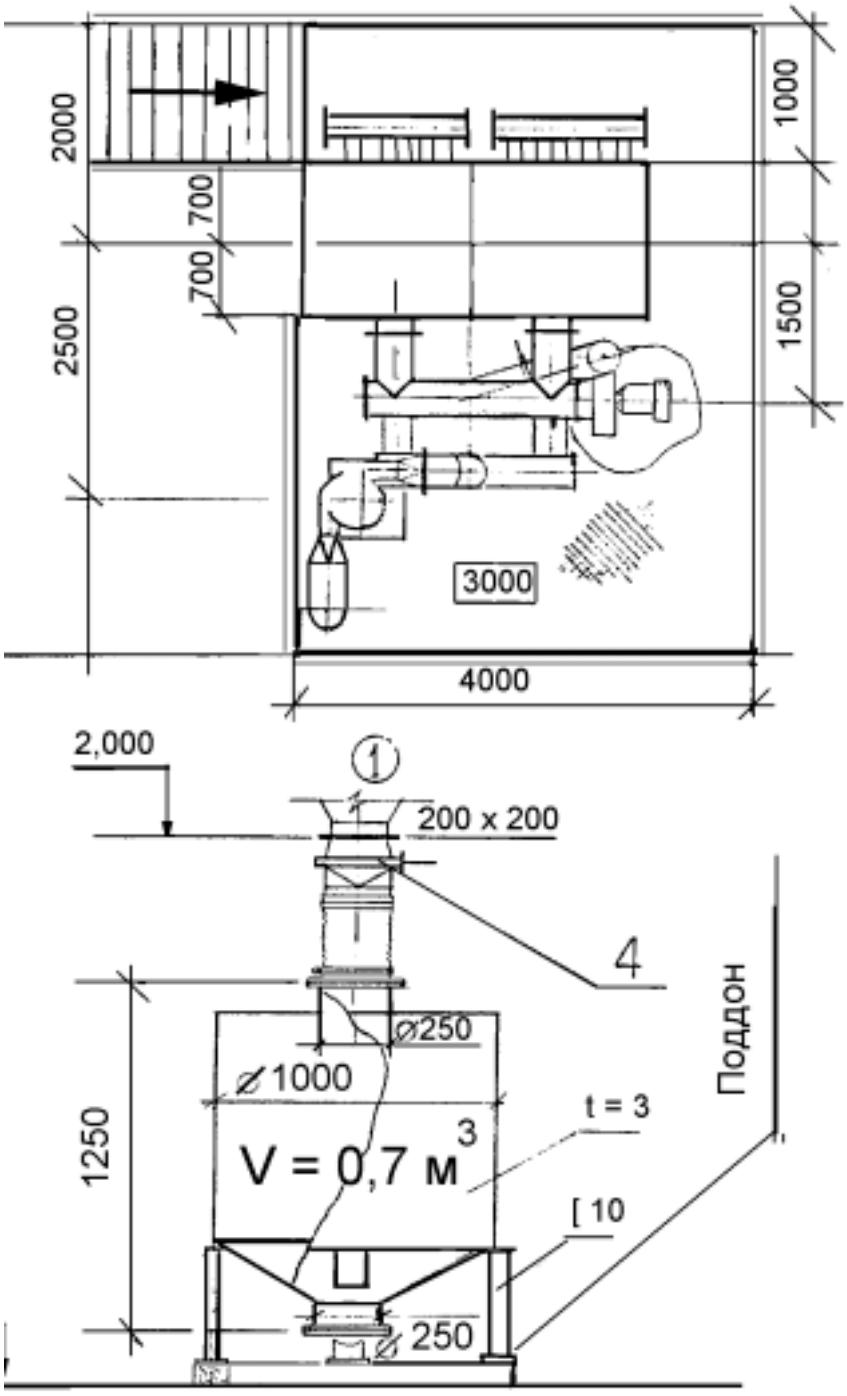


*Figure A.2*

*Baghouse filter at RechiDrev Sawmill site. Air-site view (above)*
*Flue gas fan (below)*

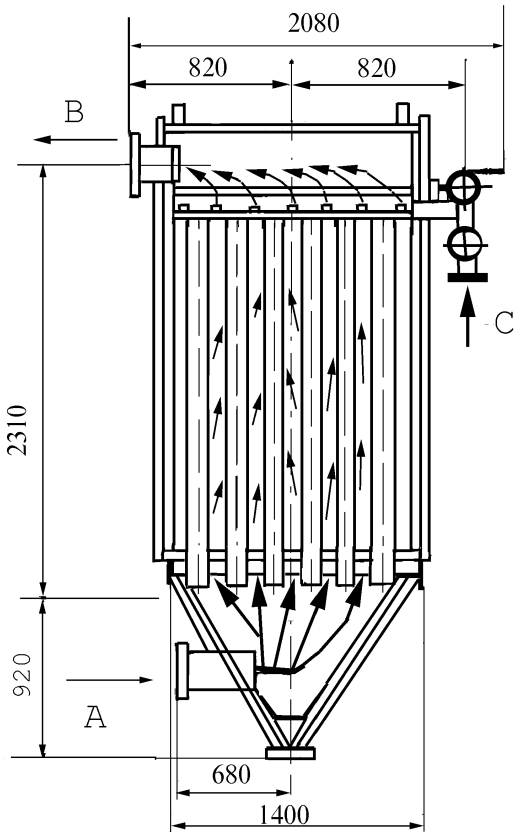


*Figure A.3 Scheme of single baghouse casing.*
*A - incoming air.*
*B - filtered air out.*
*C - compressed air for bag cleaning.*

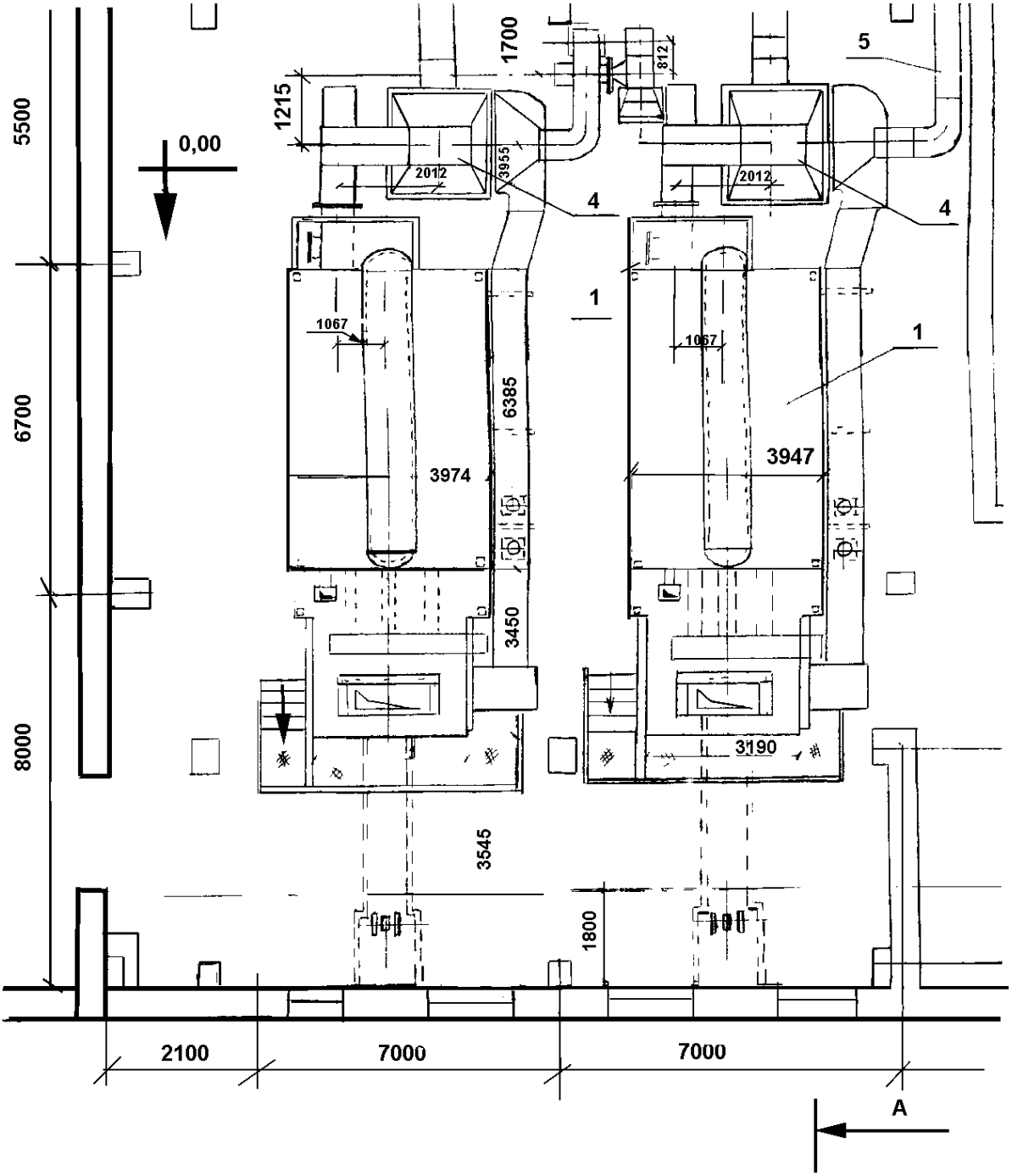


*Figure A.4 Boiler house at Rechitza Drew Sawmill. Air view on wood fired boilers*

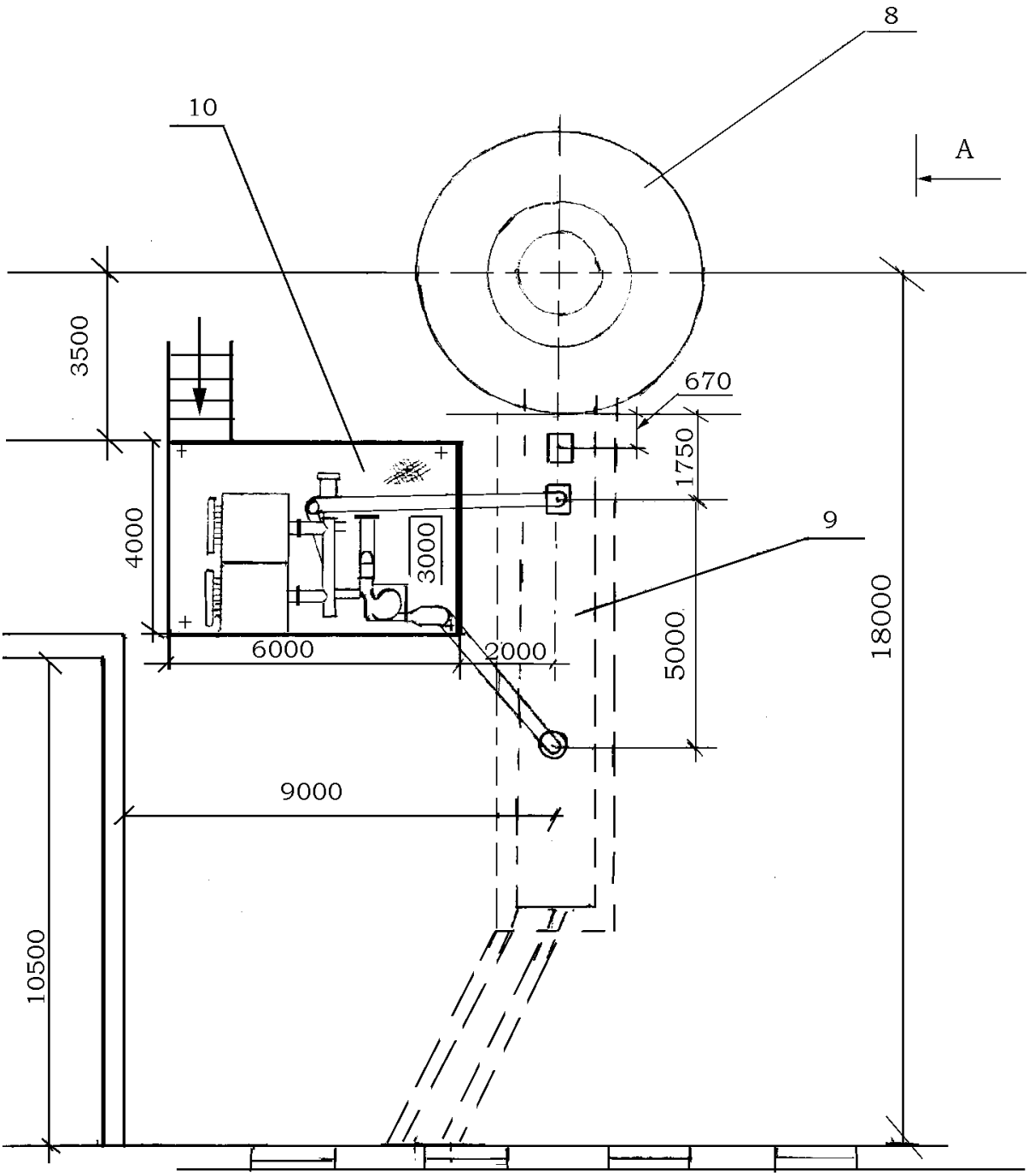


*Figure A.5 Baghouse filter at Rechitza Drew Sawmill site. Air-site view.*
*8 - Chimney; 9 - Flue gas trunk chest; 10 - Baghouse filter*

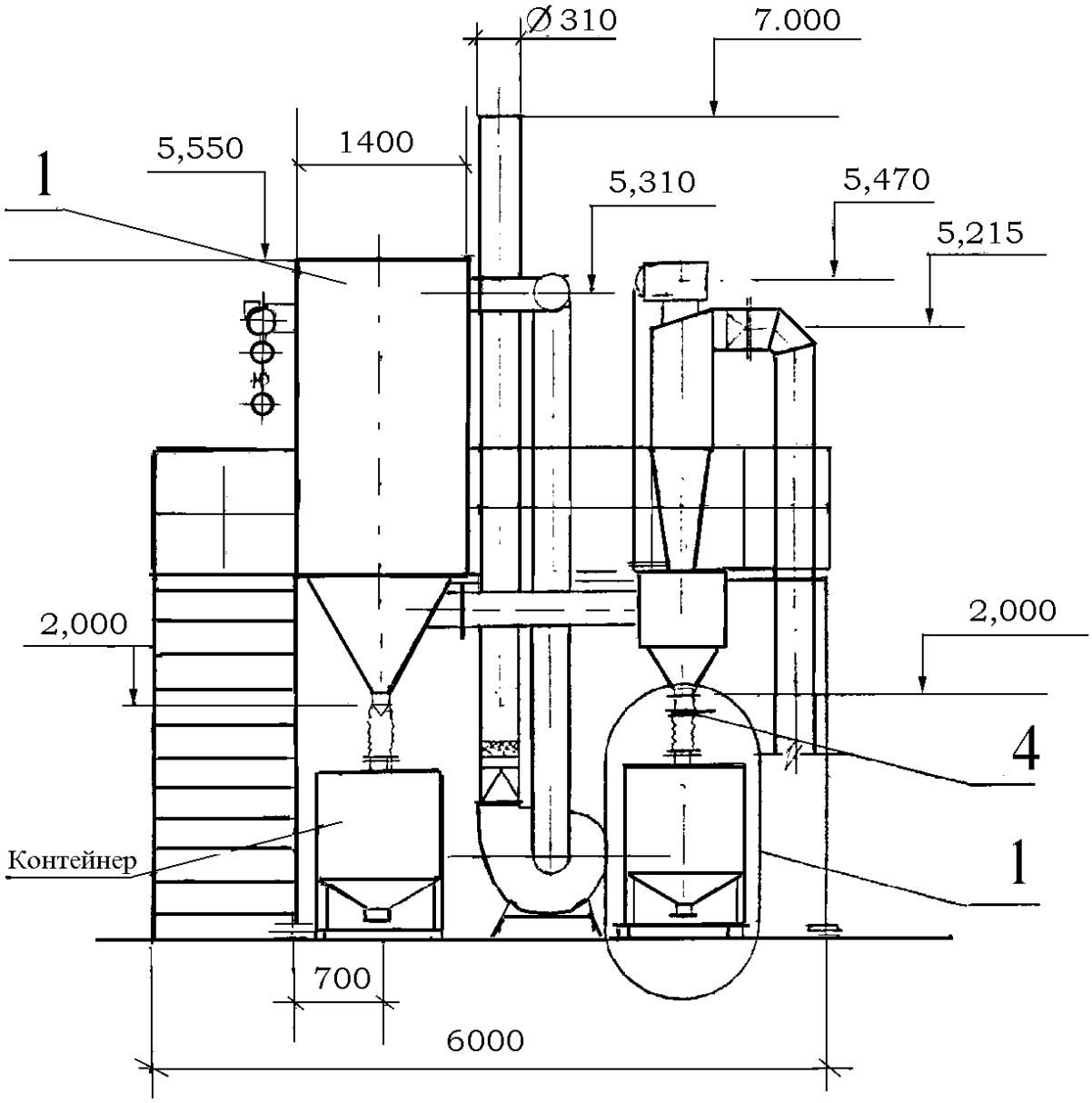


*Figure A.6 Baghouse filter at RechiDrev Sawmill site. Back-site view.*

*1 top - Baghouse filter casing*
*1 bottom - fly ash container below cyclone*

# Appendix B

**Raw Data of Impactor Measurements**

| ID | Pos. | Impactor ID | Collector surface | Foil numbers | Start time | Duration [min.] | Volume [$m^3$] |
|---|---|---|---|---|---|---|---|
| IMP-1 | S1 | 25-43 | Alu-grease | 402-411 | 16.06.99-15:05 | 8 | 0.206 |
| IMP-2 | S2L | 25-22 | Alu-grease | 451-442 | 16.06.99-18:05 | 61 | 1.549 |
| IMP-3 | S3 | 25-43 | Alu-ng | 412-421 | 16:06.99-14:32 | 240 | 6.168 |
| IMP-4 | S3 | 25-43 | Alu-ng | 352-361 | 17.06.99-08:45 | 240 | 6.168 |
| IMP-5 | S1 | 25-22 | Alu-grease | 422-431 | 17.06.99-09:00 | 2 | 0.051 |
| IMP-6 | S2 | 25-22 | Alu-grease | 392-401 | 17.06.99-10:06 | 4 | 0.102 |
| IMP-7 | S2 | 25-22 | Teflon | 242-251 | 17.06.99-12:16 | 1.333 | 0.034 |
| IMP-8 | S3 | 25-22 | Alu-grease | 452-461 | 17.06.99-14:45 | 180 | 4.572 |
| IMP-9 | S2 | 25-43 | Alu-grease | 462-471 | 17.06.99-15:33 | 1.333 | 0.034 |
| IMP-10 | S1 | 25-43 | Teflon | 252-261 | 17.06.99-16:30 | 1.333 | 0.034 |
| IMP-11 | S2 | 25-22 | Alu-ng | 362-371 | 17.06.99-18:20 | 1 | 0.025 |
| IMP-12 | S1L | 25-22 | Alu-grease | 472-481 | 18.06.99-09:29 | 1 | 0.0254 |
| IMP-13 | S2L | 25-43 | Alu-grease | 432-441 | 18.06.99-09:29 | 1 | 0.0257 |
| IMP-14 | S1L | 25-22 | Teflon | 272-281 | 18.06.99-11:05 | 1 | 0.0254 |
| IMP-15 | S2 | 25-43 | Teflon | 262-271 | 18.06.99-11:05 | 1 | 0.0257 |
| IMP-16 | S2 | 25-43 | Teflon | 282-291 | 18.06.99-14:00 | 0.75 | 0.019 |
| IMP-17 | S2 | 25-22 | Alu-ng | 342-351 | 18.06.99-14:00 | 0.75 | 0.019 |
| IMP-18 | S3TL | 25-22 | Teflon | 292-301 | 18.06.99-14:36 | 120 | 3.048 |
| IMP-19 | S2L | 25-43 | Alu-ng | 372-381 | 18.06.99-15:05 | 1 | 0.026 |
| IMP-20 | S2L | 25-43 | Teflon | 302-311 | 18.06.99-16:02 | 0.5 | 0.013 |
| IMP-21 | S2L | 25-43 | Alu-ng | 382-391 | 18.06.99-17:36 | 1 | 0.026 |
| IMP-22 | S2L | 25-22 | Alu-grease | 482-491 | 18.06.99-17:36 | 1 | 0.025 |

| IMP-2 | | Filter ID | 1. pre mass | 2. pre mass | 1. post mass | 2. post mass | Sample mass | | Conc. | |
|---|---|---|---|---|---|---|---|---|---|---|
| | [µm] | [ ] | [g] | [g] | [g] | [g] | [g] | [mg] | [mg/m$^3$] | [%] |
| | 0,021 | 442 | 0,08829 | | 0,08881 | 0,08889 | 0,00056 | 0,56 | 0,361 | 1% |
| Flow | 0,042 | 443 | 0,08847 | | 0,09051 | 0,09029 | 0,00193 | 1,93 | 1,246 | 5% |
| 1,5494 | 0,087 | 444 | 0,08811 | | 0,09081 | 0,09081 | 0,00270 | 2,7 | 1,743 | 7% |
| m$^3$ | 0,18 | 445 | 0,08782 | | 0,09014 | 0,09013 | 0,00232 | 2,315 | 1,494 | 6% |
| | 0,35 | 446 | 0,08825 | | 0,09194 | 0,09193 | 0,00368 | 3,685 | 2,378 | 9% |
| | 0,71 | 447 | 0,08825 | | 0,09832 | | 0,01007 | 10,07 | 6,499 | 24% |
| | 1,4 | 448 | 0,08810 | | 0,10286 | | 0,01476 | 14,76 | 9,526 | 36% |
| | 2,8 | 449 | 0,08764 | | 0,09218 | | 0,00454 | 4,54 | 2,930 | 11% |
| | 5,6 | 450 | 0,08833 | | 0,08897 | 0,08896 | 0,00063 | 0,635 | 0,410 | 2% |
| | 11,3 | 451 | 0,08887 | | 0,08911 | 0,08905 | 0,00021 | 0,21 | 0,136 | 1% |
| | | | | | | | | 41,4 | 26,723 | 100% |

**Impactor measurement at S2**

**between cyclone and filter**

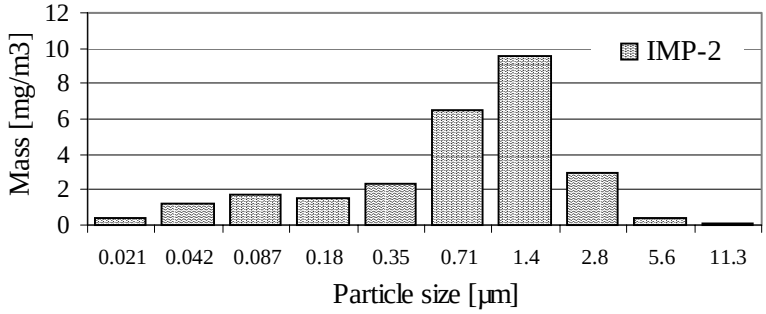


| IMP-3 | | Filter ID | 1. pre mass | 2. pre mass | 1. post mass | 2. post mass | Sample mass | | Conc. | |
|---|---|---|---|---|---|---|---|---|---|---|
| | [µm] | [ ] | [g] | [g] | [g] | [g] | [g] | [mg] | [mg/m$^3$] | [%] |
| | 0,021 | 412 | 0,08829 | | 0,08838 | 0,08833 | 0,00007 | 0,065 | 0,011 | 1% |
| Flow | 0,042 | 413 | 0,08898 | | 0,08919 | 0,08913 | 0,00018 | 0,18 | 0,029 | 2% |
| 6,168 | 0,087 | 414 | 0,08839 | | 0,08850 | 0,08843 | 0,00007 | 0,075 | 0,012 | 1% |
| m$^3$ | 0,18 | 415 | 0,08881 | | 0,08992 | 0,08989 | 0,00110 | 1,095 | 0,178 | 10% |
| | 0,35 | 416 | 0,08837 | | 0,09028 | 0,09021 | 0,00187 | 1,875 | 0,304 | 17% |
| | 0,71 | 417 | 0,08814 | | 0,08891 | 0,08889 | 0,00076 | 0,76 | 0,123 | 7% |
| | 1,4 | 418 | 0,08897 | | 0,09004 | 0,09001 | 0,00106 | 1,055 | 0,171 | 10% |
| | 2,8 | 419 | 0,08937 | | 0,09110 | 0,09107 | 0,00171 | 1,715 | 0,278 | 15% |
| | 5,6 | 420 | 0,08754 | | 0,09008 | 0,09004 | 0,00252 | 2,52 | 0,409 | 23% |
| | 11,3 | 421 | 0,08827 | | 0,09001 | 0,09001 | 0,00174 | 1,74 | 0,282 | 16% |
| | | | | | | | | 11,1 | 1,796 | 100% |

**Impactor measurement at S3**

**after the bag house filter**

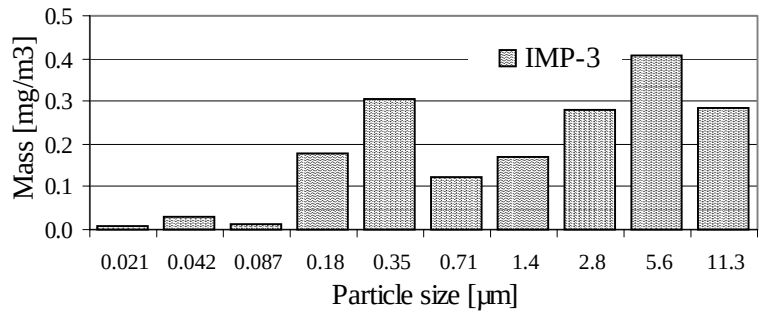

| IMP-4 | [µm] | Filter ID [ ] | 1. pre mass [g] | 2. pre mass [g] | 1. post mass [g] | 2. post mass [g] | Sample mass [g] | [mg] | Conc. [mg/m$^3$] | [%] |
|---|---|---|---|---|---|---|---|---|---|---|
| | 0,021 | 352 | 0,08773 | | 0,08778 | 0,08776 | 0,00004 | 0,04 | 0,006 | 1% |
| Flow | 0,042 | 353 | 0,08808 | | 0,08821 | 0,08819 | 0,00012 | 0,12 | 0,019 | 2% |
| 6,168 | 0,087 | 354 | 0,08770 | | 0,08789 | 0,08785 | 0,00017 | 0,17 | 0,028 | 3% |
| m$^3$ | 0,18 | 355 | 0,08812 | | 0,08954 | 0,08945 | 0,00137 | 1,375 | 0,223 | 23% |
| | 0,35 | 356 | 0,08748 | | 0,08878 | 0,08872 | 0,00127 | 1,27 | 0,206 | 21% |
| | 0,71 | 357 | 0,08751 | | 0,08843 | 0,08839 | 0,00090 | 0,9 | 0,146 | 15% |
| | 1,4 | 358 | 0,08843 | | 0,08894 | 0,08891 | 0,00050 | 0,495 | 0,080 | 8% |
| | 2,8 | 359 | 0,08783 | | 0,08841 | 0,08840 | 0,00058 | 0,575 | 0,093 | 10% |
| | 5,6 | 360 | 0,08849 | | 0,08920 | 0,08914 | 0,00068 | 0,68 | 0,110 | 11% |
| | 11,3 | 361 | 0,08859 | | 0,08903 | 0,08897 | 0,00041 | 0,41 | 0,066 | 7% |
| | | | | | | | Sum | 6,035 | 0,978 | 100% |

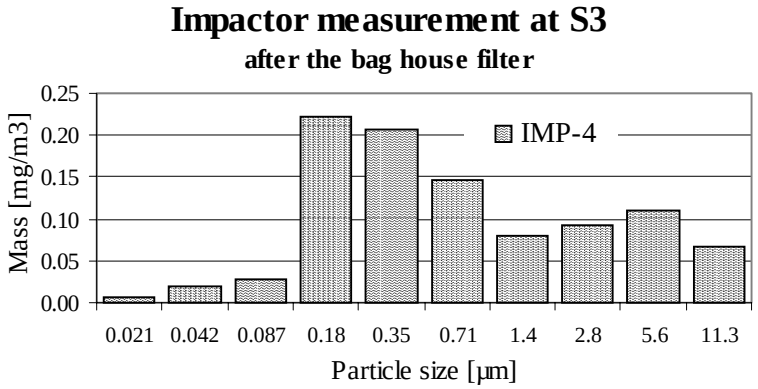


| IMP-5 | [µm] | Filter ID [ ] | 1. pre mass [g] | 2. pre mass [g] | 1. post mass [g] | 2. post mass [g] | Sample mass [g] | [mg] | Conc. [mg/m$^3$] | [%] |
|---|---|---|---|---|---|---|---|---|---|---|
| | 0,021 | 422 | 0,08808 | | 0,08822 | 0,08818 | 0,00012 | 0,12 | 0,019 | 1% |
| Flow | 0,042 | 423 | 0,08847 | | 0,08902 | 0,08900 | 0,00054 | 0,54 | 0,088 | 2% |
| 0,0508 | 0,087 | 424 | 0,08803 | | 0,08974 | 0,08971 | 0,00170 | 1,695 | 0,275 | 8% |
| m$^3$ | 0,18 | 425 | 0,08816 | | 0,09841 | | 0,01025 | 10,25 | 1,662 | 45% |
| | 0,35 | 426 | 0,08801 | | 0,09416 | | 0,00615 | 6,15 | 0,997 | 27% |
| | 0,71 | 427 | 0,08796 | | 0,09003 | | 0,00207 | 2,07 | 0,336 | 9% |
| | 1,4 | 428 | 0,08821 | | 0,08909 | | 0,00088 | 0,88 | 0,143 | 4% |
| | 2,8 | 429 | 0,08834 | | 0,08873 | 0,08873 | 0,00039 | 0,39 | 0,063 | 2% |
| | 5,6 | 430 | 0,08721 | | 0,08745 | 0,08743 | 0,00023 | 0,23 | 0,037 | 1% |
| | 11,3 | 431 | 0,08739 | | 0,08763 | 0,08761 | 0,00023 | 0,23 | 0,037 | 1% |
| | | | | | | | | 22,555 | 3,657 | 100% |

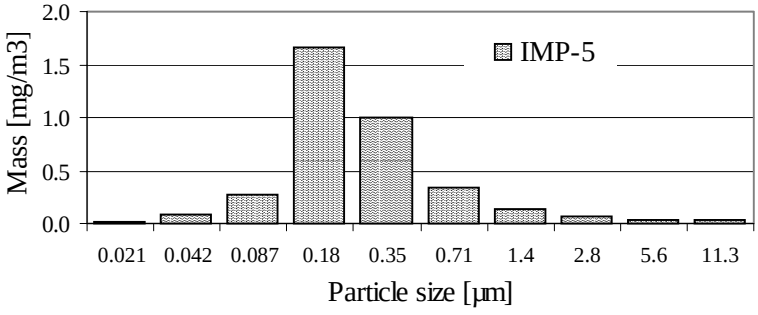

| IMP-6 | [µm] | Filter ID [ ] | 1. pre mass [g] | 2. pre mass [g] | 1. post mass [g] | 2. post mass [g] | Sample mass [g] | [mg] | Conc. [mg/m$^3$] | [%] |
|---|---|---|---|---|---|---|---|---|---|---|
| | 0,021 | 392 | 0,08742 | | 0,08744 | 0,08743 | 0,00002 | 0,015 | 0,148 | 0% |
| Flow | 0,042 | 393 | 0,08752 | | 0,08764 | 0,08755 | 0,00008 | 0,075 | 0,738 | 1% |
| 0,1016 | 0,087 | 394 | 0,08757 | | 0,08790 | 0,08788 | 0,00032 | 0,32 | 3,150 | 2% |
| m$^3$ | 0,18 | 395 | 0,08875 | | 0,09020 | 0,09020 | 0,00145 | 1,45 | 14,272 | 11% |
| | 0,35 | 396 | 0,08753 | | 0,09038 | 0,09039 | 0,00286 | 2,855 | 28,100 | 21% |
| | 0,71 | 397 | 0,08894 | | 0,09093 | 0,09092 | 0,00199 | 1,985 | 19,537 | 15% |
| | 1,4 | 398 | 0,08820 | | 0,08911 | 0,08911 | 0,00091 | 0,91 | 8,957 | 7% |
| | 2,8 | 399 | 0,08818 | | 0,08968 | 0,08965 | 0,00149 | 1,485 | 14,616 | 11% |
| | 5,6 | 400 | 0,08858 | | 0,09179 | 0,09177 | 0,00320 | 3,2 | 31,496 | 24% |
| | 11,3 | 401 | 0,08859 | | 0,08975 | 0,08976 | 0,00117 | 1,165 | 11,467 | 9% |
| | | | 0,09286 | | 0,09314 | 0,09305 | | 13,460 | 132,480 | 100% |

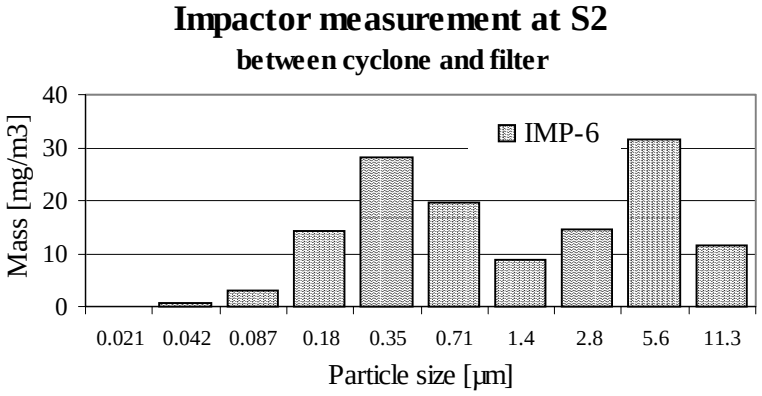


| IMP-7 | [µm] | Filter ID [ ] | 1. pre mass [g] | 2. pre mass [g] | 1. post mass [g] | 2. post mass [g] | Sample mass [g] | [mg] | Conc. [mg/m$^3$] | [%] |
|---|---|---|---|---|---|---|---|---|---|---|
| | 0,02 | 242 | 0,33041 | 0,33040 | 0,33043 | 0,33044 | 0,00003 | 0,03 | 0,886 | 1% |
| Flow | 0,04 | 243 | 0,32921 | 0,32921 | 0,32931 | 0,32922 | 0,00006 | 0,055 | 1,624 | 3% |
| 0,03386 | 0,08 | 244 | 0,33240 | 0,33239 | 0,33269 | 0,33265 | 0,00028 | 0,275 | 8,122 | 13% |
| m$^3$ | 0,18 | 245 | 0,32886 | 0,32886 | 0,32956 | 0,32966 | 0,00075 | 0,75 | 22,151 | 35% |
| | 0,35 | 246 | 0,33302 | 0,33303 | 0,33328 | 0,33323 | 0,00023 | 0,23 | 6,793 | 11% |
| | 0,71 | 247 | 0,33189 | 0,33189 | 0,33203 | 0,33195 | 0,00010 | 0,1 | 2,953 | 5% |
| | 1,4 | 248 | 0,33120 | 0,33125 | 0,33144 | 0,33146 | 0,00023 | 0,225 | 6,645 | 11% |
| | 2,8 | 249 | 0,32866 | 0,32865 | 0,32895 | 0,32896 | 0,00030 | 0,3 | 8,860 | 14% |
| | 5,6 | 250 | 0,32997 | 0,32997 | 0,33008 | 0,33008 | 0,00011 | 0,11 | 3,249 | 5% |
| | 11,3 | 251 | 0,33263 | 0,33263 | 0,33265 | 0,33269 | 0,00004 | 0,04 | 1,181 | 2% |
| | | | | | | | | 2,115 | 62,466 | 100% |

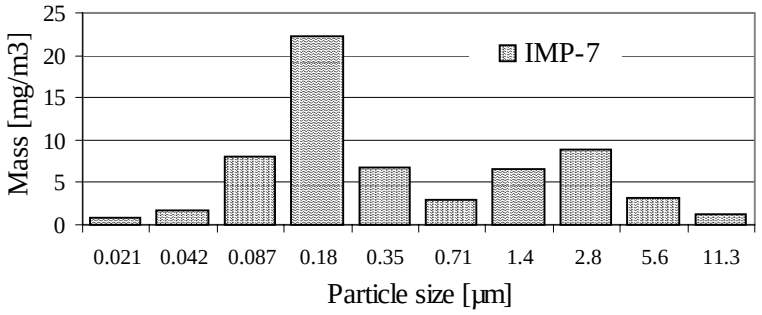

| IMP-8 | [µm] | Filter ID [ ] | 1. pre mass [g] | 2. pre mass [g] | 1. post mass [g] | 2. post mass [g] | Sample mass [g] | [mg] | Conc. [mg/m$^3$] | [%] |
|---|---|---|---|---|---|---|---|---|---|---|
| | 0,021 | 452 | 0,08812 | | 0,08816 | 0,08822 | 0,00007 | 0,07 | 0,015 | 2% |
| Flow | 0,042 | 453 | 0,08827 | | 0,08844 | 0,08840 | 0,00015 | 0,15 | 0,033 | 4% |
| 4,572 | 0,087 | 454 | 0,08746 | | 0,08757 | 0,08761 | 0,00013 | 0,13 | 0,028 | 3% |
| m$^3$ | 0,18 | 455 | 0,08822 | | 0,08890 | 0,08890 | 0,00068 | 0,68 | 0,149 | 17% |
| | 0,35 | 456 | 0,08825 | | 0,08879 | 0,08870 | 0,00049 | 0,495 | 0,108 | 13% |
| | 0,71 | 457 | 0,08710 | | 0,08746 | 0,08740 | 0,00033 | 0,33 | 0,072 | 8% |
| | 1,4 | 458 | 0,08713 | | 0,08766 | 0,08760 | 0,00050 | 0,5 | 0,109 | 13% |
| | 2,8 | 459 | 0,08815 | | 0,08870 | 0,08864 | 0,00052 | 0,52 | 0,114 | 13% |
| | 5,6 | 460 | 0,08809 | | 0,08871 | 0,08873 | 0,00063 | 0,63 | 0,138 | 16% |
| | 11,3 | 461 | 0,08745 | | 0,08787 | 0,08786 | 0,00041 | 0,415 | 0,091 | 11% |
| | | | | | | | | 3,920 | 0,857 | 100% |

**Impactor measurement at S3**

**after the bag house filter**

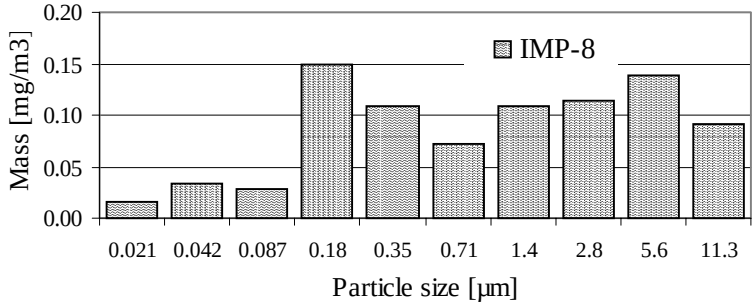


| IMP-9 | [µm] | Filter ID [ ] | 1. pre mass [g] | 2. pre mass [g] | 1. post mass [g] | 2. post mass [g] | Sample mass [g] | [mg] | Conc. [mg/m$^3$] | [%] |
|---|---|---|---|---|---|---|---|---|---|---|
| | 0,02 | 462 | 0,08815 | | 0,08818 | 0,08821 | 0,00004 | 0,045 | 1,314 | 4% |
| Flow | 0,04 | 463 | 0,08980 | | 0,08984 | 0,08986 | 0,00005 | 0,05 | 1,460 | 4% |
| 0,03426 | 0,08 | 464 | 0,08962 | | 0,08974 | 0,08969 | 0,00009 | 0,095 | 2,773 | 8% |
| m$^3$ | 0,18 | 465 | 0,08873 | | 0,08913 | 0,08909 | 0,00038 | 0,38 | 11,092 | 32% |
| | 0,35 | 466 | 0,08946 | | 0,08959 | 0,08959 | 0,00013 | 0,13 | 3,795 | 11% |
| | 0,71 | 467 | 0,08919 | | 0,08924 | 0,08927 | 0,00006 | 0,065 | 1,897 | 6% |
| | 1,4 | 468 | 0,08849 | | 0,08861 | 0,08861 | 0,00012 | 0,12 | 3,503 | 10% |
| | 2,8 | 469 | 0,08828 | | 0,08851 | 0,08846 | 0,00021 | 0,205 | 5,984 | 17% |
| | 5,6 | 470 | 0,08807 | | 0,08815 | 0,08816 | 0,00009 | 0,085 | 2,481 | 7% |
| | 11,3 | 471 | 0,08816 | | 0,08818 | 0,08814 | 0,00000 | - | 0,000 | 0% |
| | | | | | | | | 1,175 | 34,298 | 100% |

**Impactor measurement at S2**

**between cyclone and filter**

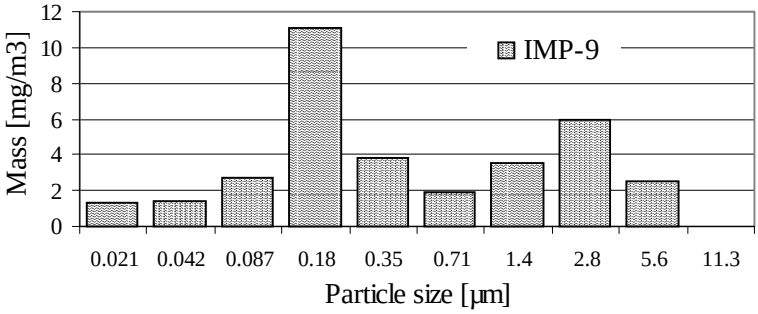

| IMP-10 | | Filter ID | 1. pre mass | 2. pre mass | 1. post mass | 2. post mass | Sample mass | | Conc. | |
|---|---|---|---|---|---|---|---|---|---|---|
| | [µm] | [ ] | [g] | [g] | [g] | [g] | [g] | [mg] | [mg/m$^3$] | [%] |
| | 0,02 | 252 | 0,32893 | 0,32890 | 0,32899 | 0,32898 | 0,00007 | 0,07 | 2,0 | 4% |
| Flow | 0,04 | 253 | 0,32993 | 0,32993 | 0,33005 | 0,33001 | 0,00010 | 0,1 | 2,9 | 6% |
| 0,0342 | 0,08 | 254 | 0,33127 | 0,33123 | 0,33155 | 0,33154 | 0,00029 | 0,295 | 8,6 | 18% |
| m$^3$ | 0,18 | 255 | 0,33344 | 0,33332 | 0,33398 | 0,33393 | 0,00057 | 0,575 | 16,8 | 35% |
| | 0,35 | 256 | 0,33362 | 0,33362 | 0,33377 | 0,33379 | 0,00016 | 0,16 | 4,7 | 10% |
| | 0,71 | 257 | 0,33220 | 0,33218 | 0,33226 | 0,33225 | 0,00006 | 0,065 | 1,9 | 4% |
| | 1,4 | 258 | 0,33026 | 0,33027 | 0,33029 | 0,33030 | 0,00003 | 0,03 | 0,9 | 2% |
| | 2,8 | 259 | | 0,33008 | 0,33009 | 0,33008 | 0,00000 | 0,005 | 0,1 | 0% |
| | 5,6 | 260 | 0,33137 | 0,33197 | 0,33203 | 0,33198 | 0,00033 | 0,335 | 9,8 | 20% |
| | 11,3 | 261 | 0,33141 | 0,33135 | 0,33144 | 0,33137 | 0,00002 | 0,025 | 0,7 | 2% |
| | | | | | | | | 1,660 | 48,5 | 100% |

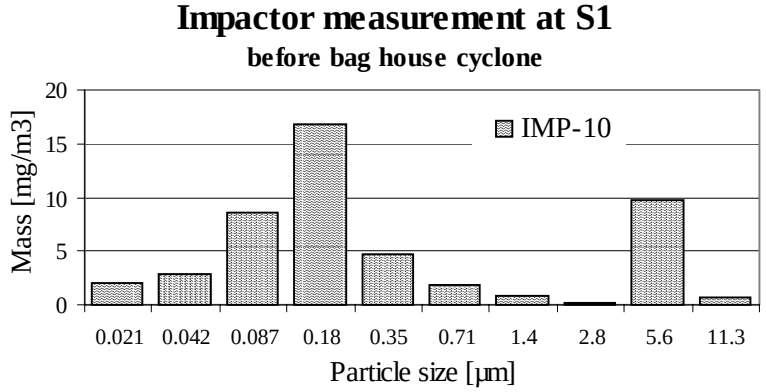


| IMP-11 | | Filter ID | 1. pre mass | 2. pre mass | 1. post mass | 2. post mass | Sample mass | | Conc. | |
|---|---|---|---|---|---|---|---|---|---|---|
| | [µm] | [ ] | [g] | [g] | [g] | [g] | [g] | [mg] | [mg/m$^3$] | [%] |
| | 0,02 | 362 | 0,08774 | | 0,08788 | 0,08783 | 0,00012 | 0,115 | 4,528 | 24% |
| Flow | 0,04 | 363 | 0,08773 | | 0,08767 | 0,08766 | -0,00007 | -0,065 | -2,559 | -14% |
| 0,0254 | 0,08 | 364 | 0,08789 | | 0,08796 | 0,08795 | 0,00007 | 0,065 | 2,559 | 14% |
| m$^3$ | 0,18 | 365 | 0,08815 | | 0,08824 | 0,08825 | 0,00009 | 0,095 | 3,740 | 20% |
| | 0,35 | 366 | 0,08826 | | 0,08830 | 0,08831 | 0,00004 | 0,045 | 1,772 | 9% |
| | 0,71 | 367 | 0,08792 | | 0,08800 | 0,08799 | 0,00007 | 0,075 | 2,953 | 16% |
| | 1,4 | 368 | 0,08800 | | | 0,08806 | 0,00006 | 0,06 | 2,362 | 13% |
| | 2,8 | 369 | 0,08855 | | 0,08863 | 0,08860 | 0,00006 | 0,065 | 2,559 | 14% |
| | 5,6 | 370 | 0,08797 | | 0,08802 | 0,08798 | 0,00003 | 0,03 | 1,181 | 6% |
| | 11,3 | 371 | 0,08794 | | 0,08792 | 0,08794 | -0,00001 | -0,01 | -0,394 | -2% |
| | | | | | | | | 0,475 | 18,701 | 100% |

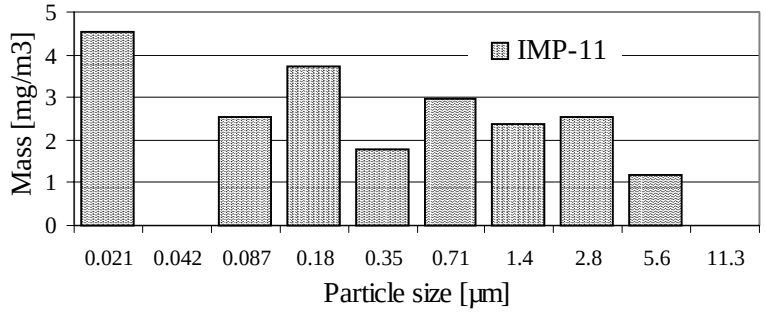

| IMP-12 | [µm] | Filter ID [ ] | 1. pre mass [g] | 2. pre mass [g] | 1. post mass [g] | 2. post mass [g] | Sample mass [g] | [mg] | Conc. [mg/m$^3$] | [%] |
|---|---|---|---|---|---|---|---|---|---|---|
| | 0.021 | 472 | 0.08719 | | 0.08738 | 0.08728 | 0.00014 | 0.14 | 5.512 | 3% |
| Flow | 0.042 | 473 | 0.08755 | | 0.08770 | 0.08778 | 0.00019 | 0.19 | 7.480 | 5% |
| 0.0254 | 0.087 | 474 | 0.08733 | | 0.08768 | 0.08790 | 0.00046 | 0.46 | 18.110 | 11% |
| m$^3$ | 0.18 | 475 | 0.08787 | | 0.08925 | 0.08926 | 0.00139 | 1.385 | 54.528 | 33% |
| | 0.35 | 476 | 0.08792 | | 0.08863 | 0.08878 | 0.00079 | 0.785 | 30.906 | 19% |
| | 0.71 | 477 | 0.08785 | | 0.08806 | 0.08805 | 0.00020 | 0.205 | 8.071 | 5% |
| | 1.4 | 478 | 0.08905 | | 0.08928 | 0.08922 | 0.00020 | 0.2 | 7.874 | 5% |
| | 2.8 | 479 | 0.08918 | | 0.08943 | 0.08956 | 0.00031 | 0.315 | 12.402 | 8% |
| | 5.6 | 480 | 0.08884 | | 0.08914 | 0.08914 | 0.00030 | 0.3 | 11.811 | 7% |
| | 11.3 | 481 | 0.08865 | | 0.08881 | 0.08891 | 0.00021 | 0.21 | 8.268 | 5% |
| | | | | | | | | 4.190 | 164.961 | 100% |

**Impactor measurement at S1**

**before bag house cyclone**

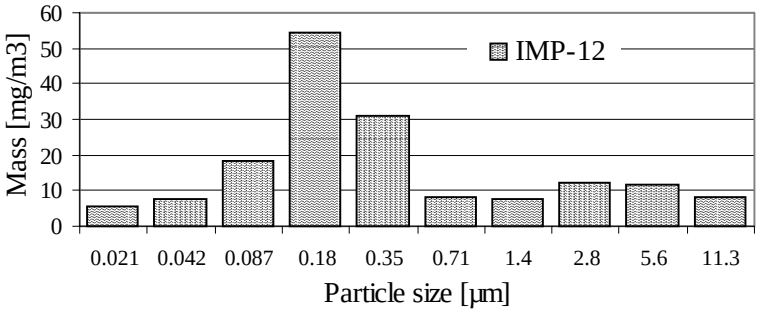


| IMP-13 | [µm] | Filter ID [ ] | 1. pre mass [g] | 2. pre mass [g] | 1. post mass [g] | 2. post mass [g] | Sample mass [g] | [mg] | Conc. [mg/m$^3$] | [%] |
|---|---|---|---|---|---|---|---|---|---|---|
| | 0,02 | 432 | 0,08759 | | 0,08767 | 0,08764 | 0,00006 | 0,065 | 2,529 | 2% |
| Flow | 0,04 | 433 | 0,08833 | | 0,08840 | 0,08851 | 0,00013 | 0,125 | 4,864 | 3% |
| 0,0257 | 0,08 | 434 | 0,08802 | | 0,08851 | 0,08854 | 0,00050 | 0,505 | 19,650 | 14% |
| m$^3$ | 0,18 | 435 | 0,08710 | | 0,08831 | 0,08834 | 0,00123 | 1,225 | 47,665 | 34% |
| | 0,35 | 436 | 0,08892 | | 0,08963 | 0,08960 | 0,00070 | 0,695 | 27,043 | 19% |
| | 0,71 | 437 | 0,08886 | | 0,08914 | 0,08917 | 0,00030 | 0,295 | 11,479 | 8% |
| | 1,4 | 438 | 0,08903 | | 0,08919 | 0,08919 | 0,00016 | 0,16 | 6,226 | 4% |
| | 2,8 | 439 | 0,08841 | | 0,08866 | 0,08855 | 0,00020 | 0,195 | 7,588 | 5% |
| | 5,6 | 440 | 0,08908 | | 0,08927 | 0,08922 | 0,00016 | 0,165 | 6,420 | 5% |
| | 11,3 | 441 | 0,08906 | | 0,08927 | 0,08926 | 0,00021 | 0,205 | 7,977 | 6% |
| | | | | | | | | 3,635 | 141,440 | 100% |

**Impactor measurement at S2**

**between cyclone and filter**

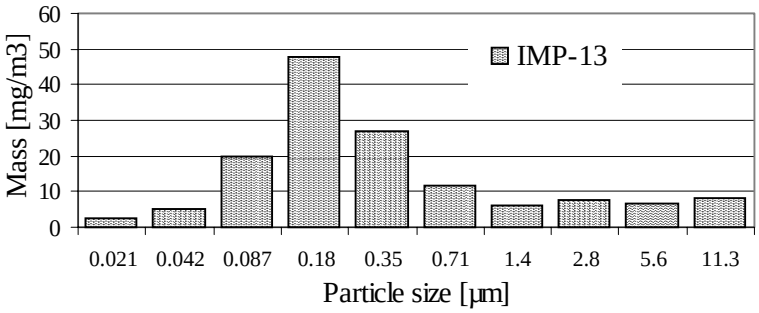

| IMP-14 | | Filter ID | 1. pre mass | 2. pre mass | 1. post mass | 2. post mass | Sample mass | | Conc. | |
|---|---|---|---|---|---|---|---|---|---|---|
| | [µm] | [ ] | [g] | [g] | [g] | [g] | [g] | [mg] | [mg/m$^3$] | [%] |
| | 0,02 | 272 | 0,32859 | 0,32861 | 0,32870 | 0,32871 | 0,00011 | 0,105 | 4,134 | 2% |
| Flow | 0,04 | 273 | 0,32982 | 0,32982 | 0,33014 | 0,33015 | 0,00033 | 0,325 | 12,795 | 5% |
| 0,0254 | 0,08 | 274 | 0,32922 | 0,32923 | 0,32980 | 0,32981 | 0,00058 | 0,58 | 22,835 | 9% |
| m$^3$ | 0,18 | 275 | 0,32997 | 0,32995 | 0,33269 | 0,33254 | 0,00265 | 2,655 | 104,528 | 40% |
| | 0,35 | 276 | 0,32995 | 0,32992 | 0,33140 | 0,33132 | 0,00143 | 1,425 | 56,102 | 22% |
| | 0,71 | 277 | 0,33191 | 0,33195 | 0,33261 | 0,33264 | 0,00070 | 0,695 | 27,362 | 10% |
| | 1,4 | 278 | 0,32943 | 0,32943 | 0,32971 | 0,32982 | 0,00033 | 0,335 | 13,189 | 5% |
| | 2,8 | 279 | 0,33197 | 0,33198 | 0,33224 | 0,33209 | 0,00019 | 0,19 | 7,480 | 3% |
| | 5,6 | 280 | 0,32876 | 0,32876 | 0,32890 | 0,32885 | 0,00012 | 0,115 | 4,528 | 2% |
| | 11,3 | 281 | 0,33056 | 0,33059 | 0,33081 | 0,33074 | 0,00020 | 0,2 | 7,874 | 3% |
| | | | | | | | | 6,625 | 260,827 | 100% |

## Impactor measurement at S1

**before bag house cyclone**

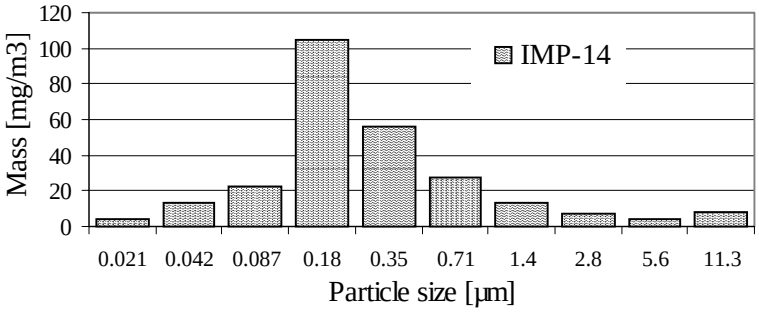


| IMP-15 | | Filter ID | 1. pre mass | 2. pre mass | 1. post mass | 2. post mass | Sample mass | | Conc. | |
|---|---|---|---|---|---|---|---|---|---|---|
| | [µm] | [ ] | [g] | [g] | [g] | [g] | [g] | [mg] | [mg/m$^3$] | [%] |
| | 0,02 | 262 | 0,33080 | 0,33078 | 0,33087 | 0,33093 | 0,00011 | 0,11 | 4,280 | 2% |
| Flow | 0,04 | 263 | 0,33046 | 0,33043 | 0,33061 | 0,33076 | 0,00024 | 0,24 | 9,339 | 4% |
| 0,0257 | 0,08 | 264 | | 0,32901 | 0,32945 | 0,32951 | 0,00047 | 0,47 | 18,288 | 8% |
| m$^3$ | 0,18 | 265 | | 0,32953 | 0,33213 | 0,33209 | 0,00258 | 2,58 | 100,389 | 42% |
| | 0,35 | 266 | | 0,32976 | 0,33102 | 0,33100 | 0,00125 | 1,25 | 48,638 | 20% |
| | 0,71 | 267 | 0,33245 | 0,33250 | 0,33310 | 0,33306 | 0,00061 | 0,605 | 23,541 | 10% |
| | 1,4 | 268 | 0,33156 | 0,33159 | 0,33187 | 0,33193 | 0,00032 | 0,325 | 12,646 | 5% |
| | 2,8 | 269 | 0,32969 | 0,32970 | 0,32990 | 0,32996 | 0,00024 | 0,235 | 9,144 | 4% |
| | 5,6 | 270 | 0,33180 | 0,33178 | 0,33184 | 0,33200 | 0,00013 | 0,13 | 5,058 | 2% |
| | 11,3 | 271 | 0,32980 | 0,32983 | 0,33001 | 0,32995 | 0,00017 | 0,165 | 6,420 | 3% |
| | | | | | | | | 6,110 | 237,743 | 100% |

## Impactor measurement at S2

**between cyclone and filter**

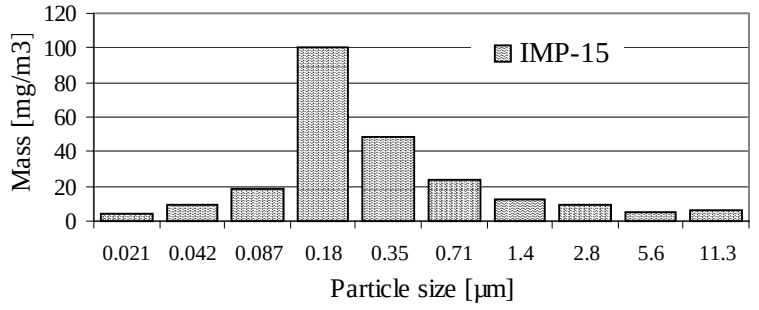

| IMP-16 | | Filter ID | 1. pre mass | 2. pre mass | 1. post mass | 2. post mass | Sample mass | | Conc. | |
|---|---|---|---|---|---|---|---|---|---|---|
| | [µm] | [ ] | [g] | [g] | [g] | [g] | [g] | [mg] | [mg/m$^3$] | [%] |
| | 0,02 | 282 | 0,32965 | 0,32964 | 0,32971 | 0,32969 | 5,5E-05 | 0,055 | 2,853 | 1% |
| Flow | 0,04 | 283 | 0,32831 | 0,32829 | 0,32858 | 0,32855 | 0,000265 | 0,265 | 13,748 | 3% |
| 0,0193 | 0,08 | 284 | 0,32661 | 0,32664 | 0,32742 | 0,3274 | 0,000785 | 0,785 | 40,726 | 8% |
| m$^3$ | 0,18 | 285 | 0,33539 | 0,33541 | 0,33821 | | 0,00281 | 2,81 | 145,785 | 30% |
| | 0,35 | 286 | 0,32836 | 0,32835 | 0,33195 | | 0,003595 | 3,595 | 186,511 | 38% |
| | 0,71 | 287 | 0,32946 | 0,32948 | 0,33036 | | 0,00089 | 0,89 | 46,174 | 10% |
| | 1,4 | 288 | 0,33036 | 0,33032 | 0,33087 | 0,33081 | 0,0005 | 0,5 | 25,940 | 5% |
| | 2,8 | 289 | 0,32524 | 0,32525 | 0,32548 | 0,32552 | 0,000255 | 0,255 | 13,230 | 3% |
| | 5,6 | 290 | 0,32864 | 0,32863 | 0,32879 | 0,32873 | 0,000125 | 0,125 | 6,485 | 1% |
| | 11,3 | 291 | 0,32858 | 0,3286 | 0,32869 | 0,32866 | 8,5E-05 | 0,085 | 4,410 | 1% |
| | | | | | | | | 9,365 | 485,863 | 100% |

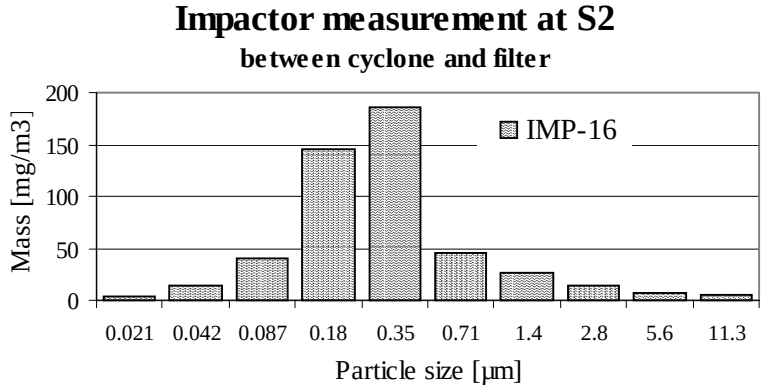


| IMP-17 | | Filter ID | 1. pre mass | 2. pre mass | 1. post mass | 2. post mass | Sample mass | | Conc. | |
|---|---|---|---|---|---|---|---|---|---|---|
| | [µm] | [ ] | [g] | [g] | [g] | [g] | [g] | [mg] | [mg/m$^3$] | [%] |
| | 0,02 | 342 | 0,08833 | 0,08833 | 0,08838 | 0,08847 | 0,00009 | 0,095 | 5,0 | 1% |
| Flow | 0,04 | 343 | 0,08805 | 0,08805 | 0,08826 | 0,08826 | 0,00021 | 0,21 | 11,0 | 2% |
| 0,01905 | 0,08 | 344 | 0,08775 | 0,08774 | 0,08850 | 0,08852 | 0,00077 | 0,765 | 40,2 | 7% |
| m$^3$ | 0,18 | 345 | 0,08782 | 0,08780 | 0,09131 | 0,09146 | 0,00357 | 3,575 | 187,7 | 31% |
| | 0,35 | 346 | 0,08821 | 0,08819 | 0,09327 | 0,09294 | 0,00490 | 4,905 | 257,5 | 43% |
| | 0,71 | 347 | 0,08827 | 0,08828 | 0,08938 | 0,08941 | 0,00112 | 1,12 | 58,8 | 10% |
| | 1,4 | 348 | 0,08901 | 0,08905 | 0,08953 | 0,08955 | 0,00051 | 0,51 | 26,8 | 4% |
| | 2,8 | 349 | 0,08895 | 0,08895 | 0,08917 | 0,08912 | 0,00020 | 0,195 | 10,2 | 2% |
| | 5,6 | 350 | 0,08809 | 0,08811 | 0,08820 | 0,08813 | 0,00006 | 0,065 | 3,4 | 1% |
| | 11,3 | 351 | 0,08850 | 0,08844 | 0,08849 | 0,08843 | -0,00001 | -0,01 | -0,5 | 0% |
| | | | | | | | Sum | 11,4 | 600 | 100% |

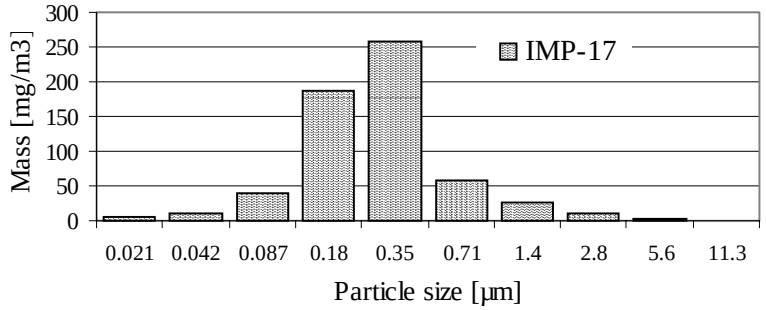

| IMP-18 | | Filter ID | 1. pre mass | 2. pre mass | 1. post mass | 2. post mass | Sample mass | | Conc. | |
|---|---|---|---|---|---|---|---|---|---|---|
| | [µm] | [ ] | [g] | [g] | [g] | [g] | [g] | [mg] | [mg/m$^3$] | [%] |
| | 1 | 292 | 0,32788 | 0,32790 | 0,32802 | 0,32800 | 0,00012 | 0,12 | 0,039 | 6% |
| Flow | 2 | 293 | 0,33063 | 0,33061 | 0,33076 | 0,33078 | 0,00015 | 0,15 | 0,049 | 8% |
| 3,048 | 3 | 294 | 0,32888 | 0,32884 | 0,32906 | 0,32885 | 0,00009 | 0,095 | 0,031 | 5% |
| m$^3$ | 4 | 295 | 0,32981 | 0,32983 | 0,33036 | 0,33017 | 0,00045 | 0,445 | 0,146 | 23% |
| | 5 | 296 | 0,33265 | 0,33263 | 0,33288 | 0,33283 | 0,00022 | 0,215 | 0,071 | 11% |
| | 6 | 297 | 0,32925 | 0,32926 | 0,32942 | 0,32944 | 0,00018 | 0,175 | 0,057 | 9% |
| | 7 | 298 | 0,32946 | 0,32948 | 0,32954 | 0,32970 | 0,00015 | 0,15 | 0,049 | 8% |
| | 8 | 299 | 0,32880 | 0,32881 | 0,32895 | 0,32903 | 0,00018 | 0,185 | 0,061 | 9% |
| | 9 | 300 | 0,33376 | 0,33373 | 0,33400 | 0,33392 | 0,00022 | 0,215 | 0,071 | 11% |
| | 10 | 301 | 0,32748 | 0,32747 | 0,32765 | 0,32770 | 0,00020 | 0,2 | 0,066 | 10% |
| | | | | | | | Sum | 1,950 | 0,640 | 100% |

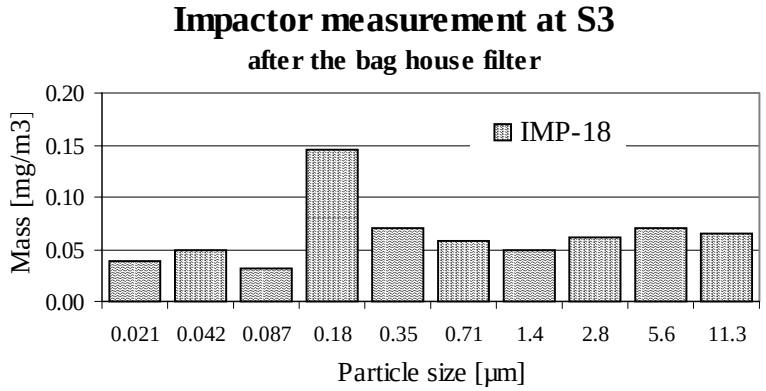


| IMP-19 | | Filter ID | 1. pre mass | 2. pre mass | 1. post mass | 2. post mass | Sample mass | | Conc. | |
|---|---|---|---|---|---|---|---|---|---|---|
| | [µm] | [ ] | [g] | [g] | [g] | [g] | [g] | [mg] | [mg/m$^3$] | [%] |
| | 1 | 372 | 0,08799 | | 0,08805 | 0,08802 | 0,00005 | 0,0450 | 1,8 | 1% |
| Flow | 2 | 373 | 0,08820 | | 0,08836 | 0,08836 | 0,00016 | 0,1600 | 6,2 | 2% |
| 0,0257 | 3 | 374 | 0,08837 | | 0,08915 | 0,08912 | 0,00076 | 0,7650 | 29,8 | 10% |
| m$^3$ | 4 | 375 | 0,08844 | | 0,09153 | 0,09214 | 0,00340 | 3,3950 | 132,1 | 45% |
| | 5 | 376 | 0,08860 | | 0,09072 | 0,09068 | 0,00210 | 2,1000 | 81,7 | 28% |
| | 6 | 377 | 0,08806 | | 0,08858 | 0,08854 | 0,00050 | 0,5000 | 19,5 | 7% |
| | 7 | 378 | 0,08882 | | 0,08924 | 0,08929 | 0,00045 | 0,4450 | 17,3 | 6% |
| | 8 | 379 | 0,08880 | | 0,08896 | 0,08895 | 0,00016 | 0,1550 | 6,0 | 2% |
| | 9 | 380 | 0,08839 | | 0,08842 | 0,08843 | 0,00004 | 0,0350 | 1,4 | 0% |
| | 10 | 381 | 0,08889 | | 0,08890 | 0,08887 | 0,00000 | -0,0050 | -0,2 | 0% |
| | | | | | | | Sum | 7,5950 | 295,5 | 100% |

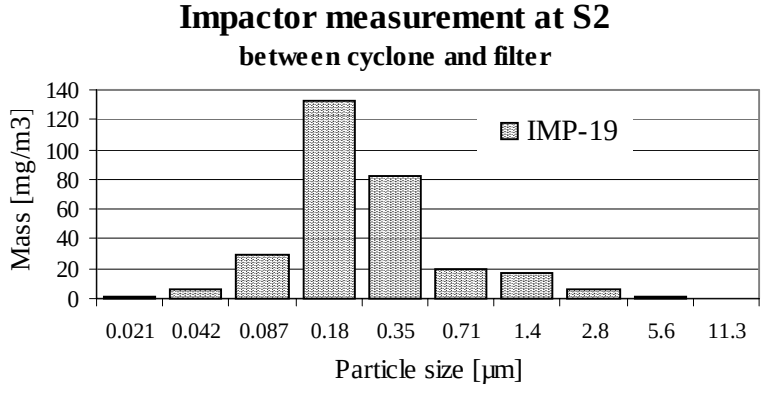

| IMP-20 | | Filter ID | 1. pre mass | 2. pre mass | 1. post mass | 2. post mass | Sample mass | | Conc. | |
|---|---|---|---|---|---|---|---|---|---|---|
| | [µm] | [ ] | [g] | [g] | [g] | [g] | [g] | [mg] | [mg/m$^3$] | [%] |
| | 1 | 302 | 0,33375 | 0,33372 | 0,33369 | 0,33377 | -0,00001 | -0,005 | -0,002 | -1% |
| Flow | 2 | 303 | 0,32519 | 0,32514 | 0,32521 | 0,32522 | 0,00005 | 0,05 | 0,016 | 7% |
| 0,01285 | 3 | 304 | 0,32756 | 0,32758 | 0,32773 | 0,32771 | 0,00015 | 0,15 | 0,049 | 20% |
| m$^3$ | 4 | 305 | 0,32759 | 0,32757 | 0,32779 | 0,32793 | 0,00028 | 0,28 | 0,092 | 37% |
| | 5 | 306 | 0,32801 | 0,32801 | 0,32809 | 0,32804 | 0,00005 | 0,055 | 0,018 | 7% |
| | 6 | 307 | 0,32821 | 0,32819 | 0,32823 | 0,32819 | 0,00001 | 0,01 | 0,003 | 1% |
| | 7 | 308 | 0,32716 | 0,32713 | 0,32722 | 0,32719 | 0,00006 | 0,06 | 0,020 | 8% |
| | 8 | 309 | 0,32904 | 0,32903 | 0,32910 | 0,32908 | 0,00006 | 0,055 | 0,018 | 7% |
| | 9 | 310 | 0,32704 | 0,32712 | 0,32712 | 0,32712 | 0,00004 | 0,04 | 0,013 | 5% |
| | 10 | 311 | 0,32638 | 0,32633 | 0,32647 | 0,32636 | 0,00006 | 0,06 | 0,020 | 8% |
| | | | | | | | Sum | 0,755 | 0,248 | 100% |

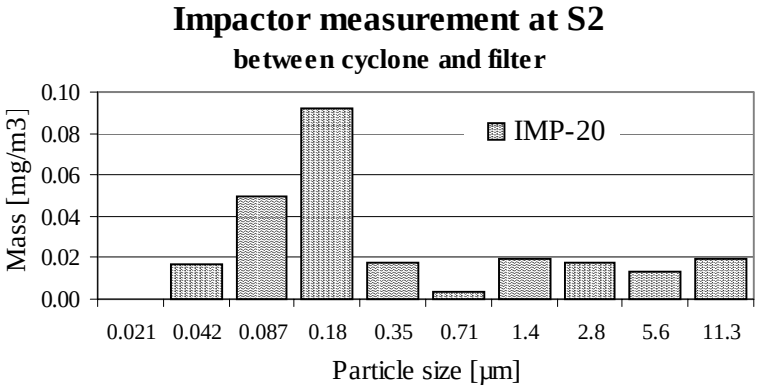


| IMP-21 | | Filter ID | 1. pre mass | 2. pre mass | 1. post mass | 2. post mass | Sample mass | | Conc. | |
|---|---|---|---|---|---|---|---|---|---|---|
| | [µm] | [ ] | [g] | [g] | [g] | [g] | [g] | [mg] | [mg/m$^3$] | [%] |
| | 0,02 | 382 | 0,08833 | | 0,08831 | 0,08826 | -0,00005 | -0,045 | -1,751 | -6% |
| Flow | 0,04 | 383 | 0,08802 | | 0,08801 | 0,08796 | -0,00003 | -0,035 | -1,362 | -4% |
| 0,0257 | 0,08 | 384 | 0,08802 | | 0,08812 | 0,08812 | 0,00010 | 0,1 | 3,891 | 13% |
| m$^3$ | 0,18 | 385 | 0,08804 | | 0,08854 | 0,08849 | 0,00048 | 0,475 | 18,482 | 60% |
| | 0,35 | 386 | 0,08768 | | 0,08775 | 0,08777 | 0,00008 | 0,08 | 3,113 | 10% |
| | 0,71 | 387 | 0,08782 | | 0,08793 | 0,08788 | 0,00009 | 0,085 | 3,307 | 11% |
| | 1,4 | 388 | 0,08769 | | 0,08773 | 0,08773 | 0,00004 | 0,04 | 1,556 | 5% |
| | 2,8 | 389 | 0,08803 | | 0,08809 | 0,08808 | 0,00005 | 0,055 | 2,140 | 7% |
| | 5,6 | 390 | 0,08772 | | 0,08775 | 0,08774 | 0,00002 | 0,025 | 0,973 | 3% |
| | 11,3 | 391 | 0,08742 | | 0,08744 | 0,08743 | 0,00002 | 0,015 | 0,584 | 2% |
| | | | | | | | Sum | 0,795 | 30,934 | 100% |

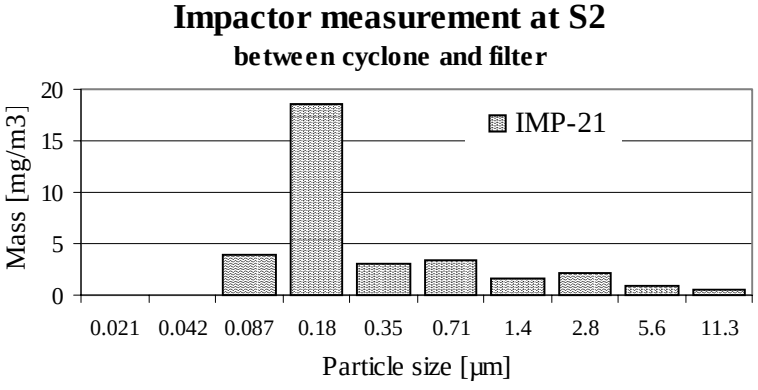

| IMP-22 | [µm] | Filter ID [ ] | 1. pre mass [g] | 2. pre mass [g] | 1. post mass [g] | 2. post mass [g] | Sample mass [g] | [mg] | Conc. [mg/m$^3$] | [%] |
|---|---|---|---|---|---|---|---|---|---|---|
| | 0,02 | 482 | 0,08928 | | 0,08927 | 0,08928 | -0,00001 | -0,005 | -0,197 | -1% |
| Flow | 0,04 | 483 | 0,09807 | | 0,09808 | 0,09811 | 0,00002 | 0,025 | 0,984 | 3% |
| 0,0254 | 0,08 | 484 | 0,08836 | | 0,08841 | 0,08836 | 0,00002 | 0,025 | 0,984 | 3% |
| m$^3$ | 0,18 | 485 | 0,08879 | | 0,08909 | 0,08913 | 0,00032 | 0,32 | 12,598 | 44% |
| | 0,35 | 486 | 0,08890 | | 0,08905 | 0,08904 | 0,00014 | 0,145 | 5,709 | 20% |
| | 0,71 | 487 | 0,08871 | | 0,08869 | 0,08872 | 0,00000 | -0,005 | -0,197 | -1% |
| | 1,4 | 488 | 0,08867 | | 0,08872 | 0,08872 | 0,00005 | 0,05 | 1,969 | 7% |
| | 2,8 | 489 | 0,08833 | | 0,08840 | 0,08848 | 0,00011 | 0,11 | 4,331 | 15% |
| | 5,6 | 490 | 0,08943 | | 0,08941 | 0,08950 | 0,00003 | 0,025 | 0,984 | 3% |
| | 11,3 | 491 | 0,08844 | | 0,08842 | 0,08854 | 0,00004 | 0,04 | 1,575 | 5% |
| | | | | | | | Sum | 0,730 | 28,740 | 100% |

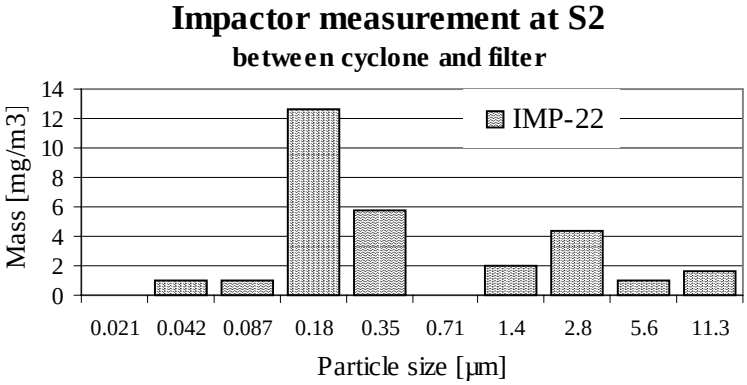

# Appendix C

Review of activity measurement on impactor foils. The data have been summed for particles less than 1 µm (stage 1 to 6) and particles larger than 1 µm (stage 7 - 10) for activity and mass. Specific activities have then been calculated for the two size groups.

| Measurement | | Particles smaller than 1 µm | | | Particles larger than 1 µm | | |
|---|---|---|---|---|---|---|---|
| ID | Position | Mass [mg] | Activity [Bq] | Specific act. [Bq/g] | Mass [mg] | Activity [Bq] | Specific act. [Bq/g] |
| IMP 3 | S3 | 4,1 | 0,123 | 30 | 7,0 | 0,045 | 6 |
| IMP 4 | S3 | 3,9 | 0,0656 | 17 | 2,2 | 0,034 | 16 |
| IMP 5 | S1 | 20,8 | 0,179 | 9 | 1,7 | 0,034 | 20 |
| IMP 6 | S2 | 6,7 | 0,2791 | 42 | 6,8 | 0,150 | 22 |
| IMP 12 | S1 | 3,2 | 0,085 | 27 | 1,0 | 0,023 | 23 |
| IMP 13 | S2 | 2,9 | 0,058 | 20 | 0,7 | 0,023 | 31 |
| IMP 17 | S2 | 10,7 | 0,012 | 1 | | BDL | |

**Detailed results:**

| **IMP 3** Stage | Par. Size [µm] | Cs-137 [Bq] | s.d. [Bq] | Load [mg] | Mass load [mg/m3] | Specifi act. [Bq/g] |
|---|---|---|---|---|---|---|
| 1 | 0.021 | -0.0023 | 0.0038 | 0.0650 | 0.01 | -35 |
| 2 | 0.042 | 0.0029 | 0.0038 | 0.1800 | 0.03 | 16 |
| 3 | 0.087 | 0.0047 | 0.0048 | 0.0750 | 0.01 | 63 |
| 4 | 0.18 | 0.0458 | 0.0052 | 1.0950 | 0.18 | 42 |
| 5 | 0.35 | 0.0582 | 0.0061 | 1.8750 | 0.30 | 31 |
| 6 | 0.71 | 0.0132 | 0.0041 | 0.7600 | 0.12 | 17 |
| 7 | 1.4 | 0.0056 | 0.0053 | 1.0550 | 0.17 | 5 |
| 8 | 2.8 | 0.0102 | 0.0037 | 1.7150 | 0.28 | 6 |
| 9 | 5.6 | 0.01838 | 0.00445 | 2.5200 | 0.41 | 7 |
| 10 | 11.3 | 0.011 | 0.00445 | 1.7400 | 0.28 | 6 |

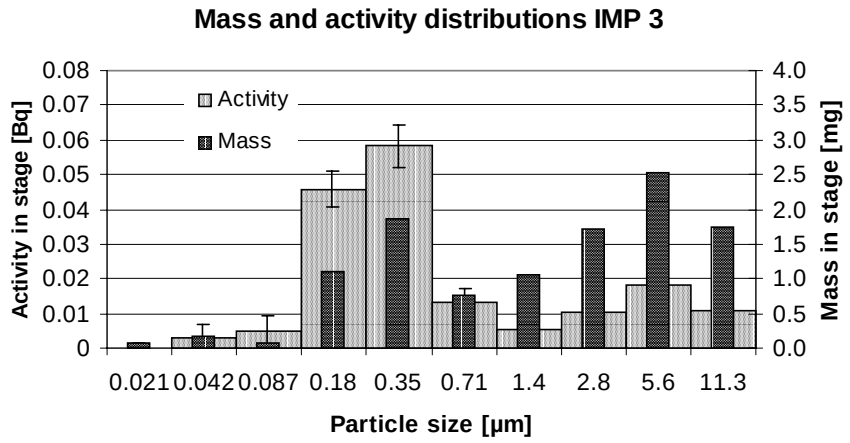

| **IMP4** Stage | Par. Size [µm] | Cs-137 [Bq] | s.d. [Bq] | Load [mg] [mg] | Mass load [mg/m3] | Specifi act. [Bq/g] |
|---|---|---|---|---|---|---|
| 1 | 0,021 | -0,0002 | 0,0052 | 0,0400 | 0,01 | -5 |
| 2 | 0,042 | 0,0106 | 0,0052 | 0,1200 | 0,02 | 88 |
| 3 | 0,087 | 0,0074 | 0,0031 | 0,1700 | 0,03 | 44 |
| 4 | 0,18 | 0,021 | 0,0039 | 1,3750 | 0,22 | 15 |
| 5 | 0,35 | 0,0133 | 0,0042 | 1,2700 | 0,21 | 10 |
| 6 | 0,71 | 0,0135 | 0,0048 | 0,9000 | 0,15 | 15 |
| 7 | 1,4 | 0,006 | 0,0042 | 0,4950 | 0,08 | 12 |
| 8 | 2,8 | 0,0093 | 0,0045 | 0,5750 | 0,09 | 16 |
| 9 | 5,6 | 0,0077 | 0,0051 | 0,6800 | 0,11 | 11 |
| 10 | 11,3 | 0,011 | 0,0051 | 0,4100 | 0,07 | 27 |

**Mass and activity distributions IMP 4**

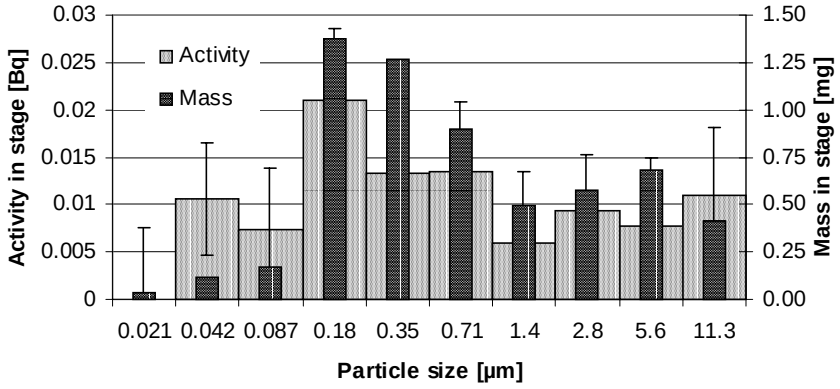


| **IMP 5** Stage | Par. Size [µm] | Cs-137 [Bq] | s.d. [Bq] | Load [mg] [g] | Mass load [mg/m3] | Specifi act. [Bq/g] |
|---|---|---|---|---|---|---|
| 1 | 0.021 | 0.0174 | 0.006 | 0.12 | 0.02 | 145 |
| 2 | 0.042 | 0.0108 | 0.006 | 0.54 | 0.09 | 20 |
| 3 | 0.087 | 0.0283 | 0.0065 | 1.695 | 0.27 | 17 |
| 4 | 0.18 | 0.0654 | 0.0076 | 10.25 | 1.66 | 6 |
| 5 | 0.35 | 0.0375 | 0.0089 | 6.15 | 1.00 | 6 |
| 6 | 0.71 | 0.0199 | 0.0073 | 2.07 | 0.34 | 10 |
| 7 | 1.4 | 0.0081 | 0.0074 | 0.88 | 0.14 | 9 |
| 8 | 2.8 | 0.0146 | 0.006 | 0.39 | 0.06 | 37 |
| 9 | 5.6 | 0.0057 | 0.0072 | 0.23 | 0.04 | 25 |
| 10 | 11.3 | 0.011 | 0.0072 | 0.23 | 0.04 | 48 |

**Mass and activity distributions IMP 5**

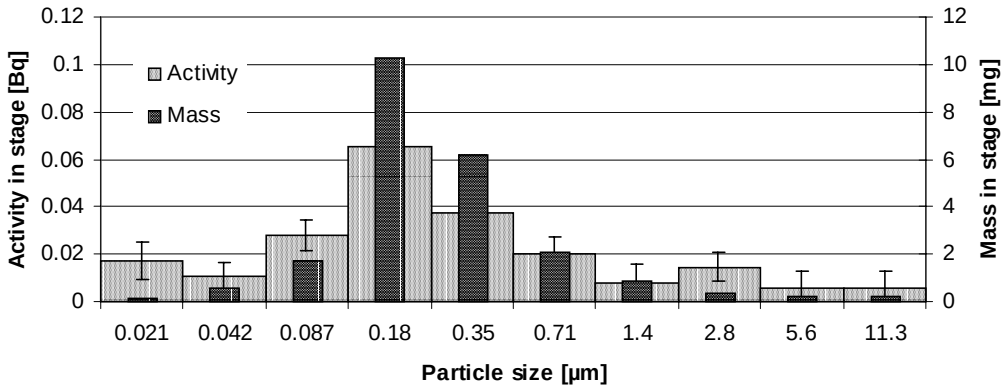

| **IMP 6** Stage | Par. Size [µm] | Cs-137 [Bq] | s.d. [Bq] | Load [mg] | Mass load [mg/m3] | Specifi act. [Bq/g] |
|---|---|---|---|---|---|---|
| 1 | 0.021 | 0.0073 | 0.0071 | 0.0150 | 1.31 | 487 |
| 2 | 0.042 | 0.0073 | 0.0071 | 0.0750 | 1.46 | 97 |
| 3 | 0.087 | 0.0484 | 0.0084 | 0.3200 | 2.77 | 151 |
| 4 | 0.18 | 0.1075 | 0.009 | 1.4500 | 11.09 | 74 |
| 5 | 0.35 | 0.0683 | 0.0085 | 2.8550 | 3.79 | 24 |
| 6 | 0.71 | 0.0403 | 0.0082 | 1.9850 | 1.90 | 20 |
| 7 | 1.4 | 0.0368 | 0.0091 | 0.9100 | 3.50 | 40 |
| 8 | 2.8 | 0.0685 | 0.008 | 1.4850 | 5.98 | 46 |
| 9 | 5.6 | 0.0333 | 0.0069 | 3.2000 | 2.48 | 10 |
| 10 | 11.3 | 0.011 | 0.0069 | 1.1650 | 0.00 | 9 |

**Mass and activity distributions IMP 6**

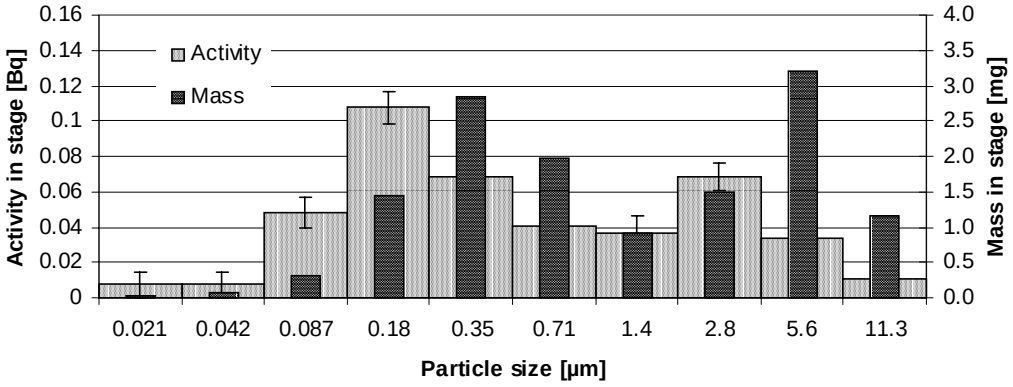


| **IMP 12** Stage | Par. Size [µm] | Cs-137 [Bq] | s.d. [Bq] | Load [mg] [g] | Mass load [mg/m3] | Specifi act. [Bq/g] |
|---|---|---|---|---|---|---|
| | 0.021 | 0.0037 | 0.0059 | 0.14 | 5.51 | 27 |
| 1+2 | 0.042 | 0.0037 | 0.0059 | 0.19 | 7.48 | 20 |
| 3 | 0.087 | 0.0177 | 0.0050 | 0.46 | 18.11 | 39 |
| 4 | 0.18 | 0.0347 | 0.0084 | 1.39 | 54.53 | 25 |
| 5 | 0.35 | 0.0110 | 0.0061 | 0.79 | 30.91 | 14 |
| 6 | 0.71 | 0.0138 | 0.0058 | 0.21 | 8.07 | 67 |
| 7 | 1.4 | 0.0041 | 0.0049 | 0.20 | 7.87 | 20 |
| 8 | 2.8 | 0.0060 | 0.0054 | 0.32 | 12.40 | 19 |
| 9+10 | 5.6 | 0.0065 | 0.0070 | 0.30 | 11.81 | 22 |
| | 11.3 | 0.0065 | 0.0070 | 0.21 | 8.27 | 31 |

**Mass and activity distributions IMP 12**

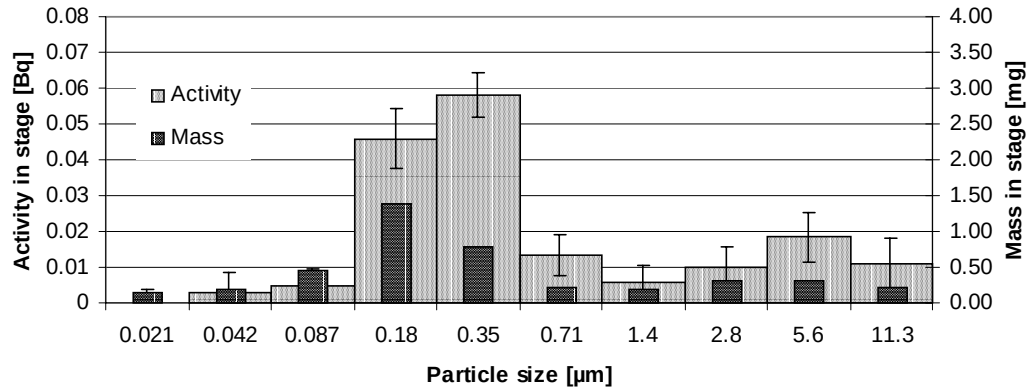

| **IMP 13** Stage | Par. Size [µm] | Cs-137 [Bq] | s.d. [Bq] | Load [mg] [g] | Mass load [mg/m3] | Specifi act. [Bq/g] |
|---|---|---|---|---|---|---|
| | 0.021 | -0.0012 | 0.0055 | 0.065 | 2.53 | -18.2 |
| 1+2 | 0.042 | -0.0012 | 0.0055 | 0.125 | 4.86 | -9.5 |
| 3 | 0.087 | 0.0111 | 0.0060 | 0.505 | 19.65 | 21.9 |
| 4 | 0.18 | 0.0219 | 0.0074 | 1.225 | 47.67 | 17.9 |
| 5 | 0.35 | 0.0195 | 0.0071 | 0.695 | 27.04 | 28.0 |
| 6 | 0.71 | 0.0083 | 0.0038 | 0.295 | 11.48 | 28.2 |
| 7 | 1.4 | 0.0055 | 0.0054 | 0.16 | 6.23 | 34.4 |
| 8 | 2.8 | 0.0030 | 0.0050 | 0.195 | 7.59 | 15.5 |
| 9+10 | 5.6 | 0.0071 | 0.0063 | 0.165 | 6.42 | 42.7 |
| | 11.3 | 0.0071 | 0.0063 | 0.205 | 7.98 | 34.4 |

**Mass and activity distributions IMP 13**

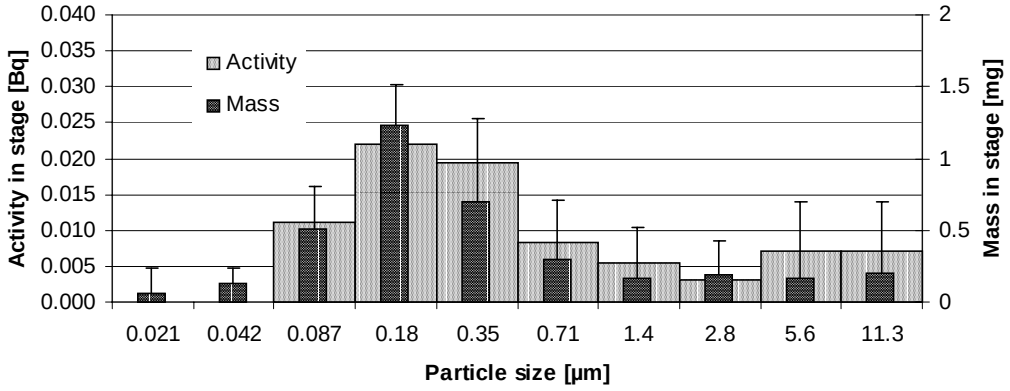


| **IMP 17** Stage | Par. Size [µm] | Cs-137 [Bq] | s.d. [Bq] | Load [mg] [g] | Mass load [mg/m3] | Specifi act. [Bq/g] |
|---|---|---|---|---|---|---|
| | | | | 0.095 | | |
| | | | | 0.21 | | |
| 3 | 0.087 | 0.0000 | 0.0037 | 0.765 | | |
| 4 | 0.18 | 0.0044 | 0.0026 | 3.575 | | 1.22 |
| 5 | 0.35 | 0.0075 | 0.0020 | 4.905 | | 1.53 |
| 6 | 0.71 | 0.0000 | 0.0037 | 1.12 | | |
| | | | | 0.51 | | |
| | | | | 0.195 | | |
| | | | | 0.065 | | |
| | | | | -0.01 | | |

# Appendix D. Fuel Sample Measurements

*Table D.1 Description of fuel samples*

| Time of sampling | | ***Log. # of sample: W1*** Type of fuel | Approximate weight, kg | Moisture content, % |
|---|---|---|---|---|
| 16.06.99 | 15:30 | Sawdust and shavings | 1 | 35.7 |
| 17.06.99 | 9:35 | Sawdust, shavings and chips | 2 | 37.3 |
| 17.06.99 | 10:35 | Sawdust, shavings and chips | 2 | 40.6 |
| 17.06.99 | 11:35 | Sawdust, shavings and chips | 3 | 37.8 |
| 17.06.99 | 12:35 | Sawdust, shavings and chips | 2 | 35.5 |
| 17.06.99 | 13:35 | Sawdust, shavings and chips | 2 | 55.6 |
| 17.06.99 | 14:35 | Chips | 3 | 48.7 |
| 17.06.99 | 15:35 | Chips | 3 | 47.1 |
| 17.06.99 | 16:35 | Chips | 2 | 40.2 |
| 17.06.99 | 17:35 | Chips | 3 | 31.2 |
| 17.06.99 | 18:35 | Chips | 3 | 34.7 |
| 18.06.99 | 8:40 | Shavings and chips | 2.5 | 55.6 |
| 18.06.99 | 9:40 | Shavings and chips | 3 | 32.2 |
| 18.06.99 | 10:40 | Shavings and chips | 3 | 45.8 |
| 18.06.99 | 15:40 | Shavings and chips | 2 | 42.0 |
| 18.06.99 | 16:40 | Shavings and chips | 3 | 42.6 |

*Table D.2 $^{137}$Cs specific activity in the collected samples*

| Log # | Time of sampling | Activity of sample, kBq | Specific activity, Bq/kg | Total error, Bq/kg | Ratio error, % | Average value of specific activity, Bq/kg |
|---|---|---|---|---|---|---|
| 17.06.99, Wood fuel samples | | | | | | |
| W1 | 9:35 | 3.526242 | 154.0126 | 19.01092 | 12.34374 | |
| | | 3.060448 | 134.475 | 19.04222 | 14.16042 | 154.2334 |
| | | 4.023388 | 174.2126 | 18.93535 | 10.8691 | |
| W1 | 10:35 | 3.97336 | 136.5576 | 15.09487 | 11.05386 | |
| | | 4.677195 | 160.9695 | 14.36632 | 8.924868 | 144.6513 |
| | | 3.99044 | 136.4267 | 15.02423 | 11.01267 | |
| W1 | 11:35 | 2.38735 | 79.75698 | 14.47878 | 18.15362 | |
| | | 1.856712 | 61.60783 | 14.31218 | 23.2311 | 77.87527 |
| | | 2.824774 | 92.26101 | 14.13809 | 15.32401 | |
| W1 | 12:35 | 2.152453 | 76.39287 | 15.3277 | 20.06431 | |
| | | 2.352752 | 82.919 | 15.23253 | 18.37037 | 86.88519 |
| | | 2.862128 | 101.3437 | 15.39125 | 15.18719 | |
| 18.06.99, Wood fuel samples | | | | | | |
| W1 | 16:40 | 2.909738 | 94.86039 | 14.20572 | 14.9754 | |
| | | 2.657956 | 88.90287 | 14.53174 | 16.34564 | 83.27103 |
| | | 1.96742 | 66.04985 | 13.76341 | 20.83791 | |
| 17.06.99, Integrated ash samples from ash containers | | | | | | |
| Z2(1) | 19:30 | 193.9456 | 12206.59 | 99.94555 | 0.818784 | |
| | | 194.4717 | 11863.02 | 96.99882 | 0.817657 | 12029.56 |
| | | 188.0934 | 12019.06 | 100.2406 | 0.834014 | |
| Z2(2) | 19:30 | 149.0406 | 10622.39 | 102.1841 | 0.961969 | |
| | | 145.301 | 10670.72 | 104.2791 | 0.977245 | 10671.13 |
| | | 140.3393 | 10720.29 | 107.0576 | 0.998645 | |
| Z1 | 19:30 | 188.9679 | 3052.936 | 26.00639 | 0.851849 | |
| | | 191.4775 | 3040.29 | 25.70578 | 0.845504 | 3106.86 |
| | | 196.4473 | 3227.353 | 26.83651 | 0.831533 | |
| 18.06.99, Integrated ash samples from ash containers | | | | | | |
| Z2(1) | 17:20 | 140.5509 | 10038.56 | 100.2032 | 0.998182 | |
| | | 140.4934 | 10291.13 | 115.2985 | 1.120368 | 10154.34 |
| | | 135.5475 | 10133.33 | 103.4692 | 1.021077 | |
| Z2(2) | 17:20 | 103.5323 | 8897.053 | 108.1458 | 1.215524 | |
| | | 102.9445 | 8876.059 | 108.2977 | 1.22011 | 8919.375 |
| | | 114.5706 | 8985.011 | 102.2217 | 1.137691 | |
| Z1 | 17:20 | 274.4037 | 4083.783 | 27.93747 | 0.684108 | |
| | | 270.5271 | 4022.218 | 27.74597 | 0.689818 | 4040.704 |
| | | 264.3481 | 4016.112 | 27.70138 | 0.689756 | |

*Table D.2 (continued)*

| Log # | Time of sampling | Activity of sample, kBq | Specific activity, Bq/kg | Total error, Bq/kg | Ratio error, % | Average value of specific activity, Bq/kg |
|---|---|---|---|---|---|---|
| 20.06.99, Integrated bottom ash/slag samples | | | | | | |
| Z0 (bottom ash) | entire test | 369.0455 | 2144.742 | 12.98399 | 0.605387 | |
| | | 344.7667 | 1986.645 | 12.5535 | 0.631895 | 2139.896 |
| | | 389.4241 | 2288.301 | 13.44751 | 0.587663 | |
| Z0 (slag) | entire test | 422.7815 | 2701.961 | 13.82323 | 0.5116 | |
| | | 414.2413 | 2667.974 | 13.79473 | 0.517049 | 2692.138 |
| | | 411.4077 | 2706.48 | 14.0212 | 0.51806 | |
| Z0 (slag) | entire test | 379.8315 | 2458.798 | 13.33426 | 0.542308 | |
| | | 378.524 | 2419.648 | 13.16188 | 0.543959 | 2440.328 |
| | | 385.9617 | 2442.537 | 13.15497 | 0.538578 | |
| 17.06.99, Time-dependent ash samples | | | | | | |
| Z2(1) | 9:45 | 12.21338 | 10725.72 | 205.2852 | 1.913953 | |
| Z2(2) | 9:45 | 0.868946 | 2257.002 | 529.7599 | 23.47184 | |
| Z1 | 11:15 | 0.649847 | 2008.801 | 550.027 | 27.38086 | |
| Z2(1) | 11:15 | 1.638177 | 6386.654 | 893.7692 | 13.99433 | |
| Z2(1) | 12:30 | 1.225071 | 7680.697 | 1354.46 | 17.63459 | |
| Z2(2) | 12:30 | 1.140318 | 9278.421 | 1032.783 | 11.13102 | |
| Z2(1) | 14:00 | 2.859481 | 10005.18 | 381.3261 | 3.811286 | |
| Z2(1) | 15:20 | 5.749388 | 10376.08 | 531.395 | 5.121344 | |
| Z1 | 17:45 | 10.89116 | 4372.206 | 132.1397 | 3.022267 | |
| Z2(1) | 17:45 | 5.33275 | 10923.29 | 592.4054 | 5.423323 | |
| 18.06.99, Time-dependent ash samples | | | | | | |
| Z1 | 8:50 | 0.315403 | 3879.492 | 398.0913 | 10.26143 | |
| Z2(1) | 8:50 | 2.764798 | 15637.99 | 1387.189 | 8.870631 | |
| Z1 | 10:10 | 0.993884 | 2170.526 | 414.6168 | 19.10213 | |
| Z2(1) | 10:10 | 1.629808 | 12924.73 | 878.59 | 6.797746 | |
| Z1 | 11:20 | 0.441726 | 3166.496 | 704.9007 | 22.26122 | |
| Z1 | 12:35 | 1.312436 | 2850.644 | 434.9649 | 15.25848 | |
| Z2(1) | 12:35 | 1.777488 | 8603.524 | 1064.39 | 12.37156 | |
| Z1 | 14:00 | 0.249144 | 4280.817 | 586.1751 | 13.69306 | |
| Z2(1) | 14:00 | 8.079776 | 7360.642 | 309.0678 | 4.198925 | |
| Z2(1) | 15:10 | 0.942915 | 8045.353 | 1605.246 | 19.95246 | |
| Z1 | 15:20 | 5.952381 | 3266.411 | 193.5427 | 5.925241 | |
| Z1 | 16:20 | 3.785104 | 3190.68 | 254.7268 | 7.983464 | |
| Z2(1) | 16:20 | 7.360032 | 6540.506 | 285.3875 | 4.363386 | |
| Z2(2) | 16:20 | 9.056656 | 7406.49 | 282.3111 | 3.811672 | |
| 17.06.99, Aerosols entrapped by “absolute” filters during the total dust measurements | | | | | | |
| AD1 | 9:15 | 0.097591 | 966.2471 | 327.3552 | 33.87903 | |
| AD2 | 9:15 | 0.123448 | 2864.223 | 878.2719 | 30.66353 | |
| AD1 | 14:50 | 0.409205 | 15922.37 | 1649.297 | 10.35836 | |
| AD2 | 15:04 | 0.102285 | 14612.16 | 5107.927 | 34.9567 | |
| AD1 | 16:10 | 0.131036 | 4782.341 | 1399.768 | 29.2695 | |
| AD4 | 12:28-18:00 | 0.250352 | 1093.717 | 212.7503 | 19.45205 | |
| 18.06.99, Aerosols entrapped by “absolute” filters during the total dust measurements | | | | | | |
| AD1 | 10:25 | 0.140567 | 3872.367 | 1166.754 | 30.13025 | |
| AD2 | 10:47 | 0.089846 | 6417.565 | 2993.34 | 46.64293 | |
| AD1 | 14:41 | 0.087951 | 5143.329 | 2164.02 | 42.07431 | |
| AD2 | 16:05 | 0.100193 | 12369.5 | 4858.472 | 39.27785 | |
| AD4 | 10:00-16:45 | 0.153205 | 1758.958 | 542.567 | 30.84592 | |

# Appendix E. Laser Measurements

*Table E.1 Number of particulate of different fractions. The results of laser spectrometry of aerosols*

| **17.06.99, Port S31**, $N_2$ dilution ratio = 4.5; Volume of probe = 50 $cm^3$ | | | | | | | |
|---|---|---|---|---|---|---|---|
| **Time** | **0,2-0,25 μm** | **0,25-0,3 μm** | **0,3-0,4 μm** | **0,4-0,5 μm** | **0,5-0,7 μm** | **0,7-1,0 μm** | **1,0-2,0 μm** |
| 8:46 | 67298 | 19503 | 5139 | 4032 | 653 | 212 | 27 |
| 8:50 | 60570 | 19107 | 4752 | 3938 | 792 | 482 | 86 |
| 8:54 | 45662 | 14706 | 4964 | 5018 | 1481 | 1040 | 90 |
| 8:56 | 69561 | 19944 | 5157 | 5045 | 1211 | 761 | 77 |
| 8:59 | 32310 | 10112 | 3407 | 3182 | 950 | 644 | 54 |
| 9:00 | 19049 | 6737 | 1958 | 1611 | 320 | 171 | 23 |
| 9:03 | 17766 | 5940 | 1841 | 887 | 90 | 126 | 131 |
| 9:04 | 20651 | 6944 | 1881 | 1139 | 167 | 99 | 41 |
| 9:05 | 24570 | 8055 | 2300 | 1539 | 203 | 113 | 41 |
| 9:07 | 15089 | 5337 | 1467 | 788 | 99 | 50 | 5 |
| 9:08 | 15044 | 5247 | 1409 | 648 | 68 | 45 | 5 |
| 9:09 | 16844 | 5711 | 1818 | 833 | 68 | 59 | 27 |
| 9:10 | 22253 | 7992 | 2291 | 1436 | 270 | 230 | 68 |
| 9:11 | 47655 | 20457 | 5895 | 5148 | 1967 | 927 | 126 |
| 9:13 | 63927 | 29061 | 8766 | 8276 | 3366 | 1418 | 207 |
| 9:14 | 54729 | 25061 | 8159 | 6638 | 2534 | 1085 | 108 |
| 9:15 | 68711 | 34304 | 12182 | 8996 | 3245 | 1557 | 140 |
| 9:16 | 35105 | 15660 | 5207 | 3551 | 1247 | 657 | 59 |
| 9:18 | 20696 | 7596 | 2124 | 1377 | 333 | 171 | 27 |
| 9:19 | 36491 | 15111 | 4599 | 3915 | 1449 | 716 | 36 |
| 9:20 | 26703 | 10701 | 3281 | 2120 | 504 | 297 | 41 |
| 9:21 | 26451 | 10395 | 3429 | 2075 | 455 | 311 | 45 |
| 9:22 | 43061 | 18972 | 6206 | 3933 | 1130 | 581 | 50 |
| 9:24 | 45725 | 19143 | 6575 | 4203 | 788 | 410 | 144 |
| 9:25 | 25925 | 10008 | 3105 | 1769 | 486 | 279 | 77 |
| 9:27 | 17361 | 6048 | 1832 | 981 | 113 | 68 | 27 |
| 9:28 | 17564 | 5787 | 1778 | 891 | 108 | 68 | 27 |
| 9:29 | 40631 | 17937 | 5589 | 3812 | 761 | 369 | 77 |
| MAX | 69561 | 34304 | 12182 | 8996 | 3366 | 1557 | 207 |
| MIN | 15044 | 5247 | 1409 | 648 | 68 | 45 | 5 |
| AVRG | 35621,5 | 13627,71 | 4182,536 | 3135,036 | 887,7857 | 462,3571 | 66,64286 |
| STDEV | 18191,43 | 7812,718 | 2594,571 | 2271,721 | 921,6206 | 424,0264 | 48,27484 |

*Table E-1 (continued)*

| **17.06.99, Port S31**, $N_2$ dilution ratio = 4.5; Volume of probe = 50 $cm^3$ | | | | | | | |
|---|---|---|---|---|---|---|---|
| **Time** | **0,2-0,25 µm** | **0,25-0,3 µm** | **0,3-0,4 µm** | **0,4-0,5 µm** | **0,5-0,7 µm** | **0,7-1,0 µm** | **1,0-2,0 µm** |
| 10:12 | 6935 | 2421 | 743 | 369 | 41 | 59 | 36 |
| 10:15 | 6597 | 1994 | 594 | 203 | 9 | 0 | 9 |
| 10:16 | 6512 | 2034 | 657 | 324 | 14 | 27 | 9 |
| 10:17 | 6804 | 2462 | 639 | 338 | 36 | 23 | 14 |
| 10:18 | 10130 | 3510 | 1008 | 513 | 72 | 90 | 9 |
| 10:23 | 26433 | 8924 | 2849 | 1719 | 135 | 153 | 41 |
| 10:24 | 23697 | 8442 | 2754 | 1269 | 144 | 176 | 68 |
| 10:25 | 22964 | 7844 | 2358 | 1166 | 104 | 135 | 68 |
| 10:26 | 23468 | 7907 | 2574 | 1256 | 86 | 140 | 41 |
| MAX | 26433 | 8924 | 2849 | 1719 | 144 | 176 | 68 |
| MIN | 6512 | 1994 | 594 | 203 | 9 | 0 | 9 |
| AVRG | 14837,78 | 5059,778 | 1575,111 | 795,2222 | 71,22222 | 89,22222 | 32,77778 |
| STDEV | 8943,146 | 3100,362 | 1019,749 | 555,7391 | 49,94692 | 64,61768 | 24,17529 |
| **17.06.99, Port S31**, $N_2$ dilution ratio = 4.5; Volume of probe = 50 $cm^3$ | | | | | | | |
| **Time** | **0,2-0,25 µm** | **0,25-0,3 µm** | **0,3-0,4 µm** | **0,4-0,5 µm** | **0,5-0,7 µm** | **0,7-1,0 µm** | **1,0-2,0 µm** |
| 12:15 | 20075 | 6773 | 2565 | 977 | 72 | 59 | 18 |
| 12:16 | 20331 | 7169 | 2736 | 1238 | 167 | 108 | 41 |
| 1217 | 22662 | 7596 | 3096 | 1431 | 207 | 117 | 36 |
| 12:18 | 20115 | 6858 | 2750 | 1409 | 239 | 117 | 32 |
| 12:20 | 18167 | 5486 | 2345 | 1175 | 180 | 108 | 9 |
| 12:21 | 15143 | 4703 | 1962 | 806 | 90 | 50 | 23 |
| 12:23 | 15282 | 4604 | 1886 | 824 | 72 | 41 | 14 |
| 12:24 | 14459 | 4559 | 1832 | 743 | 45 | 18 | 14 |
| 12:25 | 13397 | 4262 | 1688 | 590 | 36 | 36 | 5 |
| MAX | 22662 | 7596 | 3096 | 1431 | 239 | 117 | 41 |
| MIN | 13397 | 4262 | 1688 | 590 | 36 | 18 | 5 |
| AVRG | 17736,78 | 5778,889 | 2317,778 | 1021,444 | 123,1111 | 72,66667 | 21,33333 |
| STDEV | 3252,446 | 1313,383 | 496,8432 | 304,0276 | 75,53219 | 39,47151 | 12,52996 |
| **17.06.99, Port S31**, $N_2$ dilution ratio = 4.5; Volume of probe = 50 $cm^3$ | | | | | | | |
| **Time** | **0,2-0,25 µm** | **0,25-0,3 µm** | **0,3-0,4 µm** | **0,4-0,5 µm** | **0,5-0,7 µm** | **0,7-1,0 µm** | **1,0-2,0 µm** |
| 13:02 | 144000 | 8235 | 1773 | 1404 | 369 | 414 | 99 |
| 13:04 | 179703 | 8136 | 1782 | 1836 | 594 | 441 | 117 |
| 13:05 | 183483 | 8307 | 2079 | 1953 | 387 | 279 | 36 |
| 13:06 | 241857 | 9252 | 2223 | 2250 | 423 | 432 | 135 |
| MAX | 241857 | 9252 | 2223 | 2250 | 594 | 441 | 135 |
| MIN | 144000 | 8136 | 1773 | 1404 | 369 | 279 | 36 |
| AVRG | 187260,8 | 8482,5 | 1964,25 | 1860,75 | 443,25 | 391,5 | 96,75 |
| STDEV | 40511,87 | 517,7673 | 223,5403 | 350,8365 | 102,9769 | 75,83535 | 43,08422 |

*Table E-1 (continued)*

| **17.06.99, Port S31**, $N_2$ dilution ratio = 4.5; Volume of probe = 50 $cm^3$ | | | | | | | |
|---|---|---|---|---|---|---|---|
| **Time** | **0,2-0,25 µm** | **0,25-0,3 µm** | **0,3-0,4 µm** | **0,4-0,5 µm** | **0,5-0,7 µm** | **0,7-1,0 µm** | **1,0-2,0 µm** |
| 15:14 | 2277 | 725 | 275 | 86 | 14 | 9 | 0 |
| 15:16 | 2075 | 531 | 176 | 90 | 14 | 0 | 0 |
| 15:17 | 3600 | 716 | 234 | 104 | 5 | 0 | 0 |
| 15:20 | 5675 | 2083 | 765 | 374 | 41 | 32 | 5 |
| 15:22 | 3024 | 1022 | 243 | 99 | 5 | 18 | 0 |
| 15:23 | 2867 | 837 | 270 | 104 | 18 | 14 | 0 |
| 15:26 | 2588 | 878 | 275 | 99 | 0 | 5 | 5 |
| 15:27 | 2831 | 774 | 216 | 144 | 14 | 5 | 0 |
| 15:30 | 3564 | 1062 | 293 | 117 | 5 | 0 | 0 |
| 15:31 | 3861 | 1166 | 351 | 99 | 14 | 14 | 5 |
| 15:33 | 3326 | 1026 | 293 | 117 | 0 | 5 | 14 |
| 15:34 | 3618 | 1080 | 261 | 162 | 9 | 23 | 5 |
| MAX | 5675 | 2083 | 765 | 374 | 41 | 32 | 14 |
| MIN | 2075 | 531 | 176 | 86 | 0 | 0 | 0 |
| AVRG | 3275,5 | 991,6667 | 304,3333 | 132,9167 | 11,58333 | 10,41667 | 2,833333 |
| STDEV | 941,3415 | 390,7786 | 151,4796 | 79,06437 | 11,01617 | 10,10363 | 4,26046 |
| **17.06.99, Port S31**, $N_2$ dilution ratio = 4.5; Volume of probe = 50 $cm^3$ | | | | | | | |
| **Time** | **0,2-0,25 µm** | **0,25-0,3 µm** | **0,3-0,4 µm** | **0,4-0,5 µm** | **0,5-0,7 µm** | **0,7-1,0 µm** | **1,0-2,0 µm** |
| 18:20 | 1319 | 437 | 117 | 176 | 23 | 18 | 18 |
| 18:22 | 4712 | 860 | 230 | 135 | 14 | 5 | 0 |
| 18:23 | 3474 | 653 | 180 | 122 | 36 | 5 | 0 |
| 18:36 | 12011 | 2255 | 495 | 270 | 18 | 18 | 5 |
| 18:37 | 49464 | 8964 | 702 | 203 | 41 | 23 | 9 |
| 18:39 | 5670 | 1175 | 383 | 243 | 18 | 18 | 0 |
| 18:41 | 2408 | 801 | 302 | 126 | 18 | 9 | 0 |
| 18:43 | 2295 | 563 | 198 | 122 | 14 | 5 | 9 |
| 18:44 | 2075 | 603 | 216 | 144 | 36 | 23 | 0 |
| MAX | 49464 | 8964 | 702 | 270 | 41 | 23 | 18 |
| MIN | 1319 | 437 | 117 | 122 | 14 | 5 | 0 |
| AVRG | 9269,778 | 1812,333 | 313,6667 | 171,2222 | 24,22222 | 13,77778 | 4,555556 |
| STDEV | 15415,59 | 2737,178 | 185,4353 | 55,7736 | 10,52114 | 7,726218 | 6,366143 |

*Table E-1 (continued)*

| **17.06.99, Port S22**, $N_2$ dilution ratio = 135; Volume of probe = 50 $cm^3$ | | | | | | | |
|---|---|---|---|---|---|---|---|
| **Time** | **0,2-0,25 µm** | **0,25-0,3 µm** | **0,3-0,4 µm** | **0,4-0,5 µm** | **0,5-0,7 µm** | **0,7-1,0 µm** | **1,0-2,0 µm** |
| 9:38 | 169155 | 61830 | 18900 | 13500 | 1080 | 270 | 0 |
| 9:39 | 356130 | 114750 | 39690 | 30240 | 3510 | 2160 | 270 |
| 9:41 | 312525 | 84240 | 36315 | 29160 | 4995 | 2430 | 945 |
| 9:43 | 218160 | 63045 | 27810 | 21330 | 4995 | 2295 | 405 |
| 9:44 | 142830 | 43875 | 18765 | 15930 | 1755 | 945 | 540 |
| 9:46 | 87750 | 32400 | 11475 | 6750 | 945 | 405 | 270 |
| 9:47 | 115830 | 39015 | 17415 | 8910 | 1215 | 1080 | 135 |
| 9:49 | 96660 | 34965 | 11475 | 7020 | 945 | 675 | 0 |
| 9:51 | 108405 | 38340 | 12555 | 7965 | 405 | 405 | 270 |
| 9:52 | 88560 | 31995 | 13905 | 8370 | 1215 | 675 | 270 |
| 9:53 | 110160 | 33075 | 13230 | 11475 | 1080 | 540 | 0 |
| MAX | 356130 | 114750 | 39690 | 30240 | 4995 | 2430 | 945 |
| MIN | 87750 | 31995 | 11475 | 6750 | 405 | 270 | 0 |
| AVRG | 164196,8 | 52502,73 | 20139,55 | 14604,55 | 2012,727 | 1080 | 282,2727 |
| STDEV | 93129,51 | 26545,71 | 10039,1 | 8654,083 | 1672,535 | 816,7221 | 279,6459 |
| **17.06.99, Port S22**, $N_2$ dilution ratio = 135; Volume of probe = 50 $cm^3$ | | | | | | | |
| **Time** | **0,2-0,25 µm** | **0,25-0,3 µm** | **0,3-0,4 µm** | **0,4-0,5 µm** | **0,5-0,7 µm** | **0,7-1,0 µm** | **1,0-2,0 µm** |
| 11:33 | 251910 | 68175 | 16470 | 9315 | 405 | 675 | 0 |
| 11:34 | 110565 | 20385 | 6345 | 2970 | 135 | 405 | 135 |
| 11:35 | 70065 | 12420 | 6345 | 5940 | 270 | 405 | 135 |
| 11:37 | 84780 | 22275 | 6615 | 6480 | 945 | 540 | 0 |
| 11:51 | 357480 | 86130 | 19440 | 7155 | 540 | 945 | 405 |
| 11:53 | 68175 | 14310 | 6750 | 5535 | 1215 | 675 | 540 |
| 11:54 | 83295 | 19980 | 8370 | 5265 | 675 | 135 | 0 |
| MAX | 357480 | 86130 | 19440 | 9315 | 1215 | 945 | 540 |
| MIN | 68175 | 12420 | 6345 | 2970 | 135 | 135 | 0 |
| AVRG | 146610 | 34810,71 | 10047,86 | 6094,286 | 597,8571 | 540 | 173,5714 |
| STDEV | 113060,8 | 29590,72 | 5512,926 | 1933,579 | 380,6995 | 258,5053 | 216,4816 |
| **18.06.99, Port log. # S31**, $N_2$ dilution ratio = 4.5; Volume of probe = 50 $cm^3$ | | | | | | | |
| **Time** | **0,2-0,25 µm** | **0,25-0,3 µm** | **0,3-0,4 µm** | **0,4-0,5 µm** | **0,5-0,7 µm** | **0,7-1,0 µm** | **1,0-2,0 µm** |
| 12:53 | 927 | 68 | 23 | 5 | 5 | 5 | 0 |
| 12:54 | 635 | 36 | 9 | 9 | 0 | 0 | 0 |
| 12:56 | 450 | 14 | 5 | 0 | 0 | 0 | 0 |
| 12:57 | 1040 | 131 | 18 | 14 | 5 | 0 | 0 |
| MAX | 1040 | 131 | 23 | 14 | 5 | 5 | 0 |
| MIN | 450 | 14 | 5 | 0 | 0 | 0 | 0 |
| AVRG | 763 | 62,25 | 13,75 | 7 | 2,5 | 1,25 | 0 |
| STDEV | 269,554 | 50,9141 | 8,22090 | 5,94418 | 2,88675 | 2,5 | 0 |

*Table E-1 (continued)*

| **18.06.99, Port log. # S31**, $N_2$ dilution ratio = 4.5; Volume of probe = 50 $cm^3$ | | | | | | | |
|---|---|---|---|---|---|---|---|
| **Time** | **0,2-0,25 µm** | **0,25-0,3 µm** | **0,3-0,4 µm** | **0,4-0,5 µm** | **0,5-0,7 µm** | **0,7-1,0 µm** | **1,0-2,0 µm** |
| 15:57 | 20876 | 1103 | 113 | 77 | 32 | 14 | 14 |
| 15:58 | 74336 | 30092 | 8487 | 1445 | 54 | 50 | 9 |
| 16:00 | | | | | | | |
| 16:04 | 83795 | 21704 | 2781 | 374 | 27 | 9 | 9 |
| 16:06 | 3056 | 428 | 126 | 162 | 32 | 14 | 5 |
| 16:07 | 3632 | 248 | 99 | 95 | 23 | 14 | 0 |
| 16:09 | 9900 | 5333 | 135 | 113 | 14 | 5 | 0 |
| MAX | 83795 | 30092 | 8487 | 1445 | 54 | 50 | 14 |
| MIN | 3056 | 248 | 99 | 77 | 14 | 5 | 0 |
| AVRG | 32599,17 | 9818 | 1956,833 | 377,6667 | 30,33333 | 17,66667 | 6,166667 |
| STDEV | 36681,21 | 12869,62 | 3371,784 | 534,0553 | 13,39652 | 16,25628 | 5,56477 |
| **18.06.99, Port log. # S31**, $N_2$ dilution ratio = 4.5; Volume of probe = 50 $cm^3$ | | | | | | | |
| **Time** | **0,2-0,25 µm** | **0,25-0,3 µm** | **0,3-0,4 µm** | **0,4-0,5 µm** | **0,5-0,7 µm** | **0,7-1,0 µm** | **1,0-2,0 µm** |
| 16:10 | 18036 | 1449 | 288 | 198 | 54 | 27 | 14 |
| 16:12 | 19593 | 1458 | 171 | 203 | 27 | 36 | 18 |
| 16:13 | 19103 | 1655 | 279 | 131 | 9 | 18 | 0 |
| 16:15 | 19125 | 1764 | 315 | 180 | 45 | 27 | 5 |
| 16:16 | 20084 | 1751 | 230 | 153 | 18 | 18 | 0 |
| 16:17 | 21740 | 1760 | 189 | 144 | 14 | 14 | 9 |
| 16:19 | 16722 | 1589 | 167 | 126 | 0 | 5 | 5 |
| 16:20 | 31338 | 2111 | 275 | 216 | 41 | 23 | 9 |
| 16:22 | 23400 | 1472 | 288 | 180 | 41 | 18 | 18 |
| 16:23 | 20619 | 842 | 149 | 99 | 32 | 9 | 0 |
| 16:24 | 21213 | 1188 | 144 | 122 | 23 | 27 | 9 |
| 16:26 | 30474 | 2097 | 216 | 126 | 18 | 14 | 0 |
| 16:27 | 18671 | 986 | 135 | 122 | 9 | 9 | 9 |
| 16:29 | 16754 | 1022 | 122 | 144 | 27 | 5 | 0 |
| MAX | 31338 | 2111 | 315 | 216 | 54 | 36 | 18 |
| MIN | 16722 | 842 | 122 | 99 | 0 | 5 | 0 |
| AVRG | 21205,14 | 1510,286 | 212 | 153,1429 | 25,57143 | 17,85714 | 6,857143 |
| STDEV | 4497,967 | 391,1156 | 66,68871 | 36,04881 | 15,60431 | 9,297288 | 6,561627 |
| **18.06.99, Port log. # S22**, $N_2$ dilution ratio = 9; Volume of probe = 50 $cm^3$ | | | | | | | |
| **Time** | **0,2-0,25 µm** | **0,25-0,3 µm** | **0,3-0,4 µm** | **0,4-0,5 µm** | **0,5-0,7 µm** | **0,7-1,0 µm** | **1,0-2,0 µm** |
| 13:02 | 144000 | 8235 | 1773 | 1404 | 369 | 414 | 99 |
| 13:04 | 179703 | 8136 | 1782 | 1836 | 594 | 441 | 117 |
| 13:05 | 183483 | 8307 | 2079 | 1953 | 387 | 279 | 36 |
| 13:06 | 241857 | 9252 | 2223 | 2250 | 423 | 432 | 135 |
| MAX | 241857 | 9252 | 2223 | 2250 | 594 | 441 | 135 |
| MIN | 144000 | 8136 | 1773 | 1404 | 369 | 279 | 36 |
| AVRG | 187260,8 | 8482,5 | 1964,25 | 1860,75 | 443,25 | 391,5 | 96,75 |
| STDEV | 40511,87 | 517,7673 | 223,5403 | 350,8365 | 102,9769 | 75,83535 | 43,08422 |

**Bibliographic Data Sheet** **Risø-R-1146(EN)**

Title and authors

Power Production from Radioactively Contaminated Biomass and Forest Litter in Belarus – Phase 1b

Jørn Roed, Kasper G. Andersson, Christian L. Fogh, Svend K. Olsen, Henrik Prip, Helle Junker, Niels Kirkegaard, Jens-Martin Jensen, Alexandre J. Grebenkov, Vitalij N. Solovjev, Gregory G. Kolchanov, Leonid A. Bida, Peter M. Klepatzky, Igor G. Pleshchenkov, Arnold A. Gvozdev and Larry Baxter

ISBN
87-550-2619-2
87-550-2620-6 (Internet)

ISSN
0106-2840

Department or group
Nuclear Safety Research and Facilities Department

Date
March 2000

Groups own reg. number(s)

Project/contract No(s)
Chernobyl Bio-energy Project phase 1b

| Pages | Tables | Illustrations | References |
|---|---|---|---|
| 93 | 27 | 58 | 7 |

Abstract (max. 2000 characters)

The Chernobyl accident has led to radioactive contamination of vast Belarussian forest areas. A total scheme for remediation of contaminated forest areas and utilisation of the removed biomass in safe energy production is being investigated in a Belarussian-American-Danish collaborative project. Here the total radiological impact of the scheme is considered. This means that not only the dose reductive effect of the forest decontamination is taken into account, but also the possible adverse health effects in connection with the much needed bio-energy production. This report presents the results of an in-country, commercial-scale investigation of the effect of a baghouse filter in retaining contaminants so that they are not released to the atmosphere in the biomass energy production process. Approximately 99.5% of the activity of a commercially representative, dust-laden boiler flue gas was removed from the stream by using a combination of a cyclone and a baghouse filter.

Descriptors INIS/EDB

AEROSOLS; BAGHOUSES; BIOMASS; BOILERS; CESIUM 137; CONTAMINATION; CYCLONE SEPARATORS; DECONTAMINATION; EFFICIENCY; FABRIC FILTERS; FLUE GAS; FLY ASH; RADIOACTIVITY; WOOD WASTES

Available on request from Information Service Department, Risø National Laboratory,
(Information Service Department, Risø National Laboratory), P.O.Box 49, DK-4000 Roskilde, Denmark.
Telephone +45 46 77 40 04, Telefax +45 46 77 40 13.